

A Census of the Young Cluster IC 348 ¹

K. L. Luhman², John R. Stauffer³, A. A. Muench⁴, G. H. Rieke⁵, E. A. Lada⁶, J. Bouvier⁷, and C. J. Lada⁸

ABSTRACT

We present a new census of the stellar and substellar members of the young cluster IC 348. We have obtained images at I and Z for a $42' \times 28'$ field encompassing the cluster and have combined these measurements with previous optical and near-infrared photometry. From spectroscopy of candidate cluster members appearing in these data, we have identified 122 new members, 15 of which have spectral types of M6.5-M9, corresponding to masses of ~ 0.08 - $0.015 M_{\odot}$ by recent evolutionary models. The latest census for IC 348 now contains a total of 288 members, 23 of which are later than M6 and thus are likely to be brown dwarfs. From an extinction-limited sample of members ($A_V \leq 4$) for a $16' \times 14'$ field centered on the cluster, we construct an IMF that is unbiased in mass and nearly complete for $M/M_{\odot} \geq 0.03$ ($\lesssim M8$). In logarithmic units where the Salpeter slope is 1.35, the mass function for IC 348 rises from high masses down to a solar mass, rises more slowly down to a maximum at 0.1 - $0.2 M_{\odot}$, and then declines into the substellar regime. In comparison, the similarly-derived IMF for Taurus from Bričeno et al. and Luhman et al. rises quickly to a peak near $0.8 M_{\odot}$ and steadily declines to lower masses. The distinctive shapes of the IMFs in IC 348 and Taurus are reflected in the distributions of spectral types, which peak at M5 and K7, respectively. These data provide compelling, model-independent evidence for a significant variation of the IMF with star-forming conditions.

Subject headings: infrared: stars — stars: evolution — stars: formation — stars: low-mass, brown dwarfs — stars: luminosity function, mass function — stars: pre-main sequence

1. Introduction

The identification of large, unbiased samples of members of star-forming regions is important for studying in detail the birth and early evolution of stars and brown dwarfs. Complete membership lists are essential

¹Based on observations obtained at Keck Observatory, Steward Observatory, the MMT Observatory, and the Canada-France-Hawaii Telescope. This publication makes use of data products from the Two Micron All Sky Survey, which is a joint project of the University of Massachusetts and the Infrared Processing and Analysis Center/California Institute of Technology, funded by the National Aeronautics and Space Administration and the National Science Foundation.

²Harvard-Smithsonian Center for Astrophysics, 60 Garden St., Cambridge, MA 02138, USA; kluhman@cfa.harvard.edu.

³SIRTF Science Center, Caltech MS 314-6, Pasadena, CA 91125, USA; stauffer@ipac.caltech.edu.

⁴SIRTF Science Center, Caltech MS 220-6, Pasadena, CA 91125, USA; muench@ipac.caltech.edu.

⁵Steward Observatory, The University of Arizona, Tucson, AZ 85721; griek@as.arizona.edu.

⁶Department of Astronomy, The University of Florida, Gainesville, FL 32611; lada@astro.ufl.edu.

⁷Laboratoire d'Astrophysique de l'Observatoire de Grenoble, BP 53, 38041 Grenoble Cedex 9, France; jbouvier@laog.obs.ujf-grenoble.fr.

⁸Harvard-Smithsonian Center for Astrophysics, 60 Garden St., Cambridge, MA 02138, USA; clada@cfa.harvard.edu.

ingredients in the analysis of data on circumstellar disks, X-ray emission, multiplicity, rotation, and kinematics. Most importantly, a thorough spectroscopic census of a young population provides a measurement of the Initial Mass Function (IMF) from massive stars down to brown dwarfs, as recently demonstrated for Taurus, IC 348, Ophiuchus, and the Trapezium Cluster (Briceño et al. 2002; Luhman et al. 2003a; Herbig 1998; Luhman et al. 1998b; Luhman 1999; Luhman & Rieke 1999; Luhman et al. 2000; Hillenbrand 1997). For measuring the IMF, these spectroscopic surveys complement alternative methods such as luminosity function modeling, which have proven successful in constraining the IMFs of the more compact and denser clusters (Muench et al. 2002, 2003).

The young cluster IC 348 is well-suited for a membership survey. The cluster is young (2 Myr), nearby (315 pc), rich (~ 400 members), compact ($D \sim 20'$), and most of its members exhibit relatively low extinction ($A_V = 0-4$). As a result, a large fraction of the membership can be identified down to very low masses through efficient observations of a small area of sky that can be performed at both optical and infrared (IR) wavelengths. Previous searches for members of IC 348 have utilized proper motion measurements (Fredrick 1956; Scholz et al. 1999), optical spectroscopy and photometry (Gingrich 1922; Harris et al. 1954; Strom et al. 1974), IR photometry (Lada & Lada 1995; Muench et al. 2003), imaging in H α (Herbig 1954, 1998), extensive spectroscopy and photometry at optical and IR wavelengths (Herbig 1998; Luhman et al. 1998b; Luhman 1999), and narrow-band IR photometry (Najita et al. 2000) (hereafter NTC00). The membership information and spectral types from these studies have provided an important basis for recent work in IC 348 on multiplicity (Duchêne et al. 1999; Luhman et al. 2003b), near-IR and millimeter disk emission (Haisch et al. 2001; Carpenter 2002; Liu et al. 2003), variability (Herbst et al. 2000; Ripepi et al. 2002), and X-ray emission (Preibisch & Zinnecker 2001, 2002).

In this paper, we present our latest results in a continuing effort to identify all of the stellar and substellar members of IC 348. We use new data at I and Z and recently published near-IR photometry to select candidate members of the cluster across a larger area and down to lower masses than in previous surveys. We describe spectroscopy of these candidates and evaluate the membership status of all objects toward IC 348 that have been observed spectroscopically in this work and in previous studies. For this list of known cluster members, we estimate extinctions, luminosities, and effective temperatures, and construct a Hertzsprung-Russell (H-R) diagram. Using the evolutionary models that provide the best agreement with observational constraints for young stars (Palla & Stahler 1999; Baraffe et al. 1998; Chabrier et al. 2000) (hereafter BCAH98 and CBAH00), we infer individual masses and derive an IMF for the cluster, which is compared to the mass functions in other star-forming regions and open clusters.

2. Observations and Data Analysis

2.1. Optical Photometry

Images of the IC 348 cluster were obtained with the CFH12K camera on the Canada-France-Hawaii Telescope on the night of 1999 September 30. The instrument contained twelve 2048×4096 CCDs separated by $\sim 7''$ and arranged in a 6×2 mosaic. With a plate scale of $0''.206 \text{ pixel}^{-1}$, the total field of view was $42' \times 28'$. Images were obtained with exposure times of 1, 30, and 900 s through the I and Z filters at one pointing centered at $\alpha = 3^{\text{h}}44^{\text{m}}33^{\text{s}}.2$, $\delta = +32^{\circ}09'48''$ (J2000). Data from various targets during the observing run were used to construct sky flat field frames. The IC 348 images were bias subtracted and flat-fielded. A typical point source in these images exhibited a FWHM of three pixels, or $0''.6$. Photometry and image coordinates of the sources in these data were measured with DAOFIND and PHOT under the IRAF

package APPHOT. For most stars, aperture photometry was extracted with a radius of six pixels. Smaller apertures were used for closely separated stars. The photometry was calibrated in the Cousins I system by combining data for standards across a range of colors (Landolt 1992) with the appropriate aperture and airmass corrections. The transmission profile for the Z filter is described by Moraux et al. (2003). The Z data were calibrated by assuming $I - Z = 0$ for A0 standard stars. This type of calibration is sufficient since the analysis in this study relies only on the relative precision of the Z photometry. To compare our Z photometry to data from another instrument, one would need to calibrate the latter in the manner applied to our data and to account for any differences in the filter and instrument transmission profiles. Saturation in the 1 sec exposures occurred near magnitudes of 11-12 in both filters. The completeness limits of the long exposures were $I \sim 22$ and $Z \sim 21$. Typical photometric uncertainties were 0.04 mag at $I = 21.25$ and $Z = 20.25$ and 0.1 mag at $I = 22.25$ and $Z = 21.25$. The plate solution was derived from coordinates measured in the Two-Micron All-Sky Survey (2MASS) Spring 1999 Release Point Source Catalog for stars that appeared in the optical images and were not saturated.

2.2. Spectroscopy

The 241 targets of our new spectroscopy are listed in Table 1, which are selected in § 3.1. The gratings and spectral resolutions for these data are also provided in Table 1. During the observations with the Keck low-resolution imaging spectrometer (LRIS; Oke et al. (1995)), we used both the long-slit and multi-slit modes. All long-slit spectra were obtained with the slit rotated to the parallactic angle. The exposure times ranged from 60 to 3600 s. After bias subtraction and flat-fielding, the spectra were extracted and calibrated in wavelength with arc lamp data. The spectra were then corrected for the sensitivity functions of the detectors, which were measured from observations of spectrophotometric standard stars.

In addition to the optical data, we obtained K -band spectra of a small sample of objects using the near-IR long-slit spectrometer FSpec (Williams et al. 1993). These data were collected at the MMT Observatory on 2000 December 7. Sources were stepped through four positions along the slit. At each position, the integration times ranged between 30 and 120 s. At one grating setting, we obtained a spectrum extending from 2.0 to 2.4 μm with a two-pixel resolution of $R = \lambda/\Delta\lambda = 800$. We observed a nearby A0 V star (HR 1019), which acted as the telluric standard. After dark subtraction and flat-fielding, adjacent images along the slit were subtracted from each other to remove sky emission. The sky-subtracted images were aligned and combined, during which most bad pixels and cosmic rays were rejected. A spectrum was extracted from this final image, divided by the extracted A0 V standard spectrum, and wavelength calibrated using OH airglow lines. The intrinsic spectral slope of the telluric standard was removed with an artificial blackbody spectrum of $T_{\text{eff}} = 10000$ K.

Among the several dozen candidate members of IC 348 that were observed spectroscopically by Luhman (1999), only sources with spectral types of M4 or later were presented in that study. The 42 stars that were earlier than M4 are included in Table 1. The observations of these stars were conducted on 1998 August 7 and 1998 December 23 and 26 and are described by Luhman (1999). Table 1 contains a total of 268 objects, some of which were observed on more than one date.

3. New Members of IC 348

3.1. Selection of Candidate Members

Previous studies have searched for members of IC 348 through measurements of proper motions (Fredrick 1956), imaging in H α emission (Herbig 1954, 1998), IR luminosity functions (Lada & Lada 1995; Luhman et al. 1998b; Muench et al. 2003), and optical color-magnitude diagrams (Herbig 1998; Luhman 1999). We extend the latter surveys to greater depth and to a larger area of the cluster by including our new I and Z data. We have focused our membership survey on the $16' \times 14'$ region centered at $\alpha = 3^{\text{h}}44^{\text{m}}31^{\text{s}}$, $\delta = +32^{\circ}06'45''$ (J2000), which is indicated in Figure 1. The color-magnitude diagrams and completeness analysis (§ 3.3) apply to this area.

To identify the stars toward IC 348 that have both the colors and the absolute photometry expected of cluster members, we have constructed extinction-corrected diagrams of $I - K_s$ versus H and $I - Z$ versus H in the manner described by Luhman et al. (2003a). The near-IR photometry for these diagrams is from the references listed in § 4.1. When the known members of IC 348 are placed on a H-R diagram, most of them appear above the model isochrone for an age of 10 Myr from Baraffe et al. (1998) (Luhman 1999). In the diagrams of $I - K_s$ versus H and $I - Z$ versus H in Figure 2, we plot the 10 Myr isochrone from 0.015 to $1 M_{\odot}$ by combining the predicted effective temperatures and bolometric luminosities (Baraffe et al. 1998), a temperature scale that is compatible with the adopted models (§ 4.3), intrinsic colors in $I - K$ (Leggett 1992) and $I - Z$ (§ 4.2), dwarf bolometric corrections (see references in Luhman (1999)), and a distance modulus of 7.5 (Herbig 1998). We have defined boundaries below this isochrone to separate candidate members of IC 348 and probable field stars, as shown in Figure 2. For spectroscopy, we selected 148 objects that appeared above both of these boundaries. Although we focused on the $16' \times 14'$ field in Figure 1, a small number of the targets are outside of this area. We also obtained spectra for 49 objects from previous studies to improve their spectral type measurements.

Young stars that are observed only in scattered light (e.g., edge-on disks) can appear well below the cluster sequence in a color-magnitude diagram (Briceño et al. 2002). As a result, such sources are rejected as field stars when candidate members are selected through color-magnitude diagrams. However, scattered-light objects can be identified through other indicators of youth, such as the presence of reflection nebulosity, variability, emission in H α and in X-rays, and excess emission at near- and mid-IR wavelengths. After checking the stars below the boundaries in Figure 2 for these signatures, we found that sources 203 and 435 were detected in X-rays by Preibisch & Zinnecker (2001) and have near-IR excess emission. The former was also detected in the H α survey of Herbig (1998). These two stars were included in our spectroscopic sample.

Many of the above targets were observed with multi-slit spectroscopy. After designing a slit mask for a set of these objects, we included additional slitlets as space allowed for stars that were below one or both of the boundaries in Figure 2. The highest priority was given to stars that appeared to be M-type by the data from NTC00 or that were just below the boundaries. In this way, useful spectra were obtained for 69 objects.

3.2. Classification of Candidate Members

In this section, we measure spectral types for the 268 objects toward IC 348 that we observed spectroscopically. We then evaluate the membership of each candidate with the spectral types, spectral features (H α , Na I, K I), and photometry. For determining spectral types and membership, we used low-resolution

optical spectroscopy from 6000 to 9000 Å. At the M spectral types that are expected for most of the members of IC 348, the K I and Na I absorption lines vary significantly between dwarfs and pre-main-sequence stars (Martín et al. 1996; Luhman et al. 1998a,b; Luhman 1999). Because these features are easily detected in low-resolution spectra, higher-resolution data for Li were unnecessary for distinguishing young members from field dwarfs among most of the candidates. Meanwhile, for faint M-type sources, both high sensitivity and accurate spectral types can be achieved with low spectral resolution. For a few objects with earlier spectral types, we included IR spectroscopy to better constrain the classifications.

3.2.1. Spectral Types

The low-resolution optical spectra of early-type dwarfs and giants (<K0) exhibit only a few absorption lines (H α , Ca II) and are otherwise featureless. As a result, the uncertainties in spectral types are largest at these types. In fact, we can classify some objects as only “early-type” or “giant”. In most of those cases, such a classification is sufficiently accurate to indicate that an object is a background star. However, for G and early K types, we cannot confidently distinguish between giants, dwarfs, and pre-main sequence stars based on the low-resolution optical data. Because absorption in the *K*-band CO band heads is much stronger in the former than in the latter two, we obtained *K*-band spectra of some of the stars with these ambiguous classifications and compared the data to those of standard dwarfs and giants (Luhman & Rieke 1998) to distinguish background giants from dwarfs and pre-main-sequence stars. In addition, we measured the strength of Li absorption at 6707 Å for one these stars through moderate-resolution spectroscopy. There remains one star of this kind that lacks IR spectra or Li data and thus has an uncertain classification (§ A.1).

For K and M-type field dwarfs and for K0-M5 members of IC 348, we measured spectral types by comparison to the spectra of standard dwarfs from Allen & Strom (1995), Kirkpatrick et al. (1991), Henry et al. (1994), and Kirkpatrick et al. (1997). Spectral types for members later than M5 were derived with the averages of dwarf and giant spectra as described by Luhman (1999). The same system has been used in classifying young late-type objects in Taurus (Briceño et al. 2002; Luhman et al. 2003a), MBM 12A (Luhman 2001), Ophiuchus (Luhman et al. 1997), and IC 348 (Luhman et al. 1998b; Luhman 1999). Spectra of the 23 known members of IC 348 with spectral types later than M6 are presented in Figs. 3 and 4. The typical uncertainties in the optical spectral types from Luhman et al. (1998b), Luhman (1999), and this work are ± 0.5 and ± 0.25 for K and M types, respectively, unless noted otherwise.

3.2.2. Membership

Stars projected against IC 348 can be background stars, foreground stars, or young members of the cluster. We now evaluate the membership status of all objects toward IC 348 that have been observed spectroscopically in this work and in previous studies.

Members of IC 348 can be identified by several indicators. Nine of the brightest stars toward IC 348 have relative proper motions that imply membership in the cluster (Fredrick 1956). Meanwhile, the deeper proper motion measurements of Scholz et al. (1999) cannot reliably distinguish members from background stars. Because IC 348 is a star-forming cluster, objects that show evidence of youth are likely to be members of the cluster. Signatures of youth include H α emission above the levels observed for active field dwarfs ($W_\lambda \gtrsim 15$ Å for M types), Br γ emission, IR excess emission in photometry or spectra, and spectral features implying low gravity. Examples of the latter are K I, Na I, and the overall shape of the red optical spectra, which differ

noticeably between dwarfs and pre-main-sequence objects at spectral types later than M2. Finally, for a given star, the presence of significant reddening in the spectrum or colors ($A_V > 1$) and a position above the main sequence for the distance of IC 348 indicate that it cannot be in the foreground or the background of the cluster, respectively, and therefore must be a member of the cluster.

Field dwarfs in the foreground of IC 348 have large proper motions relative to cluster members or background stars, and thus are easily identified in proper motion surveys (Blaauw 1952; Scholz et al. 1999). Foreground dwarfs are also characterized by little or no reddening, strong absorption in the optical Na I and K I transitions at M types, and a lack of Li absorption or any other indicator of youth.

Field stars in the background of IC 348 consist of dwarfs and giants. At brighter levels, most background stars are giants and early-type dwarfs. However, because of the depth of our spectroscopy, we detected a large number of background field M dwarfs as well. Background dwarfs fall below the main sequence if placed on the H-R diagram for the distance of the cluster. These M dwarfs also can be identified by their strong absorption in Na I and K I, just as for foreground dwarfs. For some of the M-type stars falling below the main sequence, we cannot use these features to confirm their nature as field dwarfs because of insufficient signal-to-noise in the spectra. As discussed in § 3.1, young stars that are seen in scattered light can appear low on the H-R diagram, even below the main sequence. As a result, some of the objects that we identify as background M dwarfs could be scattered-light members of IC 348. However, these stars show none of the signatures of youth mentioned at the end of § 3.1.

We list the spectral types from this work and from previous studies for objects that we classify as members of IC 348, as foreground stars, and as background stars in Tables 2, 3, and 4, respectively. The evidence for the assigned membership status of each member and foreground star is provided. The background stars were identified by either a position below the main sequence and a lack of youth indicators or by a classification as a giant. Stars that have uncertain membership status by available data are found in Table 5. In Table 6, our source identifications are listed with those from Herbig (1998), NTC00, Preibisch & Zinnecker (2001), and the 2MASS Point Source Catalog. A few mistakes in the cross-identifications from NTC00 and Preibisch & Zinnecker (2001) have been corrected here. In our new spectroscopic sample of 268 objects, there are 47 members that have previously published spectra, 122 newly confirmed members (15 later than M6), 97 field stars, and two stars with uncertain membership status. Additional comments on the spectral and membership classifications of individual sources are in § A.1.

The membership list in Table 2 contains 288 entries. Three stars are close secondaries that lack resolved spectroscopy. Source 51 exhibits a featureless IR spectrum that is indicative of a young star with a class I spectral energy distribution. The spectrum of object 46 confirms its youth and membership, but did not have sufficient signal-to-noise for an accurate spectral classification. The remaining 283 members have measured spectral types. The positions of these objects are plotted on the map in Figure 1.

3.3. Completeness of Census

In the following discussion, we assess the completeness of the new census of members within the $16' \times 14'$ field toward IC 348 that is shown in Figure 1.

We first examine our photometry for candidate cluster members that have not been observed spectroscopically. In Figure 2, we indicate the confirmed members from the previous section, while omitting the known field stars. Next, we use this diagram to identify candidate members among the stars that lack

spectroscopy in the $16' \times 14'$ field. At $I > 22$, we cannot use the boundaries in Figure 2 to reliably separate field stars and candidate members because the photometric uncertainties are too large. Therefore, we apply this diagram only to stars with $I \leq 22$. Objects that are above this limit and that fall below either of the boundaries in Figure 2 are likely to be field stars, and thus are not shown. Similarly, we also omit stars that appear below the boundary in the diagram of $R - I$ versus I from Luhman (1999). The one exception is 2MASS 03444520+3201197, which falls below the boundary in $I - Z$ versus H , but is surrounded by reflection nebulosity in our I and Z images, and thus is probably a cluster member observed in scattered light. Sources that are earlier than M2 by the narrow-band photometry of NTC00 and that have $K = 14-16$ are likely field stars as well (see Figure 6). After rejecting these field stars, in Figure 2 there remain 23 candidate members in the $16' \times 14'$ field that have not been observed with spectroscopy. In comparison, 261 cluster members have been confirmed in this region in this work and previous studies (§ 3.2.2).

Because the mass and reddening vectors are roughly perpendicular in a near-IR color-magnitude diagram and because cool and reddened sources are most easily detected at near-IR wavelengths, we use the diagram of $J - H$ versus H in Figure 5 to evaluate the completeness of the current census in terms of mass and extinction. The photometry in Figure 5 is compiled from references in § 4.1. The deepest of those data sets is from Muench et al. (2003), which encompassed the entire $16' \times 14'$ field. The completeness limits of the photometry from Muench et al. (2003) are taken to be the magnitudes at which the logarithm of the number of sources as a function of magnitude departs from a linear slope and begins to turn over ($J \sim 17.5$, $H \sim 17.0$, $K_s \sim 16.5$). In Figure 5, we have plotted the reddening vectors from $A_V = 0-4$ for cluster members with masses of 0.03 and $0.08 M_\odot$ and ages of 3 and 10 Myr, where the latter is the maximum age implied by the H-R diagram of the cluster (§ 4.4). These vectors are derived in the manner described by Briceño et al. (2002) with the evolutionary models of CBAH00 for the distance of IC 348. As demonstrated in Figure 5, the IR photometric data should be complete for members of IC 348 with $M/M_\odot \geq 0.03$ and $A_V \leq 4$, with the exception of close companions.

In Figure 5, we omit known and likely field stars in the same manner as in Figure 2. The remaining IR sources consist of confirmed members and objects that lack spectroscopic data. The latter are divided into candidate members from Figure 2, stars with uncertain optical photometry ($I > 22$), and sources detected only in the IR data. In Figure 5, there are only three objects that lack spectral classifications and that would have $M/M_\odot > 0.03$ and $A_V \leq 4$ if they were members ($H < 16$, $J - H < 1.2$), all of which are candidate members by Figure 2. Because of the small number of these candidates, the current sample of confirmed members is nearly complete for these extinction and mass limits. Therefore, in § 4.5, we will derive the IMF from a sample of known members defined by $A_V \leq 4$ and we will refer to $0.03 M_\odot$ as the completeness limit. Just as this survey is incomplete for low-mass members with high extinction ($A_V > 4$), it is not sensitive to objects that are seen in scattered light (e.g., edge-on disks), particularly those at low-masses.

3.4. Implications for the Survey of NTC00

Using the spectral type and membership data compiled in § 3.2, we evaluate the survey for low-mass members of IC 348 by NTC00. In that study, the $5' \times 5'$ center of the cluster was imaged with NICMOS on *HST* in narrow-band filters that sampled the near-IR steam absorption bands. They estimated spectral types from those data and constructed an empirical H-R diagram, which is reproduced in Figure 6. From that diagram, they identified 20-30 brown dwarfs candidates ($>M6$).

We first discuss the membership status of the sources detected by NTC00. We place their observations

in the context of previous surveys by indicating in Figure 6 the sources that had already been observed spectroscopically by Herbig (1998), Luhman (1999), and Luhman et al. (1998b). We mark the objects that have spectra for the first time from this work, two of which, 603 and 624, had been previously reported as candidate low-mass members (Luhman et al. 2000). Next, we indicate the NICMOS sources that are field stars by the spectroscopic analysis of the previous section or by the positions in the color-magnitude diagrams in Figure 2 and in Luhman et al. (2003b). Several objects that appear to have spectral types of late M by the NICMOS data – and thus were taken as probable low-mass members by NTC00 – are field stars. Sources 609, 618, and 1426 have NICMOS spectral types of $M7.9\pm3.9$, $M5.5\pm2.9$, and $>M14$, respectively, but are background stars by both spectroscopy and the color-magnitude diagrams. While NICMOS objects 021-05, 022-03, 052-05, 071-02, and 075-01 were classified as $M11.1\pm5.2$, $>M14$, $>M14$, $M7.6\pm6.7$, and $M11.1\pm6.6$ by NTC00, they are probably field stars by their positions in an optical color-magnitude diagram constructed from *HST* WFPC2 data by Luhman et al. (2003b). Finally, we examine the objects that are not labeled as field stars and that lack spectra. Three NICMOS sources near the cluster sequence at $K < 14$ have not been observed spectroscopically. Two of them are the close companions 60B and 78B. One other object, 073-01 from NTC00, is a candidate member by our optical color-magnitude diagrams. At $K > 14$, the remaining candidate members by the NICMOS data are 014-06, 024-02, 072-01, 082-02, and 104-01 which have NICMOS types of $M6.8\pm12.1$, $M9.2\pm4.8$, $>M14$, $>M14$, and $M5.9\pm3.9$. Given the large uncertainties in these classifications and the fact that these stars are not detected in our optical images, they could be either reddened background stars ($A_V \gtrsim 3$) or cool sources that are intrinsically red (field dwarfs or members).

We now investigate the accuracy and precision of the spectral types that were estimated from the NICMOS narrow-band photometry by NTC00. In Figure 7, we plot spectral types from NTC00 and spectral types measured from ground-based spectroscopy for all NICMOS sources for which the latter data are available. Most of the ground-based spectral types are derived from optical data. The small number of IR types included here were measured with optically-classified standards. Therefore, the ground-based classifications are assured to be accurate, and in fact effectively define the spectral types for young objects at late M types. As for the precision of the optical spectral types, the measurement errors are ± 1 subclass or less for most of the objects in question. The accuracy of the NICMOS spectral types is illustrated in Figure 7, where the NICMOS classifications are systematically later than those measured from the optical data by an average of ~ 1 -2 subclasses. The spectral type calibration of the NICMOS measurements was derived from both optically-classified members of IC 348 and field dwarf standards. The offset in classifications in Figure 7 is probably due to differences in the steam band strengths between dwarfs and young objects at a given spectral type, which is a behavior that has been noticed previously (Luhman & Rieke 1999; Lucas et al. 2001; Allard et al. 2001). The precision of the NICMOS spectral types is quantified by the measurement errors reported by NTC00, which are largest for early types and for faint objects; the NICMOS types at $<M2$ are uncertain because little steam absorption is present at higher temperatures, as pointed out by NTC00, while the increase in errors at faint levels is a reflection of photometric uncertainties.

As demonstrated in the novel study of NTC00, measurements of near-IR steam absorption through narrow-band photometry can be used to efficiently identify cool objects that may be low-mass members of a dense cluster. However, to arrive at an accurate calibration of spectral types, optically-classified young M-type objects rather than M dwarfs should be used as the spectral type standards. As narrow-band photometry does not distinguish between cool field stars and cool members, membership of candidates should be confirmed through other means (e.g., spectroscopy, proper motions). In addition, useful estimates of spectral types can be derived only well above the detection limit where the photometry is accurate.

4. The IC 348 Stellar Population

In this section, we begin by tabulating photometry and spectral types for all known members of the IC 348 cluster and estimating their extinctions, effective temperatures, and bolometric luminosities (§ 4.1, § 4.2, § 4.3). The latter three parameters are estimated for the 283 members of IC 348 in Table 2 that have resolved spectral types. We place these sources on the H-R diagram and interpret their positions with the most suitable set of theoretical evolutionary models (§ 4.4). Because the current census of members is unbiased in mass at $M/M_{\odot} \geq 0.03$ and $A_V \leq 4$ for the $16' \times 14'$ region shown in Figure 1, we will restrict the IMF sample to include only members within this extinction limit and in this area. The resulting IMF is compared to data from other stellar populations such as the Taurus star-forming region (§ 4.5). Finally, we discuss the implications of our new data for the X-ray observations of Preibisch & Zinnecker (2001) (§ 4.6).

4.1. Adopted Data

The latest membership list for IC 348 was compiled in § 3.2.2 and is given in Table 2. High-resolution imaging has resolved some of these sources into close binaries. To facilitate comparisons of the populations in IC 348 and other young regions, we treat a binary system in IC 348 with a separation less than $1''$ as one object for the remainder of this section. In order of preference, we adopt the $R - I$ colors from Luhman (1999) and Herbig (1998), the I -band measurements from this work, Luhman (1999), and Herbig (1998), and the near-IR data from Muench et al. (2003), Luhman et al. (1998b), the 2MASS Point Source Catalog, and Lada & Lada (1995). For reasons given in Luhman (1999), we do not use the $R - I$ colors of Herbig (1998) for $R - I \geq 1.5$. The J , H , and K measurements of Luhman et al. (1998b) are an average of 0.09, 0.19, and 0.16 mag fainter than the 2MASS photometry for sources in common between the two data sets. We subtract these offsets from the data of Luhman et al. (1998b) for this study. The data from Muench et al. (2003) are used only when $J > 10$, $H > 10.5$, and $K_s > 11$, which are below the saturation limits of that survey. We adopt the coordinates measured from our I -band images and otherwise use the values from 2MASS. Coordinates are not available for source 91 from either of these sets of data. For this star, we measure the average offset between the coordinates of stars in the image containing 91 from NTC00 and in our I -band images. We use this offset and the coordinates reported for 91 by NTC00 to arrive at coordinates that are on the reference frame of our I -band images. These adopted measurements, the $I - Z$ colors from this work, and the available spectral types are presented in Table 2.

4.2. Extinctions

In the following analysis, standard dwarf colors are taken from the compilation of Kenyon & Hartmann (1995) for types earlier than M0 and from the young disk populations described by Leggett (1992) for types of M0 and later. The IR colors from Kenyon & Hartmann (1995) are transformed from the Johnson-Glass photometric system to the CIT system (Bessell & Brett 1988). Near-IR colors in the 2MASS and CIT photometric systems agree at a level of < 0.1 mag (Carpenter 2001). From the distributions of $E(R - I)$ and $E(I - Z)$ versus $E(J - H)$ produced later in this section, we inferred $E(I - Z) = 0.77 E(J - H)$ and $E(R - I) = 1.7 E(J - H)$. When these relations were combined with the extinction law of Rieke & Lebofsky (1985), we arrived at $E(I - Z) = 0.082 A_V = 0.29 A_J$ and $E(R - I) = 0.18 A_V = 0.64 A_J$.

The amount of extinction towards a young star can be estimated from the reddening of its broad-band colors. To ensure that the color excesses reflect only the effect of extinction, contamination from short and

long wavelength excess emission is minimized by selecting colors between the R and J bands. Therefore, our extinction estimates are based on $R - I$ and $I - Z$. To measure extinctions from the observed colors, we need the intrinsic values of $R - I$ and $I - Z$ as a function of spectral type, which were estimated in the following manner. Although $J - H$ is more susceptible to contamination from emission from circumstellar material than $R - I$ and $I - Z$, only a small minority of the members of IC 348 exhibit such excess emission in $J - H$. In addition, the intrinsic photospheric $J - H$ colors of members of IC 348 were shown to be dwarf-like by Luhman (1999). As a result, by assuming dwarf intrinsic colors for the sources with no near-IR excess emission, we were able to calculate reliable extinctions for a large sample of members. We then combined these extinctions with the observed $R - I$ and $I - Z$ for IC 348 members to arrive at average intrinsic colors as a function of spectral type. At M2 through M5, these estimates of $R - I$ were bluer than the values for dwarfs, which is a departure toward giant-like colors. We found a similar result in a previous study of a smaller sample of sources in IC 348 (Luhman 1999). For other spectral types, the $R - I$ colors that we derived were consistent with dwarf colors, and so we adopted the latter at these types. The intrinsic $R - I$ and $I - Z$ at each spectral type from K0 through M9 are listed in Table 7. Because of the paucity of members earlier than K0, we did not estimate the average intrinsic $I - Z$ at those types. Since $R - I$ data are not available for many of the members later than M6, we also measured reddenings from the optical spectra during the process of spectral classification of these sources. The final extinctions are averages of the values implied by $R - I$, $I - Z$ (\geq K0), and the optical spectra ($>$ M6). None of these three measurements are available for 23 sources, which are either saturated or below the detection limit in the optical data or are earlier than K0. For these stars, we measured extinctions from $E(J - H)$ assuming dwarf-like intrinsic colors. One exception is source 13, which exhibits strong IR excess emission. The extinction for this object was estimated by dereddening the $J - H$ and $H - K_s$ colors to the locus observed for classical T Tauri stars (Meyer et al. 1997).

4.3. Effective Temperatures and Bolometric Luminosities

Spectral types of M0 and earlier are converted to effective temperatures with the dwarf temperature scale of Schmidt-Kaler (1982). For spectral types later than M0, Luhman (1999) developed a temperature scale for use with the evolutionary models of BCAH98 with $l_{mix}/H_p = 1.0$ and 1.9 at $M/M_\odot \leq 0.6$ and $M/M_\odot > 0.6$, respectively. This temperature scale was designed such that the members of the young quadruple system GG Tau, which spanned types of K7 through M7.5, were coeval when placed on the BCAH98 model isochrones. On this scale, a spectral type of M7.5 corresponded to a temperature that was roughly an average of the values for a dwarf and a giant. To extend the scale to M8 and M9, Luhman (1999) followed this trend and arbitrarily assigned temperatures that were intermediate between dwarf and giant scales. We now revise the temperature conversion from Luhman (1999) in the following manner. From the new surveys for low-mass members of IC 348 (this work) and Taurus (Briceño et al. 2002; Luhman et al. 2003a), we have membership lists that are reasonably well-populated down to M9. As with the members of GG Tau, the sequences for IC 348 and Taurus on the H-R diagram form empirical isochrones that can be used in defining a temperature scale that is compatible with the models of BCAH98 and CBAH00. When the populations of these two regions are placed on the H-R diagram with the temperature scale from Luhman (1999), they are parallel to the isochrones of BCAH98 and CBAH00 down to the latest spectral type present in GG Tau (M7.5). At M8 and M9, we now adjust the temperatures from Luhman (1999) so that the sequences for IC 348 and Taurus continue to fall parallel to the isochrones. The H-R diagrams of Taurus and IC 348 with this scale are plotted in the next section. The revised temperature scale is tabulated in Table 8 and is illustrated in Figure 8. The temperature conversion is likely to be inaccurate at some level, but

because it falls between the scales for dwarfs and giants, the errors are probably modest. However, regardless of the sizes of the errors and the true temperature scale for young objects, the scale we have described is an appropriate choice for use with the models of BCAH98 and CBAH00 because this combination of scale and models is consistent with the available observational constraints.

For reasons described in previous studies (e.g., Luhman (1999)), I and J are the preferred bands for measuring bolometric luminosities of young objects. The adopted bolometric corrections for spectral types earlier than M9 are described in Luhman (1999). The components of four binaries with separations of 1-3'' (12AB, 42AB, 99AB, 259AB) are better resolved in the optical data. For the eight stars in these systems, the luminosities are computed by combining the bolometric corrections, the dereddened I -band measurements, and a distance modulus of 7.5. For all other objects, we use J instead of I . The extinctions, adopted spectral types, effective temperatures, and bolometric luminosities are listed in Table 2. Additional comments on the estimates of extinctions and luminosities for individual sources are in § A.2.

4.4. H-R Diagram

The effective temperatures and bolometric luminosities for the members of IC 348 can be converted to masses and ages with theoretical evolutionary models. Several sets of models for young, low-mass stars have been published in recent years (Burrows et al. 1997; D’Antona & Mazzitelli 1997; Baraffe et al. 1998; Palla & Stahler 1999; Chabrier et al. 2000; Siess et al. 2000), among which there are large differences in the predicted paths of young objects on the H-R diagram. In § B, we examine various observational tests of the available models at young ages to select the best calculations for interpreting the data in IC 348. In summary, the evolutionary models of Palla & Stahler (1999) are computed for masses of 0.1-6 M_{\odot} and agree well with dynamical mass estimates of young stars at 1-6 M_{\odot} . Meanwhile, the calculations of BCAH98 and CBAH00 consider masses of 0.001-1.4 M_{\odot} and provide the best agreement among available models with observational constraints below a solar mass. Therefore, for the subsequent analysis in this paper, we use the models of Palla & Stahler (1999) for $M/M_{\odot} > 1$ and the models of BCAH98 and CBAH00 for $M/M_{\odot} \leq 1$. Since the mass tracks of Palla & Stahler (1999) and BCAH98 are similar near a solar mass, a continuous mass function can be derived for the full range of masses in IC 348. The low- and high-mass members of IC 348 are plotted with the evolutionary models on the H-R diagrams in Figs. 9 and 10. We differentiate between members that are included and excluded from the sample from which the IMF is generated (§ 4.5.1). In Figure 9, we also show the sources in the IMF sample for Taurus from Luhman et al. (2003a) and the components of the quadruple system GG Tau.

As with previous H-R diagrams of populations in star-forming regions, the sequences for Taurus and IC 348 exhibit finite widths that could correspond to distributions of ages within each region. For IC 348, the data would seem to imply ages ranging from 1 to 10 Myr. However, there are several other potential sources of the observed thickness in a cluster sequence, such as extinction uncertainties, unresolved binaries, variability from accretion and from rotation of spotted surfaces, and differences in distances to individual members in extended regions like Taurus. As a result, it is difficult to confidently measure star formation histories from H-R diagrams of star-forming regions (Kenyon & Hartmann 1990; Hartmann 2001) and it is unclear whether a spread of ages is actually reflected in the data for IC 348.

As long as unresolved binaries are not the dominant component of the width of the cluster sequence, the median of the sequence should be a reflection of the median age of the population, which is a useful characteristic age that can be compared among young populations. In Figure 9, the models indicate median

ages of about 1 and 2 Myr for Taurus and IC 348, respectively. It is unlikely that errors in the distances to these regions are responsible for these apparent age differences since isochrones of 1 and 2 Myr differ by one magnitude in luminosity, which is larger than the uncertainties in the distance moduli. These relative ages for Taurus and IC 348 are consistent with the relative evolutionary stages of disks in these regions (Kenyon & Hartmann 1995; Haisch et al. 2000, 2001).

We briefly describe nine objects in IC 348 that are anomalously faint for their spectral types or colors, and therefore are possibly observed in scattered light. The first object, source 51, falls below the boundary separating candidate members from probable field stars in the diagram of $R - I$ versus I from Luhman (1999). The presence of K -band excess emission and a red, featureless K -band spectrum are indicative of a star with a class I spectral energy distribution (Luhman et al. 1998b). This star also exhibits emission in X-rays and is surrounded by reflection nebulosity in our optical images. Eight sources fall near or below the main sequence on the H-R diagram in Figure 9. Sources 203, 228, 276, 435, 621, 622, and 725 exhibit strong emission in $H\alpha$. Objects 203 and 435 show emission in forbidden lines. These two stars and object 276 also were detected in X-rays by Preibisch & Zinnecker (2001). Source 1434 appears to have strong $H\alpha$ emission and weak Na I absorption, each of which are indicative of youth, but given the low signal to noise of the spectrum, there is a small possibility that this star is a background field dwarf. If this is the case, it must be close to the opposite side of the cluster by its location on the H-R diagram. With the possible exception of 1434, these sources exhibit photometry and signatures of youth that are consistent with young stars occulted by circumstellar structures, resulting in their detection primarily in scattered light.

Finally, the H-R diagram of the most massive members of IC 348 provides constraints on the distance of the cluster. In Figure 10, the presence of cluster members on or near the zero-age main sequence indicates that IC 348 cannot be much closer than the adopted distance modulus of 7.5. The recent analysis of δ Scuti-like pulsations in source 4 by Ripepi et al. (2002) also supports this distance.

4.5. Initial Mass Function

4.5.1. The IC 348 Sample

We now measure the IMF for the $16' \times 14'$ region in IC 348 shown in Figure 1. From the members in this field, we attempt to construct a sample that is an accurate reflection of the cluster population. In particular, the sample must be unbiased in mass so that the resulting IMF is a meaningful representation of the cluster. For the IMF sample, we begin by selecting all members that are in the $16' \times 14'$ field and that have extinctions of $A_V \leq 4$, which is high enough to include a large number of members while low enough that the completeness limit reaches low masses. As demonstrated in § 3.3, the current census of members in this field in IC 348 is unbiased in mass down to $0.03 M_\odot$ for $A_V \leq 4$. The extinctions used in creating the extinction-limited sample are those listed in Table 2. The anomalously faint stars listed in § 4.4 that fall near or below the main sequence in Figure 9 are rejected from the IMF sample because the membership census is not complete for objects of this type (§ 3.3).

There are five sources in Table 2 that lack measurements of extinctions and luminosities. Should any of these objects be included in the IMF sample? The spectra and IR colors of sources 46 and 51 imply extinctions that are higher than the limit defining the IMF sample. The other three stars, 60B, 78B, and 187B, are secondaries that lack measured spectral types. Because 60A and 187A have extinctions that place them in the IMF sample, we include their companions as well. To estimate the masses of 60B and 187B, we assume that the components of each binary have the same reddenings and ages and that the ratios of their

luminosities are equal to the ratios of the fluxes at I and Z for 60B (this work) and at H for 187B (Duchêne et al. 1999). By combining these assumptions with the evolutionary models, we arrive at masses of 0.34 and $0.1 M_{\odot}$ for 60B and 187B.

After applying the above criteria, the IMF sample contains 194 objects. With the exception of 60B and 187B, these sources are indicated in the H-R diagrams in Figs. 9 and 10. The masses for these objects are inferred from the choice of theoretical evolutionary models described in the previous section.

4.5.2. Previous Studies of IC 348

Our measurement of the IMF in IC 348 should be placed in the context of previous work on this cluster. We have derived an IMF for IC 348 by combining the positions of cluster members on the H-R diagram with evolutionary models. The sample includes all known members with $A_V \leq 4$ in a $16' \times 14'$ region of the cluster and is unbiased in mass for $M/M_{\odot} \geq 0.03$. Herbig (1998), Luhman et al. (1998b), and NTC00 also used H-R diagrams and evolutionary models to infer mass functions. Herbig (1998) presented an IMF that contained all probable members in a $14' \times 8'$ field and that reached down to masses of $\sim 0.2 M_{\odot}$. The IMF from Luhman et al. (1998b) for the $5' \times 5'$ center of IC 348 was complete for $M/M_{\odot} \gtrsim 0.1$ and extended to $0.02 M_{\odot}$. Because all of the membership information and other relevant data from Herbig (1998) and Luhman et al. (1998b) are included in our analysis and because of our improved methods of interpreting the data (e.g., choice of evolutionary models), we do not compare our IMF to the results of those studies.

Studies by Muench et al. (2003) and Tej et al. (2002) have arrived at IMFs for IC 348 through analysis of broad-band photometry. Muench et al. (2003) obtained deep IR photometry for the entire cluster and estimated an IMF from the resulting luminosity functions. The IMFs from Muench et al. (2003) and this work are generally consistent with each other. For instance, both IMF measurements exhibit peaks near 0.1 - $0.2 M_{\odot}$. The uncertainties in the IMF of Muench et al. (2003) are largest below the hydrogen burning limit because of the rapidly increasing contamination by background stars at the fainter levels of the IR luminosity functions. Meanwhile, Tej et al. (2002) used optical and IR photometry from the Guide Star Catalog and 2MASS to identify candidate members within a radius of $20'$ from the cluster center. They estimated masses for these candidates by combining K photometry, evolutionary models, and the mean age and extinction for cluster members. We find several problems in the analysis of Tej et al. (2002). First, the assumption of fixed values for extinction and age for the cluster members is overly simplified, as demonstrated by the scatter in the sequence for IC 348 on the H-R diagram and the range of extinctions that we derive. Second, to correct for field star contamination in their sample of candidate cluster members, they subtracted data from off-cluster control fields. However, to properly correct for field stars in this way, one must estimate the distribution of extinctions toward background stars in the cluster field, apply extinction to the data from the control field to duplicate that reddening distribution, and then perform the subtraction. Tej et al. (2002) did not apply an extinction model to their control field, which is especially necessary when optical data are involved. Finally, their IMF sample, like that of NTC00 later in this section, is susceptible to a bias against low-mass sources because it includes all candidate members rather than only those within an extinction threshold.

In the empirical H-R diagram constructed from the narrowband steam measurements, NTC00 assumed that objects appearing near the cluster sequence were members. From these sources, they derived an IMF that was reported to be complete to the deuterium burning limit ($K \sim 16.5$ for $A_V = 3$, 0.013 - $0.015 M_{\odot}$; Burrows et al. (1997)). How do our findings in § 3.4 regarding the membership and spectral types of the

NICMOS sources affect the IMF reported by NTC00? At $K > 14$, photometric uncertainties in the NICMOS narrow-band photometry translated into very large errors in the estimated spectral types. Consequently, several field stars were mistaken for objects with spectral types of late M. In addition, because the spectral types from the steam data were systematically too late by 1-2 subclasses, the masses were underestimated. An offset of one subclass in the substellar regime corresponds to a change of a factor of ~ 2 in the inferred mass. These two effects both resulted in an overestimate of the number of brown dwarfs by NTC00. In Figure 7, 28 sources have NICMOS classifications later than M6, when only 9 of these sources actually have optical spectral types in that range. NTC00 concluded that their spectral types were accurate down to $K = 16.5$, or the brightness of objects at the deuterium burning mass limit for the average age and extinction of cluster members (3 Myr, $A_V = 3$). This mass was thus quoted as the completeness limit of their IMF for the NICMOS fields in IC 348. However, if an IMF sample includes all probable members, as in NTC00, then the mass completeness limit is the lowest mass at which the sample is complete to the *maximum* age and extinction. To be representative of the population down to the deuterium burning limit, an IMF from the data of NTC00 would need to contain only sources with ages and reddenings below the mean values. In addition, it is not clear that their spectral classifications are sufficiently accurate down to $K = 16.5$ for mass estimates and for the measurement of an IMF; the average uncertainties for the spectral types reported by NTC00 are ± 3.5 subclasses for types later than M2 with $K = 14.5$ to 16.5 . Indeed, in § 3.4 we showed that at least two objects at $K < 16.5$ with NICMOS classifications later than M6 are field stars. Also, because of the large uncertainties in both their spectral types and dereddened K magnitudes, the cluster sequence overlaps with the field star population (Figure 6). Without a clear separation of the two populations or other membership information, the low-mass members cannot be reliably identified and added into the IMF. Given these various issues, the IMF from NTC00 is probably not accurate in the substellar regime or complete to the deuterium burning mass limit.

4.5.3. Comparison of IMFs in Different Environments

By using methods similar to those in this study, Luhman (2000), Briceño et al. (2002), and Luhman et al. (2003a) surveyed 8.4 deg^2 in the Taurus star-forming region and arrived at a census of members that is complete for $M/M_\odot \geq 0.02$ and $A_V \leq 4$. Luhman et al. (2003a) presented an IMF from the 92 Taurus members within this extinction threshold and in the survey fields. We now compare that IMF sample for Taurus to the one that we have defined for IC 348. Because of the vertical nature of the mass tracks for low-mass stars on the H-R diagram, the spectral types of young objects should be well-correlated with their masses. Very little evolution in temperature is expected between the ages of Taurus and IC 348 (1 and 2 Myr), implying virtually identical relations between spectral types and masses for these two populations. In addition, a spectral type is a simple, observable quantity that can be measured to good accuracy with relative ease, particularly at M types. Therefore, we use the distributions of spectral types for IC 348 and Taurus as IMF proxies that can be compared in a straightforward, reliable fashion without the involvement of evolutionary models. The IMF samples for IC 348 and Taurus are unbiased in mass down to 0.03 and $0.02 M_\odot$, respectively, which correspond to types of \sim M8 and M9 for young ages. One and two sources in the IMFs for Taurus and IC 348, respectively, lack measured spectral types. After omitting these three stars, the numbers of objects as a function of spectral type in the IMF samples for IC 348 and Taurus are plotted in Figure 11. The distribution for IC 348 reaches a maximum at M5, while primary and secondary peaks appear at K7 and M5 in Taurus. Spectral types of M5 and K7 correspond to masses near 0.15 and $0.8 M_\odot$ for ages of a few million years by the models of BCAH98. The spectral type distributions for IC 348 and Taurus provide clear, unambiguous evidence for a significant variation of the IMF with star-forming

conditions. Previous studies have noted that a difference of this kind might be present between Taurus and clusters like Orion (e.g., Hillenbrand (1997)). However, most previous samples of members of star-forming regions have been derived by combining disparate surveys that utilized biased selection techniques (e.g., $H\alpha$, IR excess). It was unclear whether the predominance of K7 and M0 stars in Taurus was an accurate reflection of the region or simply a result of incompleteness at later types. But because of the new magnitude-limited membership surveys in IC 348 and Taurus, we have been able to make the first comparison of spectral type distributions in which the samples are complete down to late spectral types and contain relatively large numbers of members.

When the data for the samples in IC 348 and Taurus are transformed to individual masses with evolutionary models (§ 4.5.1; Briceño et al. (2002); Luhman et al. (2003a)), the IMFs in Figure 12 are produced. Because the same techniques and evolutionary models were employed in converting from data to masses for each population, we can be confident in the validity of any differences we find in the IMFs for IC 348 and Taurus. The IMF for Taurus peaks near $0.8 M_{\odot}$ and steadily declines to lower masses. While two peaks are present in the distribution of spectral types for Taurus, only one is found at a significant level in the IMF. Apparently, the bimodal appearance of the spectral type distribution is simply the product of stellar evolution convolved with the particular form of single-peaked IMF found in Taurus. Meanwhile, the mass function for IC 348 rises from high masses down to a solar mass in a roughly Salpeter fashion, rises more slowly down to a maximum at $0.1\text{-}0.2 M_{\odot}$, and then declines into the substellar regime. We have quantified the significance of the differences in the distributions of spectral types and masses for IC 348 and Taurus by performing a two-sided Kolmogorov-Smirnov test between the distributions for spectral types of $\leq M8$ and for masses of $M/M_{\odot} \geq 0.03$. In terms of both spectral types and masses, the probability that the samples for IC 348 and Taurus are drawn from the same distribution is $\sim 0.01\%$.

It is unlikely that the IMFs of single objects – both isolated sources and individual components of multiple systems – in IC 348 and Taurus are the same and these observed differences are simply the result of dynamical effects, such as more frequent stripping of low-mass companions in the denser environment of IC 348. Companions at separations greater than $1''$ and $2''$ in IC 348 and Taurus, respectively, were included in both IMFs. As a result, the disruption of wide binaries should have no effect on our results as long as the components remain within the cluster, which is likely for these loosely bound systems. In order for the spectral type distributions for all objects earlier than M9 to be the same in Taurus and IC 348, enormous numbers of M stars would need to be hidden as close companions in Taurus (~ 10 per primary). In addition, if the Taurus IMF is computed for only the most compact aggregate, L1495E, which has a stellar density only five times lower than that of IC 348, than the IMF variations between these two regions persist. Finally, out of the various types of stellar populations in which mass functions are measured, star-forming clusters with low to moderate stellar densities like Taurus and IC 348 are the least likely sites to be affected significantly by dynamical evolution. For instance, in IC 348, the crossing time of a star moving at the escape velocity ($\sim 0.8 \text{ km s}^{-1}$, Herbig (1998)) is comparable to the age of the cluster (2 Myr). When the members of IC 348 were younger and less evolved, they likely had even lower velocities than they do now, as indicated by the protostellar clumps in this cluster (Bachiller, Guilloteau, & Kahane 1987).

The shapes of the IMFs derived for Taurus and IC 348 are sensitive to the adopted temperature scale and evolutionary models. The combination used here was designed to produce the best agreement with the various observational constraints (§ B). In particular, the IMFs above $\sim 0.5 M_{\odot}$ should be fairly accurate since our choices of temperature scale and models implies masses from the H-R diagram that are consistent with the dynamical mass estimates of young stars. However, because fewer constraints are available at low masses, the IMFs below $\sim 0.5 M_{\odot}$ could be subject to systematic errors.

Even with the extensive spectroscopic work that has been done in Orion, one can define a well-populated sample of members that is complete down to only mid-M types in that region. To extend the IMF in Orion to lower masses, studies have relied on luminosity function modeling (Hillenbrand & Carpenter 2000; Luhman et al. 2000; Muench et al. 2002). As a result, a comparison of the IMFs in Taurus and IC 348 to that in Orion is less definitive than the comparison between the first two regions. We consider the IMF reported by Luhman et al. (2000) for the Trapezium Cluster, which was derived with similar methods to the ones used for Taurus and IC 348. The IMF from Luhman et al. (2000) peaks near $0.6 M_{\odot}$ and is roughly flat to lower masses, and thus differs somewhat from the IMF for IC 348 in Figure 12. It is unclear whether this difference is real or is the result of a shortcoming in the merging of the spectroscopic data and the luminosity function modeling for the Trapezium. Meanwhile, the IMFs for IC 348 and the Trapezium derived from luminosity function modeling are similar (Muench et al. 2003), but do allow for subtle variations of this type. To reliably compare these IMFs at this level of detail, the completeness limit of the spectroscopic work in the Trapezium must be extended to later spectral types.

The data for the Trapezium and other young clusters are more amenable to a comparison of the global properties of the IMFs. We define ratios to quantify the relative numbers of brown dwarfs and stars and the relative numbers of low-mass and high-mass stars:

$$\mathcal{R}_1 = N(0.02 \leq M/M_{\odot} \leq 0.08)/N(0.08 < M/M_{\odot} \leq 10)$$

$$\mathcal{R}_2 = N(1 < M/M_{\odot} \leq 10)/N(0.15 < M/M_{\odot} \leq 1)$$

In Table 9, we compare these ratios for IMFs in IC 348 (this work), Taurus (Briceño et al. 2002; Luhman et al. 2003a), and the Trapezium (Luhman et al. 2000) and in the open clusters of the Pleiades (Bouvier et al. 1998) and M35 (Barrado y Navascués et al. 2001). The values for the latter three clusters were compiled by Briceño et al. (2002). For Taurus, we update the ratios in Briceño et al. (2002) by adding the new members from Luhman et al. (2003a), producing $\mathcal{R}_1 = 11/80 = 0.14 \pm 0.04$ and $\mathcal{R}_2 = 5/61 = 0.08 \pm 0.04$. From the IMF for IC 348, we have $\mathcal{R}_1 = 21/169 = 0.12 \pm 0.03$ and $\mathcal{R}_2 = 18/99 = 0.18 \pm 0.04$. The former quantity could be slightly underestimated since the IC 348 sample may be incomplete at $0.02\text{-}0.03 M_{\odot}$ (§ 3.3). Note that this measurement of \mathcal{R}_1 is consistent with the value implied by the luminosity function modeling of Muench et al. (2003). As shown in Table 9, the relative numbers of high- and low-mass stars in IC 348 are similar to those found in the Trapezium and in the open clusters, while the frequency of brown dwarfs appears to be lower in IC 348 than in the Trapezium and near the value for Taurus. The IMF measured for the Ophiuchus star-forming cluster, which is comparable to IC 348 in stellar density ($n = 100\text{-}1000 \text{ pc}^{-3}$), is consistent with that of IC 348 (Luhman & Rieke 1999; Luhman et al. 2000). However, because the number statistics are relatively poor in the data for Ophiuchus, we do not include it in Table 9.

The implications of the variations in the IMF among Taurus, the Trapezium, and the open clusters for models of the IMF were discussed by Briceño et al. (2002). They suggested that the lower frequency of brown dwarfs in Taurus relative to the Trapezium could reflect differences in the typical Jeans masses of the two regions. This scenario continues to be plausible when the data for IC 348 are included. IC 348 contains a much higher frequency of low-mass stars ($0.1\text{-}0.2 M_{\odot}$) than Taurus, but a comparable fraction of brown dwarfs, which would imply an average Jeans mass for IC 348 that is intermediate between those of Taurus and the Trapezium. The observed IMF variations between Taurus and IC348 might also be explained through the recent model of turbulent fragmentation by Padoan & Nordlund (2002). In those calculations, the IMF peaks at a higher mass for lower values of the gas density and the Mach number. Indeed, Taurus exhibits a higher

peak mass than IC 348 and is less dense and more quiescent than most star-forming regions. Meanwhile, these variations would seem difficult to explain with models in which the shape of the IMF is determined by the competition between accretion and outflows (Adams & Fatuzzo 1996). The significant variation that we find in the IMF, which is particularly well-established between Taurus and IC 348, comprises a new and important test for any model of the IMF.

4.6. X-ray Properties

The X-ray properties of young stars in IC 348 have been described by Preibisch et al. (1996), Preibisch & Zinnecker (2001), and Preibisch & Zinnecker (2002). We update the results of those studies with the data from our survey for new members.

The deepest X-ray observations of IC 348 to date were conducted by Preibisch & Zinnecker (2001) with the *Chandra X-ray Observatory*. In a $17' \times 17'$ field toward the cluster, they detected 219 sources, which included 119 previously known members and 58 potential new members. Among the 283 known members of IC 348 that have measured spectral types, 154 members are detected in X-rays. The fraction of members with observed X-ray emission as a function of spectral type is illustrated by the distributions of spectral types in Figure 13. Source 51, which lacks a spectral type measurement and is a probable class I object, is an X-ray source as well. We now examine the nature of the remaining 64 X-ray detections. Most of the 39 X-ray sources that lack counterparts in available optical and IR data are probably in the background of IC 348 and unrelated to the cluster (Preibisch & Zinnecker 2001). One X-ray source, object 77, is identified as a field star through proper motions measurements (§ 3.2.2). Ten objects are candidate members, one of which is within the $16' \times 14'$ field in Figure 1 and thus appears in Figure 2. The 12 X-ray sources that are below the boundary are probably in the foreground or background of the cluster. It is possible that a few of these sources could be cluster members observed in scattered light, which would make them appear subluminescent on a color-magnitude diagram, but none of these objects show any other evidence of youth or membership. Finally, two X-ray sources are detected only in IR data. Preibisch & Zinnecker (2001) identified one of these sources, 2MASS 03444330+3201315, as a possible class I object by its strong *K*-band excess emission and high extinction. At the position of this object in our *I* and *Z* images, we detect reflection nebulosity extended across $15''$ and no point source. The IR counterpart to the second X-ray source is 2MASS 03441977+3159190, which has been detected only at *K_s*. Our optical images show faint nebulosity in the vicinity of this object's position. If 2MASS 03441977+3159190 is a member of IC 348, it must be highly embedded, probably at the class I stage. Both 2MASS 03444330+3201315 and 2MASS 03441977+3159190 are in the southern part of IC 348 where the cluster merges into the Perseus molecular cloud and where the most embedded and least evolved known members of the cluster reside, such as sources 51 and 13 (IC 348-IR) and a likely class 0 object (McCaughrean et al. 1994).

Preibisch & Zinnecker (2001) referred to several objects in IC 348 as brown dwarfs or brown dwarf candidates because of the late spectral types implied by the steam measurements of NTC00. However, most of these sources have optical spectral types that are earlier than M6 and therefore are probably low-mass stars rather than brown dwarfs (§ 3.4). There are three known members of IC 348 (329, 355, 613) that are likely brown dwarfs ($>M6$) and that have been detected in X-rays.

5. Conclusions

The results of our new census of young stars and brown dwarfs in the IC 348 star-forming cluster are summarized as follows:

We have obtained deep images at I and Z for a $42' \times 28'$ field encompassing the IC 348 cluster. By combining these data with optical and IR photometry from previous surveys, we have constructed extinction-corrected color-magnitude diagrams and used them to select candidate members. Through spectroscopy of these candidates, we have identified 122 new members, 15 of which have spectral types of M6.5-M9, corresponding to masses of ~ 0.08 - $0.015 M_{\odot}$ by the evolutionary models of BCAH98 and CBAH00. After examining the membership status of all objects toward IC 348 that have been observed spectroscopically in this work and in previous studies, we have arrived at a list of 288 known members of IC 348, 23 of which are later than M6 and thus are likely to be brown dwarfs. We find a lower proportion of such late-type members than in the study of NTC00 because of a systematic calibration error in the translation of their photometric data to spectral types, and their identification of a number of faint background stars as low-mass cluster members.

We have estimated extinctions, luminosities, and effective temperatures for the known members of IC 348 and have placed these sources on the H-R diagram. To select the best calculations with which to interpret these data, we have compiled observational constraints from previous studies (White et al. 1999; Simon et al. 2000) and from this work on IC 348 and have applied them to the available evolutionary models. These tests tend to support the validity of the models of Palla & Stahler (1999) at $M/M_{\odot} \gtrsim 1$ and the models of BCAH98 and CBAH00 at $M/M_{\odot} \lesssim 1$. We have combined these models with the H-R diagram for IC 348 to infer masses for individual members of the cluster. For a $16' \times 14'$ field centered on IC 348, we have defined an extinction-limited sample of known members ($A_V \leq 4$) that is unbiased in mass and nearly 100% complete for $M/M_{\odot} \geq 0.03$ ($\lesssim M8$). In logarithmic units where the Salpeter slope is 1.35, the IMF for this sample in IC 348 rises from high masses down to a solar mass, rises more slowly down to a maximum at 0.1-0.2 M_{\odot} , and then declines into the substellar regime. In comparison, the similarly-derived IMF for Taurus from Luhman et al. (2003a) rises quickly to a peak near 0.8 M_{\odot} and steadily declines to lower masses. The distinctive shapes of the IMFs in IC 348 and Taurus are reflected in the distributions of spectral types, which peak at M5 and K7, respectively. This is the first comparison of spectral type distributions between two star-forming populations that is based on samples that are complete to late spectral types and that include relatively large numbers of members, and it represents clear, model-independent evidence for a significant variation of the IMF with star-forming conditions.

We thank Perry Berlind and Mike Calkins for performing the FAST observations and Jean-Charles Cuillandre for reducing the CFH12K images. We are grateful to Isabelle Baraffe and Francesco Palla for access to their most recent calculations and to Lee Hartmann for comments on the manuscript. K. L. was supported by grant NAG5-11627 from the NASA Longterm Space Astrophysics program. The JHK data from Muench et al. (2003) were obtained with FLAMINGOS under the NOAO Survey Program “Towards a Complete Near-Infrared Imaging and Spectroscopic Survey of Giant Molecular Clouds” (PI: E. Lada) and supported by NSF grants AST97-3367 and AST02-02976 to the University of Florida. FLAMINGOS was designed and constructed by the IR instrumentation group (PI: R. Elston) at the Department of Astronomy at the University of Florida with support from NSF grant AST97-31180 and Kitt Peak National Observatory. This research has made use of the NASA/IPAC Infrared Science Archive, which is operated by the Jet Propulsion Laboratory, California Institute of Technology, under contract with the National Aeronautics and Space Administration. Some of the data presented herein were obtained at the MMT Observatory,

a joint facility of the Smithsonian Institution and the University of Arizona. Data were also obtained at the W. M. Keck Observatory, which is operated as a scientific partnership among the California Institute of Technology, the University of California, and the National Aeronautics and Space Administration. The Observatory was made possible by the generous financial support of the W. M. Keck Foundation. We wish to extend special thanks to those of Hawaiian ancestry on whose sacred mountain we are privileged to be guests. Without their generous hospitality, some of the observations presented herein would not have been possible.

A. Comments on Individual Sources

A.1. Spectral Types and Membership

As explained in § 3.2.1, our optical spectra do not differentiate well between giants, dwarfs, and pre-main-sequence objects at G and early K types. We have used IR spectra to break this degeneracy in the classifications of several objects in our sample. For another of these stars, source 44, we measured an equivalent width of $0.35 \pm 0.05 \text{ \AA}$ for Li at 6707 \AA . Because $\sim 99\%$ of field giant exhibit Li strengths below 0.1 \AA (Brown et al. 1989), this star is unlikely to be a background giant. Meanwhile, it cannot be a foreground dwarf given the significant reddening in its colors and spectrum. Therefore, we take object 44 to be a cluster member. Five of the remaining sources with ambiguous optical classifications (20, 22, 47, 53, 79) were detected in the X-ray observations of Preibisch & Zinnecker (2001). By their reddened colors, these stars must be either members of IC 348 or background giants rather than foreground stars. All of these stars have $L_X/L_{\text{bol}} > 10^{-4}$, whereas most G and K giants have $L_X/L_{\text{bol}} < 10^{-7}$ and only a few have been observed with ratios as high as 10^{-4} (Hüensch et al. 1996). Therefore, these five stars are probably members of the cluster.

One of the stars with ambiguous optical types, source 81, lacks Li and IR spectroscopic measurements and is not detected in X-rays. The membership status is uncertain for this star and for two other stars in Table 5. Source 197 is highly reddened and falls between the 30 Myr isochrone and the main sequence when placed on the H-R diagram for the distance of IC 348. This star could be a member of IC 348, possibly observed in scattered light, or a field dwarf that is near the opposite side of the cluster. Because source 1927 exhibits little or no extinction in its spectrum and colors and shows no other evidence of youth, it could be either a cluster member or a foreground M dwarf.

In a spectrum with low signal-to-noise, source 1476 appears to have strong emission in $H\alpha$ and strong absorption in Na I, which are suggestive of a young star and a field dwarf, respectively. Given its position below the main sequence on the H-R diagram for the distance of IC 348, this star is probably a background dwarf. For star 404, the presence of dwarf-like Na I absorption and the lack of reddening or evidence of youth are indicative of a foreground field dwarf. Because the spectrum of object 906 is matched better with an average of a dwarf and a giant than with a dwarf, we take it to be young and thus a cluster member. However, the low signal-to-noise of the data for this source precludes a reliable measurement of the gravity-sensitive Na I and K I features. In addition, this source lacks significant extinction or emission lines. As a result, there is a small possibility that this source is a foreground dwarf.

A.2. Luminosities

The most massive members of IC 348 are the components of the B5 binary system BD+31°643 (source 1 in Table 2), which have $\Delta K = 0.16$ and a separation of $0''.6$ (Kalas & Jewitt 1997). We computed a luminosity from the unresolved photometry of the system and divided the result by two for Table 2 and Figure 10. When estimating the luminosities for 60A, 78A, and 187A from the J -band photometry (§ 4.3), we corrected for the contribution of the secondaries by assuming that ΔJ was equal to $\Delta I, Z = 1.1$ (this work), $\Delta K = 2.65$ (NTC00), and $\Delta H = 0.99$ (Duchêne et al. 1999), respectively. For sources 12A, 12B, 42A, 42B, 99A, and 99B, we measured the luminosities from our resolved I -band photometry.

B. Evolutionary Models

B.1. Previous Tests

To evaluate the validity of the available evolutionary models at young ages, we first review the previous observational tests that have been applied to them.

The potential coevality of components of young multiple systems can be used as a test of evolutionary models (Hartigan et al. 1994; Prato 1998). White et al. (1999) obtained accurate, resolved photometry and spectroscopy for the members of the young quadruple system GG Tau, which span spectral types from K7 to M7.5. They placed these sources on the H-R diagram for dwarf and giant temperature scales and compared the resulting empirical isochrone to isochrones from various sets of models. The components of GG Tau were coeval when the models of BCAH98 with $l_{mix}/H_p = 1.0$ and 1.9 at $M/M_\odot \leq 0.6$ and $M/M_\odot > 0.6$ were combined with a temperature scale between those of dwarfs and giants. White et al. (1999) also found that these models provided the best agreement with the stellar masses estimated from the rotation of circumstellar disks around GG Tau Aa+Ab (Guilloteau et al. 1999), GM Aur (Dutrey et al. 1998), and DM Tau (Guilloteau & Dutrey 1998). Luhman (1999) updated the analysis of White et al. (1999) with revised spectral types and presented a temperature scale that produced coevality for GG Tau with the models BCAH98. The models were also tested with the empirical isochrone defined by the sequence of known members of IC 348, the stellar parameters of the eclipsing double-lined spectroscopic binaries CM Dra and YY Gem, and the positions on the H-R diagram of brown dwarfs in the Pleiades. Both White et al. (1999) and Luhman (1999) concluded that the models of BCAH98 with $l_{mix}/H_p = 1.9$ at $M/M_\odot > 0.6$ agreed most closely with the various observational constraints.

Molecular line images of disks around several young stars have been obtained by Guilloteau et al. (1999), Dutrey et al. (1998), Guilloteau & Dutrey (1998), and Simon et al. (2000). From the disk rotation measured in these data, dynamical masses were estimated for a total of nine young systems. Simon et al. (2000) placed these stars on the H-R diagram and compared the masses implied by evolutionary models to those derived from the dynamical measurements. They found that the models of BCAH98, Palla & Stahler (1999), and Siess et al. (2000) were in reasonable agreement with the observations, while the calculations of D’Antona & Mazzitelli (1997) were less consistent with the data.

Dynamical mass estimates from Simon et al. (2000) and from eclipsing binaries were used by Palla & Stahler (2001) to test the models from Palla & Stahler (1999). They considered the main sequence binaries EW Ori ($1.2 M_\odot$), HS Aur ($0.9 M_\odot$), and YY Gem ($0.6 M_\odot$) and found agreement between the masses implied by their models and the dynamical masses for first two systems but not the latter. Their comparison of the data and model predictions for YY Gem has been superseded by the thorough study of Torres &

Ribas (2002), who concluded that all available models implied physical parameters that differed significantly from the observed values. Palla & Stahler (2001) also examined young binaries, finding that the model predictions of Palla & Stahler (1999) agreed with the masses and mass ratios measured for four eclipsing and three non-eclipsing young double-lined spectroscopic binaries at 1-6 M_{\odot} . Finally, the masses inferred from their models were within 8% of the masses derived from disk rotation (Simon et al. 2000), with the exception of BP Tau and UZ Tau E, whose dynamical masses have large uncertainties.

An additional pre-main-sequence eclipsing binary, RXJ0529.4+0041, has been discovered by Covino et al. (2000). The components of this system have masses of 1.25 ± 0.05 and $0.91 \pm 0.05 M_{\odot}$ and spectral types of K1-K2 and K7-M0. When Covino et al. (2000) placed these stars on the H-R diagram, no set of models perfectly reproduced the dynamical mass estimates. The calculations of BCAH98 provided the best agreement. D’Antona et al. (2000) have found that the inclusion of magnetic fields in their models produces solar-mass tracks that are cooler and thus more closely match the data for RXJ0529.4+0041.

Steffen et al. (2001) have measured masses for the components of the pre-main-sequence binary NTT045251+3016 by combining radial velocity measurements and astrometry. For the models of BCAH98, a mixing length of $l_{mix}/H_p = 1.0$ produced the closest agreement between the masses implied by the tracks on the H-R diagram and the dynamical masses of 1.45 ± 0.19 and $0.81 \pm 0.09 M_{\odot}$. In contrast, the models with $l_{mix}/H_p = 1.9$ better fit most other observations (White et al. 1999; Simon et al. 2000). We note that Steffen et al. (2001) used $V - H$ in their H-R diagram for NTT045251+3016 rather than effective temperature, which is probably not advisable given the shortcomings of the theoretical colors and magnitudes near V for cool stars (e.g., Delfosse et al. (2000)).

B.2. Updated Tests of BCAH98 and CBAH00

The previous tests of the evolutionary models generally favor the calculations of BCAH98, particularly below a solar mass. In this section, the best available constraints at young ages are compiled from previous studies and from this work on IC 348 and are applied to these models in a consistent fashion.

In this discussion, we consider the models of BCAH98 with $l_{mix}/H_p = 1.0$ and 1.9 for $0.1 < M/M_{\odot} \leq 0.6$ and $0.6 < M/M_{\odot} \leq 1.4$ and the models of CBAH00 with $l_{mix}/H_p = 1.0$ for $0.001 \leq M/M_{\odot} \leq 0.1$. The calculations of BCAH98 and CBAH00 exclude and include dust, respectively, and produce similar mass tracks and isochrones for the effective temperatures of 2000-3000 K where they overlap (Baraffe et al. 2002). BCAH98 found that a convection mixing length of 1.9 was required to reproduce data for the Sun. Most of the observational constraints for young stars from the previous section were best matched with this mixing length as well. For masses below $0.6 M_{\odot}$, BCAH98 computed models only for $l_{mix}/H_p = 1.0$ because the results were not sensitive to the choice of mixing length for low masses and older ages. However, in a recent analysis of the uncertainties in their model predictions, Baraffe et al. (2002) derived tracks at low masses that changed significantly with mixing length for $\log g \lesssim 4$. For instance, at an age of 1 Myr and masses of 0.01-0.2 M_{\odot} , the mass tracks for $l_{mix}/H_p = 2.0$ were 100-200 K warmer than those with $l_{mix}/H_p = 1.0$. Baraffe et al. (2002) computed only a restricted grid of models at $l_{mix}/H_p = 2.0$ to demonstrate the effect of changes in the mixing length. Thus, low-mass models covering the full range of masses and ages are available only for $l_{mix}/H_p = 1.0$ at this time. Compared to the convection mixing length, changes in the initial radius and the initial deuterium abundance have less effect on the mass tracks and isochrones at ages of $\gtrsim 1$ Myr (Baraffe et al. 2002).

For testing the models of BCAH98 and CBAH00, we consider all pre-main-sequence stars that have

reasonably accurate dynamical mass estimates and are below $1.5 M_{\odot}$, which include five components of three spectroscopic binaries (RXJ0529.4+0041 A and B, NTT045251+3016 A and B, EK Cep B) and five systems from Simon et al. (2000) (DL Tau, DM Tau, LkCa 15, GM Aur, GG Tau Aa+Ab). We omit the double-lined spectroscopic binaries for which mass ratios alone are available (Covino et al. 2001; Prato et al. 2002). We compile luminosities and temperatures for this sample of stars in the manner described in § C. These measurements and the models of BCAH98 and CBAH00 are plotted on the H-R diagram in Figure 14. Before testing the masses inferred from the models with the dynamical masses, we first compare the latter measurements to each other. The relative positions of most of the stars in Figure 14 are consistent with their relative dynamical masses. The clear exceptions are the components of NTT045251+3016, which have dynamical masses that are anomalously high for their positions in the H-R diagram relative to the other stars. This discrepancy is reflected in the conclusion by Steffen et al. (2001) that the data for NTT045251+3016 were best fit by the BCAH98 models with $l_{mix}/H_p = 1.0$, whereas the studies of the other stars with dynamical masses favored $l_{mix}/H_p = 1.9$. If we exclude NTT045251+3016, then the models of BCAH98 and CBAH00 are in fairly good agreement with the data. For most of the stars, the masses implied by the models and the dynamical masses agree within the uncertainties. An exception is the primary of RXJ0529.4+0041, which has dynamical and model masses of 1.25 ± 0.05 and $\gtrsim 1.4 M_{\odot}$, respectively. The data for RXJ0529.4+0041 A and the other star above a solar mass in Figure 14, EK Cep B, are better matched by the models of Palla & Stahler (1999).

As described in the previous section, White et al. (1999) and Luhman (1999) tested evolutionary models by posing the following question: For a given set of models, is there a reasonable temperature scale that will make an empirical isochrone parallel to the model isochrones? The models of BCAH98 passed this test for the empirical isochrones defined by the GG Tau quadruple system and the IC 348 cluster. The limit in spectral type of this test was M7.5 because this was the latest type present in GG Tau and because the list of known members of IC 348 in Luhman (1999) was well-populated down to only M6. We have extended this test to M9 by using the new samples of low-mass members of Taurus and IC 348 from Briceño et al. (2002), Luhman et al. (2003a), and this work. In § 4.3, we were able to adjust the temperature scale from Luhman (1999) at M8 and M9 so that the sequences for Taurus and IC 348 are roughly parallel to the model isochrones for the full range of observed spectral types. This is illustrated in Figure 9, where we plot H-R diagrams for the extinction-limited samples that define the IMFs computed for Taurus (Briceño et al. 2002; Luhman et al. 2003a) and IC 348 (§ 4.5.1).

Overall, the best available observational constraints for the masses and ages of young stars below a solar mass tend to support the validity of the models of BCAH98 and CBAH00. The data favor the models with a convection mixing length of $l_{mix}/H_p = 1.9$. However, this choice of mixing length is not available for models at $M/M_{\odot} < 0.6$. As a result, the models at low masses, which use $l_{mix}/H_p = 1.0$, may be less accurate than at higher masses. We cannot test the accuracy of the low-mass tracks since dynamical masses have not been measured in this range. Any errors in the low-mass models should be at least partially compensated by our use of a temperature scale that is designed to produce populations that are parallel to the model isochrones. For instance, it is possible that the true temperature scale for young objects is that of dwarfs, and the deviation of our conversion from the dwarf scale (Figure 8) is a reflection of an error in the models (e.g., use of $l_{mix}/H_p = 1.0$). Further tests of the models at young ages and low masses will require the measurement of dynamical masses and the modeling of both additional mixing lengths and a birthline for brown dwarfs (e.g., Stahler (1983)).

C. Data for Stars with Dynamical Mass Estimates

We describe the derivation of the effective temperatures and luminosities that are used in placing RXJ0529.4+0041 A and B, NTT045251+3016 A and B, EK Cep B, DL Tau, DM Tau, LkCa 15, GM Aur, and GG Tau Aa+Ab on the H-R diagram in Figure 14. Spectral types are converted to temperatures with the scale in § 4.3. For the two components of RXJ0529.4+0041, we adopt spectral types of K1-K2 and K7-M0 and luminosities of 1.75 ± 0.15 and $0.35 \pm 0.15 L_{\odot}$ from Covino et al. (2000). Those authors identified a possible third component of the system and placed it on the H-R diagram, but did not provide photometry or a luminosity estimate for it. The uncertainties listed by Covino et al. (2000) for the primary’s luminosity are much smaller than the values plotted on their H-R diagram. The mistake is probably in $\sigma_L = \pm 0.15 L_{\odot}$ since the quoted measurement errors for the radius alone ($1.7 \pm 0.2 R_{\odot}$) would correspond to $\sigma_L = \pm 0.4 L_{\odot}$. We adopt the latter value for the uncertainty in the luminosity. For the primary of NTT045251+3016, we use the spectral type of K5 from Steffen et al. (2001) and adopt an uncertainty of ± 1 subclass. From the intrinsic color of $V - H = 4.04 \pm 0.33$ estimated for the secondary by Steffen et al. (2001), we infer a spectral type of M2.5 ± 1 . Those authors listed uncertainties in $\log L$ of ± 0.053 and ± 0.086 , which appear to be unrealistically small given that the distance uncertainties alone correspond to ± 0.048 in $\log L$. In addition, Walter et al. (1988) reports $H = 8.46$ for the system while 2MASS measures $H = 8.32$. Therefore, we adopt uncertainties of ± 0.1 and ± 0.15 in $\log L$ for the primary and secondary. We take $A_V = 0.15 \pm 0.09$ and $d = 145 \pm 8$ pc from Steffen et al. (2001). Using their H -band brightness ratio of 0.4 ± 0.1 and a total system magnitude of $H = 8.32$ from 2MASS, we calculate $H = 8.69$ and 9.68 for the individual components. Luminosities are derived by combining these H -band magnitudes with the distance and the appropriate bolometric corrections (§ 4.3). For the secondary in the spectroscopic binary EK Cep, we adopt $\log L = 0.19 \pm 0.07$ and $\log T_{\text{eff}} = 3.755 \pm 0.015$ from Popper (1987). Temperatures and luminosities for DL Tau, DM Tau, LkCa 15, and GM Aur are computed with the prescription described by Briceño et al. (2002) for members of Taurus. We use the same distance of 140 pc that was adopted in the dynamical mass estimates by Simon et al. (2000). We note that Kenyon & Hartmann (1995) mistakenly listed $R - I = 1.53$ for GM Aur instead of the correct value of $R - I = 0.72$ (1.53 is the measurement of $V - I$). Uncertainties of ± 1 subclass and ± 0.1 are adopted for the spectral types and for $\log L$, respectively. For GG Tau Aa and Ab, we adopt extinctions, spectral types, luminosity uncertainties, and photometry from White et al. (1999) and compute luminosities by combining the J -band photometry with the extinctions, bolometric corrections, and a distance of 140 pc.

REFERENCES

- Adams, F. C., & Fatuzzo, M. 1996, *ApJ*, 464, 256
- Allard, F., Hauschildt, P. H., Alexander, D. R., Tamanai, A., & Schweitzer, A. 2001, *ApJ*, 556, 357
- Allen, L. E., & Strom, K. M. 1995, *AJ*, 109, 1379
- Bachiller, R., Guilloteau, S., & Kahane, C. 1987, *A&A*, 173, 324
- Baraffe, I., Chabrier, G., Allard, F., & Hauschildt, P. H. 1998, *A&A*, 337, 403 (BCAH98)
- Baraffe, I., Chabrier, G., Allard, F., & Hauschildt, P. H. 2002, *A&A*, 382, 563
- Barrado y Navascués, D., Stauffer, J. R., Briceño, C., Patten, B., Hambly, N. & Adams, J. 2001, *ApJS*, 134, 103
- Bessell, M. S., & Brett, J. M. 1988, *PASP*, 100, 1134
- Blaauw, A. 1952, *B. A. N.*, 11, 412
- Bouvier, J., Stauffer, J. R., Martín, E. L., Barrado y Navascués, D., Wallace, B., & Bejar, V. J. S. 1998, *A&A*, 336, 490
- Briceño, C., Luhman, K. L., Hartmann, L., Stauffer, J. R., & Kirkpatrick, J. D. 2002, *ApJ*, 580, 317
- Brown, J. A., Sneden, C., Lambert, D. L., & Dutchover, E. 1989, *ApJS*, 71, 293
- Burgasser, A., et al. 2002, *ApJ*, 564, 421
- Burrows, A., et al. 1997, *ApJ*, 491, 856
- Carpenter, J. M. 2001, *AJ*, 121, 2851
- Carpenter, J. M. 2002, *AJ*, 124, 1593
- Chabrier, G., Baraffe, I., Allard, F., & Hauschildt, P. H. 2000, *ApJ*, 542, 464 (CBAH00)
- Covino, E., et al. 2000, *A&A*, 361, L49
- Covino, E., Melo, C., Alcalá, J. M., Torres, G., Fernández, M., Frasca, A., & Paladino, R. 2001, *A&A*, 375, 130
- D’Antona, F., & Mazzitelli, I. 1997, in *Cool Stars in Clusters and Associations*, eds. G. Micela, R. Pallavicini & S. Sciortino, *Mem. Soc. Astron. Italiana*, 68, 807
- D’Antona, F., Ventura, P., & Mazzitelli, I. 2000, *ApJ*, 543, L77
- Delfosse, X., Forveille, T., Ségransan, D., Beuzit, J.-L., Udry, S., Perrier, C., & Mayor, M. 2000, *A&A*, 364, 217
- Duchêne, G., Bouvier, J., & Simon, T. 1999, 343, 831
- Dutrey, A., Guilloteau, S., Prato, L., Simon, M., Duvert, G., Schuster, K., & Menard, F. 1998, *A&A*, 338, 63

- Fabricant, D., Cheimets, P., Caldwell, N., & Geary, J. 1998, *PASP*, 110, 79
- Fredrick, L. W. 1956, *AJ*, 61, 437
- Gingrich, C. H. 1922, *ApJ*, 56, 139
- Guilloteau, S., & Dutrey, A. 1998, *A&A*, 339, 467
- Guilloteau, S., Dutrey, A., & Simon M. 1999, *A&A*, 348, 570
- Haisch, K. E., Lada, E. A., & Lada, C. J. 2000, *AJ*, 120, 1396
- Haisch, K. E., Lada, E. A., & Lada, C. J. 2001, *AJ*, 121, 2065
- Harris, D. L., Morgan, W. W., & Roman, N. G. 1954, *ApJ*, 119, 622
- Hartigan, P., Strom, K. M., & Strom, S. E. 1994, *ApJ*, 427, 961
- Hartmann, L. 2001, *AJ*, 121, 1030
- Henry, T. J., Kirkpatrick, J. D., & Simons, D. A. 1994, *AJ*, 108, 1437
- Herbig, G. H. 1954, *PASP*, 66, 19
- Herbig, G. H. 1998, *ApJ*, 497, 736
- Herbst, W., Maley, J. A., & Williams, E. C. 2000, *AJ*, 120, 349
- Hillenbrand, L. A. 1997, *AJ*, 113, 1733
- Hillenbrand, L. A., & Carpenter, J. M. 2000, *ApJ*, 540, 236
- Hüensch, M., Schmitt, J. H. M. M., Schroeder, K.-P., & Reimers, D. 1996, *A&A*, 310, 801
- Kalas, P., & Jewitt, D. 1997, *Nature*, 386, 52
- Kenyon, S. J., & Hartmann, L. 1990, *ApJ*, 349, 197
- Kenyon, S. J., & Hartmann, L. 1995, *ApJS*, 101, 117
- Kirkpatrick, J. D., Henry, T. J., & Irwin, M. J. 1997, *AJ*, 113, 1421
- Kirkpatrick, J. D., Henry, T. J., & McCarthy, D. W. 1991, *ApJS*, 77, 417
- Lada, E. A., & Lada, C. J. 1995, *AJ*, 109, 1682
- Landolt, A. U. 1992, *AJ*, 104, 340
- Leggett, S. K. 1992, *ApJS*, 82, 351
- Leggett, S. K., Allard, F., Dahn, C., Hauschildt, P. H., Kerr, T. H., & Rayner, J. 2000, *ApJ*, 535, 965
- Leggett, S. K., Allard, F., Geballe, T. R., Hauschildt, P. H., & Schweitzer, A. 2001, *ApJ*, 548, 908
- Liu, M. C., Najita, J., & Tokunaga, A. T. 2003, *ApJ*, 585, 372
- Lucas, P. W., Roche, P. F., Allard, F., & Hauschildt, P. H. 2001, *MNRAS*, 326, 695

- Luhman, K. L. 1999, *ApJ*, 525, 466
- Luhman, K. L. 2000, *ApJ*, 544, 1044
- Luhman, K. L. 2001, *ApJ*, 560, 287
- Luhman, K. L., Briceño, C., Rieke, G. H., & Hartmann, L. W. 1998a, *ApJ*, 493, 909
- Luhman, K. L., Briceño, C., Stauffer, J. R., Hartmann, L., Barrado y Navascués, D., & Nelson, C. 2003, *ApJ*, in press
- Luhman, K. L., Liebert, J., & Rieke, G. H. 1997, *ApJ*, 489, L165
- Luhman, K. L., McLeod, K. K., & Goldenson, N. 2003, in preparation
- Luhman, K. L., & Rieke, G. H. 1998, *ApJ*, 497, 354
- Luhman, K. L., & Rieke, G. H. 1999, *ApJ*, 525, 440
- Luhman, K. L., Rieke, G. H., Lada, C. J., & Lada, E. A. 1998b, *ApJ*, 508, 347
- Luhman, K. L., et al. 2000, *ApJ*, 540, 1016
- Martín, E. L., Rebolo, R., & Zapatero Osorio, M. R. 1996, *ApJ*, 469, 706
- McCaughrean, M. J., Rayner, J. T., & Zinnecker, H. 1994, *ApJ*, 436, L189
- Meyer, M. R., Calvet, N., & Hillenbrand, L. A. 1997, *AJ*, 114, 288
- Moraux, E., Bouvier, J., Stauffer, J. R., & Cuillandre, J.-C. 2003, *A&A*, 400, 891
- Muench, A. A., Lada, E. A., Lada, C. J., & Alves, J. 2002, *ApJ*, 573, 366
- Muench, A. A., et al. 2003, *AJ*, in press
- Najita, J., Tiede, G. P., & Carr, J. S. 2000, *ApJ*, 541, 977 (NTC00)
- Oke, J.B., et al. 1995, *PASP*, 107, 375
- Padoan, P., & Nordlund, Å. 2002, *ApJ*, 576, 870
- Palla, F., & Stahler, S. W. 1999, *ApJ*, 525, 772
- Palla, F., & Stahler, S. W. 2001, *ApJ*, 553, 299
- Popper, D. M. 1987, *ApJ*, 313, 81
- Prato, L. A. 1998, Ph. D. thesis, State Univ. of New York at Stony Brook
- Prato, L., Simon, M., Mazeh, T., McLean, I. S., Norman, D., & Zucker, S. 2002, *ApJ*, 569, 863
- Preibisch, T., & Zinnecker, H. 2001, *AJ*, 122, 866
- Preibisch, T., & Zinnecker, H. 2002, *AJ*, 123, 1613
- Preibisch, T., Zinnecker, H., & Herbig, G. H. 1996, *A&A*, 310, 456

- Rieke, G. H., & Lebofsky, M. J. 1985, *ApJ*, 288, 618
- Ripepi, V., Palla, F., Marconi, M., Bernabei, S., Arellano Ferro, A., Terranegra, L., & Alcalá, J. M. 2002, *A&A*, 391, 587
- Schmidt-Kaler, T. 1982, in *Landolt-Bornstein, Group VI, Vol. 2*, ed. K.-H. Hellwege (Berlin: Springer), 454
- Scholz, R.-D., et al. 1999, *A&AS*, 137, 305
- Siess, L., Dufour, E., & Forestini, M. 2000, *A&A*, 358, 593
- Simon, M., Dutrey, A., & Guilloteau, S. 2000, *ApJ*, 545, 1034
- Stahler, S. W. 1983, *ApJ*, 274, 822
- Steffen, A. T., et al. 2001, *AJ*, 122, 997
- Strom, S. E., Strom, K. M., & Carrasco, L. 1974, *PASP*, 86, 798
- Tej, A., Sahu, K. C., Chandrasekhar, T., & Ashok, N. M. 2002, *ApJ*, 578, 523
- Torres, G., & Ribas, I. 2002, *ApJ*, 567, 1140
- Walter, F. W., Brown, A., Mathieu, R. D., Myers, P. C., & Vrba, F. J. 1988, *AJ*, 96, 297
- White, R. J., Ghez, A. M., Reid, I. N., & Schultz, G. 1999, *ApJ*, 520, 811
- Williams, D., Thompson, C. L., Rieke, G. H., & Montgomery, E. F. 1993, *ProcSPIE*, 1308, 482

Table 1. Observing Log

Date	Telescope + Instrument	Grating l mm ⁻¹	Resolution Å	ID
1998 Aug 7	Keck + LRIS	150	16	384,547,548,550,631
1998 Nov 24	Keck + LRIS	1200	2.5	435
1998 Dec 23, 26	KPNO 4 m + RCSP	158	14	31,43,48,53,55,61,69,79,81,82,84,89,92,93,105,116,119
...	123,129,146,174,177,186,188,210,212,236,246,281,282,311
...	317,339,369,462,829
1999 Dec 23	Keck + LRIS	150	16	301,382,391
2000 Dec 3	Steward 2.3 m + B&C	400	7	56,63,66,96,97,98,106,156,182,195,198,206,228,253,254,255
2000 Dec 7	MMT + FSpec	75	27	27,43,84,89,143,219
2000 Nov 25, 26	Keck + LRIS	150	16	97,115,140,143,166,182,187,190,191,198,219,221,230
...	243,248,252,255,278,291,292,295,298,302,308,322,329,342
...	347,350,358,365,367,370,373,385,391,404,415,434,435,437
...	450,468,479,486,555,598,603,609,618,621,622,624,630,681
...	689,690,694,702,703,705,709,713,719,725,738,741,746,761
...	774,813,817,842,850,863,934,935,944,958,963,983,991,1010
...	1383,1387,1389,1400,1416,1418,1424,1426,1432,1434,1461
...	1463,1464,1476,1481,1483,1511,1676,1684,1689,1903,2096
...	2110,3006,3039,3042,3051,3086,4037,4044,4048,4053,4098
...	5012,5194,5200
2001 Dec 25, 26	Steward 2.3 m + B&C	400	7	90,110,113,120,122,125,139,153,154,171,193,217,226
2002 Jan 12	MMT + Blue Channel	600	2.8	218,303,316,396
2002 Sep 12	FLWO 1.5 m + FAST	300	5	64,1937,10252,10338
2002 Sep 27	FLWO 1.5 m + FAST	300	5	114,1932,1941,10363
2002 Oct 11	FLWO 1.5 m + FAST	300	5	50,72
2002 Oct 14	FLWO 1.5 m + FAST	300	5	39,67,73,85,87,94,1863,10352
2002 Oct 15	FLWO 1.5 m + FAST	300	5	58,75,111,10226,10343
2002 Nov 10	MMT + Blue Channel	600	2.8	78A,136,149,168,176,194,200,203,213,235,241,247,259A+B
...	261,1719,1868,1928,1936,1940
2002 Nov 11	MMT + Blue Channel	600	2.8	42A,42B,46,51,99A,99B,138,157,207,214,216,262,269,276
...	300,341,344,906,1927
2002 Dec 7	FLWO 1.5 m + FAST	300	5	178,180
2002 Dec 12	FLWO 1.5 m + FAST	300	5	76,88,101,108,137,147,164,10289
2003 Jan 26	MMT + Red Channel	270	14	112,284,1939
2003 Jan 27	MMT + Red Channel	1200	2	44

Table 2. Data for Members of IC 348

ID	α (J2000) ^a h m s	δ (J2000) ^a ° ' "	Spectral Type/ W_λ (H α) ^b	Ref	Adopt	Member ^c -ship	T_{eff} ^d	A_J	L_{bol}	$R - I^e$	I^f	$I - Z^g$	$J - H$	$H - K_s$	K_s	Ref	IMF?
1 ^h	03 44 34.20	32 09 46.3	B5V,B3-B4,<F8(IR)	1,2,2	B5	A_V ,pm	15400	0.54	605	0.15	0.12	6.51	3	yes
2	03 44 35.36	32 10 04.6	A2,<F8(IR)	1,2	A2	A_V ,pm	8970	1.08	137	0.42	0.29	7.25	3	yes
3	03 44 50.65	32 19 06.8	A0,<F8(IR)	4,2	A0	A_V	9520	1.26	135	0.48	0.24	7.66	3	no
4	03 44 31.19	32 06 22.1	F0m;,<F8(IR)	1,2	F0	A_V ,pm	7200	0.50	34	0.31	0.16	7.86	3	yes
5	03 44 26.03	32 04 30.4	K0/23,F8-G8/2.1,?(IR)	5,2,2	G8	A_V ,ex,e	5520	1.50	9.9	1.35	12.44	0.72	1.21	0.73	8.14	3	no
6 ^h	03 44 36.94	32 06 45.4	F8,F8-G8,G3-G7(IR)	4,2,2	G3	A_V ,pm	5830	1.10	17	0.72	0.29	8.19	3	yes
7	03 44 08.48	32 07 16.5	A0V,<F8(IR)	1,2	A0	A_V ,pm	9520	0.26	35	0.10	0.12	8.60	3	yes
8	03 44 09.15	32 07 09.3	A2V,<F8(IR)	1,2	A2	A_V ,pm	8970	0.27	28	0.11	0.14	8.62	3	yes
9 ^h	03 44 39.17	32 09 18.3	G5-K0,G6-K1(IR)	2,2	G8	A_V	5520	1.56	11	1.39	12.30	0.68	0.93	0.36	8.77	3	no
10	03 44 24.66	32 10 15.0	F2,<F8(IR)	1,2	F2	A_V ,pm	6890	0.54	13	0.35	0.20	8.79	3	yes
11	03 45 07.96	32 04 02.1	F7-G6/1.5,G2-G7(IR)	2,2	G4	A_V ,e	5800	1.76	11	...	12.66	0.74	0.96	0.44	8.88	3	no
12A ⁱ	03 44 31.96	32 11 43.9	G0,A0-A5?,<F8?(IR)	5,2,2	G0	A_V ,e	6030	1.23	4.0	1.15	12.64	0.74	0.71	0.44	8.92	3	no
12B	03 44 32.06	32 11 44.0	A0-A5?,<F8?(IR)	2,2	A3	A_V ,e	8720	2.12	29	...	12.94	0.78	no
13	03 43 59.65	32 01 54.2	K7-M2(IR)	2	M0.5	A_V ,ex,e	3778	4.13	3.2	...	19.46	...	2.67	1.85	8.93	3	no
15	03 44 44.73	32 04 02.6	M0.5/36,K7-M1(IR)	2,2	M0.5	A_V ,ex,e	3778	1.12	1.9	...	13.34	0.74	1.09	0.60	9.33	3	yes
16	03 44 32.74	32 08 37.5	K,G5-K0,G2-G7(IR)	5,2,2	G6	A_V	5700	0.75	4.4	0.85	11.74	...	0.63	0.22	9.43	3	yes
17	03 44 47.72	32 19 11.9	A0-A9	2	A4	A_V	8460	1.51	20	...	11.98	0.60	0.60	0.33	9.38	3	no
19	03 44 30.82	32 09 55.8	A2,<F8(IR)	1,2	A2	A_V ,pm	8970	0.63	16	0.25	0.15	9.43	3	yes
20	03 45 07.61	32 10 28.1	G0-G2	4	G1	A_V	5945	0.62	4.9	...	11.23	0.33	0.52	0.19	9.41	3	yes
21	03 44 56.15	32 09 15.5	G8-K2/4.7	2	K0	A_V ,e	5250	1.52	3.9	...	13.21	0.67	1.03	0.52	9.47	3	no
22	03 43 51.24	32 13 09.4	F8-G0,G5-K0	4,2	G5	A_V	5770	0.74	4.3	...	11.54	0.39	0.61	0.20	9.50	3	no
23	03 44 38.72	32 08 42.0	G8-K4,K3-K6(IR)	2,2	K3	A_V	4730	1.93	4.1	...	13.97	0.85	1.22	0.48	9.49	3	no
24A	03 44 35.04	32 07 36.9	K7,K6/0.4,K6-M1(IR)	5,2,2	K6.5	A_V	4132	0.80	1.5	1.23	12.96	0.60	0.92	0.31	9.76	3	yes
24B	03 44 35.37	32 07 36.1	K8/32,M0.5/5,K6-M1(IR)	5,2,2	M0	A_V ,e	3850	1.07	0.69	...	14.32	0.71	1.14	0.55	10.39	3	yes
25	03 45 01.42	32 05 02.0	A0-A9	2	A4	A_V	8460	1.03	13	...	11.71	0.45	0.42	0.24	9.65	3	yes
26	03 43 56.03	32 02 13.3	K7-K8/44,K4-K7(IR)	2,2	K7	A_V ,ex,e	4060	2.07	1.5	...	15.62	0.97	1.73	1.03	9.53	3	no
29	03 44 31.53	32 08 45.0	K2,G8-K2,K2-K3(IR)	5,2,2	K2	A_V	4900	0.64	2.1	0.83	12.25	0.48	0.72	0.24	9.72	3	yes
30	03 44 19.13	32 09 31.4	F0:	1	F0	pm	7200	0.53	6.5	...	11.00	0.26	0.32	0.08	9.76	3	yes
31	03 44 18.16	32 04 57.0	F5-G6/11 \pm 0.5	6	G1	A_V ,e	5945	3.34	9.6	...	15.37	0.99	1.55	0.85	9.69	3	no
32	03 44 37.89	32 08 04.2	K7/68,K8/57,K4-K7(IR)	5,2,2	K7	A_V ,ex,e	4060	1.41	1.4	...	14.18	0.78	1.21	0.65	9.83	3	no
33	03 44 32.59	32 08 42.5	M2-M3/5.9,M4-M5(IR)	2,2	M2.5	A_V ,NaK	3488	0.71	0.87	...	13.25	...	0.91	0.31	10.07	3	yes
35	03 44 39.25	32 07 35.5	G8,G8-K4,K3-K6(IR)	5,2,2	K3	A_V	4730	1.43	3.6	1.40	13.21	0.71	0.88	0.40	9.55	3	no
36	03 44 38.47	32 07 35.7	K6/2,K5-K6/3.9,K6-M1(IR)	5,2,2	K6	A_V	4205	0.95	1.5	1.30	13.26	0.63	0.95	0.38	9.85	3	yes
37	03 44 37.99	32 03 29.8	K6/47	2	K6	A_V ,e	4205	0.79	0.99	...	13.18	0.58	1.01	0.57	9.87	3	yes
38	03 44 23.99	32 11 00.0	F8,F6-G1(IR)	4,2	G0	A_V	6030	0.73	3.1	0.83	11.84	0.38	0.52	0.17	10.03	3	yes
39	03 45 01.74	32 14 27.9	K3-K5	7	K4	A_V	4590	1.34	1.9	...	13.43	0.70	0.95	0.36	10.04	3	no
40	03 44 29.73	32 10 39.8	K6/145v?,K8-M0/104	5,2	K8	A_V ,ex,e	3955	1.01	0.76	1.44	14.10	0.66	1.17	0.62	10.14	3	yes
...	K6-M1(IR)	2
41	03 44 21.61	32 10 37.6	K7/48,K7-M2(IR)	5,2	K7	A_V ,ex,e	4060	1.59	0.79	...	14.99	0.83	1.21	0.66	10.62	3	no
42A ^j	03 44 42.02	32 09 00.1	M3/74,M4-M6(IR),M4.25/22 \pm 2	5,2,7	M4.25	A_V ,e,NaK	3234	0.93	0.37	...	14.88	0.85	1.12	0.53	10.13	3	yes
42B	03 44 42.14	32 09 02.2	M1/32,M1-M3(IR),M2-M3/55 \pm 10	5,2,7	M2.5	A_V ,e	3488	1.36	0.28	...	15.83	0.87	no
44	03 44 08.86	32 16 10.7	G8-K2	2	K0	A_V ,Li	5250	1.00	1.7	...	13.07	0.52	0.82	0.30	10.26	3	no
45	03 44 24.29	32 10 19.4	K5,K5,K4-K7(IR)	5,2,2	K5	A_V	4350	0.66	0.92	1.08	13.08	0.51	0.84	0.24	10.33	3	yes
46	03 44 11.62	32 03 13.2	G-K/4.5 \pm 1	7	?	A_V ,e	16.24	1.05	1.56	0.89	10.33	3	no

Table 2—Continued

ID	α (J2000) ^a h m s	δ (J2000) ^a ° ' "	Spectral Type/ W_λ (H α) ^b	Ref	Adopt	Member ^c -ship	T_{eff} ^d	A_J	L_{bol}	$R - I^e$	I^f	$I - Z^g$	$J - H$	$H - K_s$	K_s	Ref	IMF ^g
47	03 43 55.51	32 09 32.5	G8-K2	2	K0	A _V	5250	1.06	1.9	1.06	12.97	0.54	0.72	0.26	10.34	3	yes
48	03 44 34.88	32 06 33.6	K5-K6/1.5±0.3	6	K5.5	A _V	4278	0.85	0.99	1.18	13.45	0.60	0.90	0.29	10.31	3	yes
49	03 43 57.60	32 01 37.5	K7-M2(IR)	2	M0.5	A _V	3778	2.88	0.36	2.42	19.63	1.37	2.67	1.48	10.41	3	no
50	03 44 55.63	32 09 20.2	K3-K5/2±0.5	7	K4	A _{V,e}	4590	1.52	1.4	...	14.28	0.75	1.10	0.39	10.36	3	no
51	03 44 12.97	32 01 35.4	?(IR,op)/45±15	2,7	?	A _{V,e,ex}	1.70	19.56	0.88	2.66	2.40	10.03	3	no
52 ^h	03 44 43.53	32 07 43.0	K6,M2-M4(IR)	5,2	M1	A _V	3705	1.48	0.92	...	14.98	0.86	1.23	0.47	10.42	3	no
53	03 44 16.43	32 09 55.2	G8-K2	6	K0	A _V	5250	0.70	1.4	0.89	12.63	0.41	0.74	0.20	10.38	3	yes
55	03 44 31.36	32 00 14.7	M0-M1/38±2	6	M0.5	A _{V,e}	3778	2.63	0.68	2.51	18.06	1.18	1.98	1.01	10.64	3	no
56	03 44 05.00	32 09 53.8	K3-K4	7	K3.5	A _V	4660	0.74	0.93	1.07	13.02	0.47	0.84	0.21	10.50	3	yes
58	03 44 38.55	32 08 00.7	K7/9,K6-M1(IR),M1.25	5,2,7	M1.25	A _V	3669	1.04	0.72	...	14.24	0.74	1.04	0.43	10.47	3	yes
59	03 44 40.13	32 11 34.3	G7,G8-K2,K2-K4(IR)	5,2,2	K2	A _V	4900	1.19	1.4	1.26	13.54	0.60	0.86	0.30	10.51	3	no
60A ^k	03 44 25.58	32 11 30.5	K8/51,K7-M1(IR)	5,2	M0	A _{V,e}	3850	1.03	0.34	...	14.99	0.70	1.21	0.63	10.64	3	yes
60B	03 44 25.50	32 11 31.2	16.14	0.79	yes
61	03 44 22.29	32 05 42.7	K8/51±2	6	K8	A _{V,e}	3955	1.25	0.54	1.48	15.23	0.78	1.27	0.57	10.70	3	no
62	03 44 26.63	32 03 58.3	M4.75/10±1	8	M4.75	A _{V,NaK}	3161	0.52	0.39	...	14.03	0.79	0.86	0.35	10.59	3	yes
63	03 43 58.91	32 11 27.1	M1-M2.5/27±1	7	M1.75	A _{V,e}	3596	1.10	0.61	...	14.42	...	1.08	0.65	10.42	3	yes
64	03 44 25.57	32 12 30.0	M0.5/2.7±0.5	7	M0.5	A _V	3778	0.36	0.45	...	13.40	0.52	0.87	0.27	10.68	3	yes
65	03 44 33.98	32 08 54.1	K7+/0.9,M2-M4(IR)	2,2	M0	A _V	3850	0.61	0.56	1.20	13.69	0.55	0.87	0.28	10.70	3	yes
66	03 44 28.47	32 07 22.4	K6-K7/1.4±0.2	7	K6.5	A _V	4132	0.65	0.71	1.14	13.53	0.55	0.82	0.27	10.58	3	yes
67	03 43 44.62	32 08 17.9	M0.75/35±2	7	M0.75	A _{V,e}	3741	0.68	0.48	...	13.93	0.62	0.92	0.34	10.79	3	no
68	03 44 28.51	31 59 54.1	M3.5/5.1	2	M3.5	A _{V,NaK}	3342	0.83	0.46	...	14.16	0.76	0.87	0.36	10.77	3	yes
69	03 44 27.02	32 04 43.6	M1/3.5±0.5	6	M1	A _V	3705	0.55	0.46	1.27	13.69	0.59	0.81	0.29	10.85	3	yes
71	03 44 32.58	32 08 55.8	M2/5,M3/5,M1-M3(IR)	5,2,2	M3	A _{V,NaK}	3415	0.95	0.47	...	14.32	...	0.98	0.37	10.76	3	yes
72	03 44 22.57	32 01 53.7	M2.5/3.5±1	7	M2.5	A _{V,NaK}	3488	0.98	0.51	...	14.31	0.76	0.97	0.36	10.79	3	yes
74	03 44 34.27	32 10 49.7	M1/3,M2/5.4,M1-M3(IR)	5,2,2	M2	A _{V,NaK}	3560	1.14	0.62	...	14.36	0.79	1.01	0.32	10.81	3	no
75	03 44 43.78	32 10 30.6	K8,M2-M4(IR),M1.25	5,2,7	M1.25	A _V	3669	0.84	0.28	...	14.26	0.68	1.15	0.45	11.15	9	yes
76	03 44 39.81	32 18 04.2	M3.75/14±1	7	M3.75	A _{V,e,NaK}	3306	0.88	0.39	...	14.53	0.79	0.95	0.50	10.78	3	no
78A ^k	03 44 26.69	32 08 20.3	M2-M4(IR),M0-M1/75±10	2,7	M0.5	A _{V,e,ex}	3778	1.81	0.53	...	16.01	0.94	1.43	0.71	10.84	3	no
78B	03 44 26.56	32 08 20.6	18.71	1.31	no
79	03 45 01.52	32 10 51.5	G8-K2	6	K0	A _V	5250	0.83	0.94	...	13.23	0.47	0.74	0.25	10.88	3	yes
82	03 44 37.41	32 06 11.7	K7	6	K7	A _V	4060	0.71	0.51	1.29	13.89	0.54	0.94	0.28	10.87	3	yes
83	03 44 37.41	32 09 00.9	K8/7,M2-M4(IR)	5,2	M1	A _V	3705	1.21	0.51	...	14.93	0.78	1.05	0.45	10.99	3	no
85	03 44 28.12	32 16 00.3	M3.25/5±1	7	M3.25	A _V	3379	0.60	0.30	...	14.11	0.68	0.93	0.25	11.05	9	no
86 ^h	03 44 27.88	32 07 31.6	M3/3,M2/3.9,M1-M3(IR)	5,2,2	M2	A _{V,NaK}	3560	0.79	0.46	...	14.13	0.69	0.86	0.30	10.97	3	yes
87	03 43 59.72	32 14 03.2	M0.75/1.5±0.5	7	M0.75	A _V	3741	0.47	0.33	...	14.05	0.56	0.94	0.24	11.06	9	no
88	03 44 32.77	32 09 15.8	M2/4,K6-M1(IR),M3.25/5±0.5	5,2,7	M3.25	A _{V,NaK}	3379	1.03	0.36	...	14.63	...	1.01	0.37	11.10	9	yes
90	03 44 33.31	32 09 39.6	M1-M3(IR),M1.5-M2.5/5±1	2,7	M2	A _{V,NaK}	3560	1.08	0.41	...	14.55	...	1.07	0.46	11.01	9	yes
91	03 44 39.21	32 09 44.7	M1/8::M2-M4(IR)	5,2	M2	A _V	3560	1.08	0.39	...	14.76	...	1.07	0.38	11.14	9	yes
92 ^h	03 44 23.67	32 06 46.5	M2.5/4±0.5	6	M2.5	A _{V,NaK}	3488	0.81	0.39	...	14.20	0.71	0.87	0.29	11.08	9	yes
93	03 44 17.91	32 12 20.4	M2.5/5.5±0.5	6	M2.5	A _{V,NaK}	3488	0.50	0.31	...	13.87	0.62	0.84	0.24	11.10	9	yes
94	03 43 32.08	32 06 17.4	M0.75/1±0.5	7	M0.75	A _V	3741	0.27	0.29	...	13.74	0.50	0.80	0.25	11.13	3	no
95	03 44 21.91	32 12 11.6	M4/5.5,M2-M4(IR)	2,2	M4	A _{V,NaK}	3270	0.66	0.29	...	14.27	0.74	0.89	0.30	11.12	9	yes
96	03 44 34.87	32 09 53.4	>K5(IR),M3.5/4±1	2,7	M3.5	A _{V,NaK}	3342	0.90	0.31	...	14.91	0.78	0.93	0.37	11.21	9	yes
97	03 44 25.56	32 06 17.0	M2.25/3±1	7	M2.25	A _{V,NaK}	3524	1.70	0.54	...	15.98	0.96	1.23	0.52	11.07	9	no

Table 2—Continued

ID	α (J2000) ^a h m s	δ (J2000) ^a ° ' "	Spectral Type/ W_λ (H α) ^b	Ref	Adopt	Member ^c -ship	T_{eff} ^d	A_J	L_{bol}	$R - I^e$	I^f	$I - Z^g$	$J - H$	$H - K_s$	K_s	Ref	IMF?
98	03 44 38.62	32 05 06.5	M3.5-M4.5/4 \pm 1	7	M4	A_V ,NaK	3270	0.93	0.33	...	14.88	0.82	0.95	0.37	11.15	9	yes
99A ^j	03 44 19.24	32 07 34.7	M2/4,M3.75/9.5 \pm 1	5,7	M3.75	A_V ,NaK	3306	0.74	0.26	...	14.78	0.75	0.99	0.55	11.35	9	yes
99B	03 44 19.01	32 07 35.7	M4,M5.25	5,7	M5.25	A_V ,NaK	3091	0.78	0.041	...	17.18	0.94	yes
100	03 44 22.32	32 12 00.8	M1/90,M2-M4(IR)	2,2	M1	A_V ,e	3705	0.90	0.33	...	14.47	0.69	0.99	0.43	11.25	9	yes
101	03 44 50.97	32 16 09.6	M3.25/6 \pm 0.5	7	M3.25	A_V ,NaK	3379	0.88	0.35	...	14.38	0.76	0.89	0.28	11.18	9	no
103	03 44 44.59	32 08 12.7	K8/44v?,M2/26,M1-M3(IR)	5,2,2	M2	A_V ,e,NaK	3560	1.34	0.38	...	15.73	0.85	1.02	0.53	11.34	3	no
105	03 44 11.26	32 06 12.1	M0/2 \pm 0.3	6	M0	A_V	3850	0.76	0.39	...	14.32	0.62	0.92	0.27	11.20	9	yes
108	03 44 38.70	32 08 56.7	M2/3,M2-M4(IR),M3.25/4.5 \pm 0.5	5,2,7	M3.25	A_V ,NaK	3379	0.60	0.24	...	14.46	0.68	0.92	0.30	11.27	9	yes
110	03 44 37.40	32 12 24.3	K6-M1(IR),M1.5-M2.5/22 \pm 2	2,7	M2	A_V ,e	3560	1.48	0.34	...	15.78	0.89	1.24	0.49	11.44	9	no
111	03 43 48.76	32 07 33.4	M1.5	7	M1.5	A_V	3632	0.74	0.34	...	14.31	0.66	0.85	0.25	11.34	9	no
112	03 44 44.98	32 13 36.6	M4.75/10.5 \pm 1	7	M4.75	A_V ,NaK	3161	0.76	0.24	...	15.00	0.86	0.90	0.37	11.33	9	yes
113	03 44 37.19	32 09 16.1	K4-K7(IR),K6	2,7	K6	A_V	4205	0.77	0.32	1.22	14.41	0.56	0.99	0.26	11.38	9	yes
115	03 44 29.99	32 09 21.1	M1,K6-M1(IR),M2-M3	5,2,7	M2.5	A_V	3488	2.29	0.45	2.42	17.18	1.18	1.56	0.67	11.35	9	no
116	03 44 21.56	32 10 17.4	M1.5	6	M1.5	A_V	3632	0.81	0.29	...	14.57	0.68	0.96	0.30	11.40	9	yes
119	03 44 21.26	32 05 02.4	M2.5/8 \pm 0.5	6	M2.5	A_V	3488	1.12	0.32	...	15.19	0.80	0.96	0.38	11.46	9	yes
120	03 44 22.98	32 11 57.3	M2-M4?(IR),M2.25/1.5 \pm 0.3	2,7	M2.25	A_V ,NaK	3524	0.53	0.22	...	14.33	0.62	0.95	0.26	11.40	9	yes
122	03 44 33.22	32 15 29.1	K5-M0(IR),M2.25/2.5 \pm 0.5	2,7	M2.25	A_V	3524	0.63	0.26	0.89	0.24	11.39	9	no
123	03 44 24.57	32 03 57.1	M1/5 \pm 1	6	M1	A_V	3705	1.41	0.44	...	15.36	0.84	1.04	0.39	11.42	9	no
124	03 43 54.63	32 00 30.1	M4.25/7 \pm 1	8	M4.25	A_V ,NaK	3234	0.86	0.27	...	14.90	0.83	0.84	0.39	11.34	9	yes
125	03 44 21.66	32 06 24.8	K4-K7(IR),M2.75/4 \pm 0.5	2,7	M2.75	A_V ,NaK	3451	0.78	0.29	...	14.56	0.71	0.93	0.29	11.30	9	yes
128	03 44 20.18	32 08 56.6	M1/47,M1-M4(IR)	5,2	M2	A_V ,e	3560	1.00	0.32	...	14.84	0.75	0.90	0.36	11.47	9	yes
129	03 44 21.29	32 11 56.4	M2	6	M2	A_V	3560	0.79	0.27	...	14.54	0.69	1.01	0.32	11.37	9	yes
130	03 44 04.25	32 13 50.0	M4.75/5,>K5(IR)	2,2	M4.75	A_V ,NaK	3161	0.66	0.22	...	14.87	0.83	0.82	0.33	11.43	9	no
133	03 44 41.74	32 12 02.4	M4-M5,M5-M6(IR)	2,2	M5	A_V	3125	1.10	0.17	...	16.23	0.99	1.25	0.56	11.49	9	yes
135	03 44 39.19	32 20 09.0	M4.5/20,>K5(IR)	2,2	M4.5	A_V ,e,NaK	3198	0.55	0.20	...	14.78	0.77	0.80	0.32	11.47	9	no
136	03 44 13.62	32 15 54.3	M3/5 \pm 1	7	M3	A_V	3415	1.45	0.26	...	15.91	0.91	1.25	0.46	11.51	9	no
137	03 44 11.44	32 19 40.1	M3-M4/8,M4-M6(IR),M3/10 \pm 1	2,2,7	M3	A_V ,NaK	3415	0.52	0.20	...	14.36	0.64	0.85	0.29	11.45	9	no
138	03 44 45.11	32 14 13.4	M3.5-M4.5/2 \pm 1	7	M4	A_V ,NaK	3270	1.97	0.33	2.49	16.91	1.13	1.37	0.59	11.54	9	no
139	03 44 25.31	32 10 12.7	M3/51,>K5(IR),M4.75/55 \pm 5	5,2,7	M4.75	A_V ,e,NaK	3161	0.86	0.20	...	15.31	0.89	0.91	0.45	11.53	9	yes
140	03 44 35.69	32 03 03.6	M3.25	7	M3.25	A_V ,NaK	3379	0.94	0.13	1.75	15.78	0.77	1.16	0.66	11.65	9	yes
141	03 44 30.54	32 06 29.7	M1,K5-M0(IR)	2,2	M0.5	A_V	3778	1.09	0.35	...	15.07	0.73	1.00	0.34	11.48	9	yes
142	03 43 56.20	32 08 36.3	M0-M1/4,K5-M0(IR)	2,2	M0	A_V	3850	0.83	0.33	...	14.65	0.64	0.90	0.25	11.48	9	yes
144	03 44 38.39	32 12 59.8	M0/2,K5-M0(IR)	2,2	M0	A_V	3850	0.62	0.21	...	14.57	0.58	0.99	0.23	11.69	9	yes
145	03 44 41.31	32 10 25.3	M3/3:,M4.75/4,M2-M4(IR)	5,2,2	M4.75	A_V ,NaK	3161	0.48	0.17	...	14.69	0.78	0.85	0.33	11.47	9	yes
146	03 44 42.63	32 06 19.5	M1/1.5 \pm 0.5	7	M1	A_V	3705	0.20	0.19	1.13	13.99	0.45	0.81	0.19	11.55	9	yes
147	03 43 49.39	32 10 40.0	M3.5/11 \pm 1	7	M3.5	e,NaK	3342	0.34	0.17	...	14.62	0.62	0.78	0.26	11.54	9	no
149	03 44 36.99	32 08 34.2	M3/8:.,K6-M1?(IR),M4.75/30 \pm 5	5,2,7	M4.75	A_V ,e,NaK	3161	0.97	0.18	...	15.66	0.92	0.97	0.44	11.66	9	yes
150	03 45 02.85	32 07 00.9	M4.75/8 \pm 2	8	M4.75	A_V ,NaK	3161	0.83	0.22	...	15.21	0.88	0.84	0.37	11.54	9	yes
151	03 44 34.83	32 11 18.0	M3,K6-M1(IR)	5,2	M2	A_V	3560	0.93	0.26	...	14.84	0.73	0.91	0.34	11.62	9	yes
153	03 44 42.77	32 08 33.9	M2/91,>K5(IR),M4.75/40 \pm 10	5,2,7	M4.75	A_V ,e,NaK	3161	1.17	0.20	...	15.95	0.98	0.99	0.47	11.75	9	no
154	03 44 37.79	32 12 18.2	K6-M1(IR),M4.5/6.5 \pm 1.5	2,7	M4.5	A_V ,NaK	3198	0.90	0.19	...	15.38	0.87	0.92	0.39	11.70	9	yes
156	03 44 06.79	32 07 54.1	M4.25/10 \pm 2	7	M4.25	A_V ,NaK	3234	0.76	0.17	...	15.31	0.80	0.88	0.36	11.76	9	yes
157	03 44 18.58	32 12 53.2	M2-M3.5/115 \pm 10	7	M2.75	A_V ,e	3451	1.35	0.14	1.97	16.43	0.86	1.30	1.00	11.58	9	no
158	03 44 40.16	32 09 13.0	M5,>K5(IR)	2,2	M5	A_V ,NaK	3125	1.45	0.22	...	16.50	1.09	1.11	0.54	11.71	9	no

Table 2—Continued

ID	α (J2000) ^a h m s	δ (J2000) ^a ° ' "	Spectral Type/ W_λ (H α) ^b	Ref	Adopt	Member ^c -ship	T_{eff}^d	A_J	L_{bol}	$R - I^e$	I^f	$I - Z^g$	$J - H$	$H - K_s$	K_s	Ref	IMF?
159	03 44 47.62	32 10 55.8	M4.25/4 \pm 1	8	M4.25	A _V ,NaK	3234	1.62	0.22	...	16.60	1.05	1.28	0.54	11.75	9	no
160	03 44 02.59	32 01 35.1	M4.75/6 \pm 1	8	M4.75	NaK	3161	0.34	0.14	...	14.87	0.74	0.71	0.36	11.67	9	yes
163	03 44 11.22	32 08 16.3	M5.25/10.5 \pm 0.5	8	M5.25	NaK	3091	0.40	0.14	...	15.12	0.83	0.71	0.34	11.73	9	yes
165	03 44 35.45	32 08 56.3	M4/50:,M5.25/74 \pm 5,>K5(IR)	5,2,2	M5.25	A _V ,e,NaK	3091	1.02	0.16	...	16.15	1.01	0.95	0.54	11.79	9	yes
166	03 44 42.58	32 10 02.5	K6-M1(IR),M4.25/50 \pm 10	2,7	M4.25	A _V ,e,NaK	3234	1.78	0.24	2.48	16.85	1.10	1.22	0.62	11.81	9	no
167	03 44 41.18	32 10 10.2	M3,M2-M4(IR)	2,2	M3	A _V ,NaK	3415	1.66	0.15	2.14	16.71	0.98	1.42	0.68	11.94	9	no
168	03 44 31.35	32 10 46.9	M2/12,>K5(IR),M4.25/39 \pm 5	5,2,7	M4.25	A _V ,e,NaK	3234	0.90	0.12	...	15.84	0.84	1.12	0.56	11.84	9	yes
169	03 44 17.77	32 04 47.6	M3/5,M5.25/7 \pm 0.5,K6-M1?(IR)	5,8,2	M5.25	A _V ,NaK	3091	0.78	0.15	...	15.78	0.94	0.87	0.44	11.84	9	yes
170	03 44 28.42	32 11 22.5	M2-M4(IR)	2	M3	A _V	3415	2.40	0.19	2.52	18.62	1.24	1.89	0.81	11.84	9	no
171	03 44 44.85	32 11 05.8	M2,M3-M5(IR),M2.75/2.5 \pm 0.5	5,2,7	M2.75	A _V ,NaK	3451	0.89	0.17	...	15.28	0.74	1.02	0.33	11.84	9	yes
173	03 44 10.13	32 04 04.5	M5.75/110 \pm 10	8	M5.75	A _V ,e,NaK	3024	0.57	0.12	...	15.89	0.97	0.78	0.52	11.89	9	yes
174	03 44 04.11	32 07 17.1	M1.5/3 \pm 0.5	6	M1.5	A _V	3632	0.64	0.18	...	15.01	0.63	0.89	0.29	11.84	9	yes
175	03 44 49.80	32 03 34.2	M4.5/8 \pm 0.5	8	M4.5	A _V ,NaK	3198	0.59	0.13	...	15.31	0.78	0.81	0.35	11.97	9	yes
176	03 45 04.63	32 15 01.1	M4.25	7	M4.25	A _V ,NaK	3234	1.14	0.17	...	16.01	0.91	1.11	0.41	11.83	9	no
177	03 45 05.22	32 09 54.5	M3/2 \pm 0.5	6	M3	A _V ,NaK	3415	0.76	0.15	...	15.20	0.71	0.95	0.31	11.87	9	yes
178	03 44 48.83	32 13 22.1	M2.75/14 \pm 2	7	M2.75	A _V ,e,NaK	3451	0.51	0.13	...	14.94	0.63	0.89	0.26	11.96	9	yes
180	03 44 21.76	32 12 31.4	M3.5/4 \pm 0.5	7	M3.5	A _V ,NaK	3342	0.52	0.12	...	14.92	0.67	0.84	0.28	12.01	9	yes
182	03 44 18.20	32 09 59.3	M4.25/6 \pm 1	7	M4.25	A _V ,NaK	3234	0.86	0.15	...	15.74	0.83	0.91	0.43	11.87	9	yes
184	03 44 53.76	32 06 52.2	M4/5 \pm 1	8	M4	A _V ,NaK	3270	1.10	0.18	...	15.84	0.87	0.99	0.40	11.91	9	yes
186	03 44 46.33	32 11 16.8	M2	6	M2	A _V	3560	2.29	0.31	2.47	17.39	1.12	1.47	0.59	11.99	9	no
187A ^h	03 44 06.11	32 07 07.2	M4.25/5.5 \pm 0.5	7	M4.25	A _V	3234	1.31	0.15	...	16.36	0.96	0.89	0.42	12.00	9	no
187B	03 44 06.21	32 07 06.7	17.05	0.76	yes
188	03 44 56.12	32 05 56.7	M2.5-M3/5 \pm 0.5	6	M2.75	A _V ,NaK	3451	0.51	0.13	...	14.91	0.63	0.85	0.25	11.98	9	yes
190	03 44 29.21	32 01 15.8	M3.75/5 \pm 1	7	M3.75	A _V ,NaK	3306	2.00	0.16	2.52	17.93	1.10	1.47	0.84	12.02	9	no
191	03 44 37.84	32 10 07.4	M1-M3(IR),K7	2,7	K7	A _V	4060	2.31	0.33	2.35	17.36	0.99	1.57	0.60	11.98	9	no
192	03 44 23.64	32 01 52.8	M4-M5/40 \pm 20	8	M4.5	A _V ,e	3198	2.22	0.16	2.75	18.54	1.31	1.50	0.83	12.14	9	no
193	03 44 38.01	32 11 37.1	M2-M4(IR),M4/50 \pm 4	2,7	M4	A _V ,e,NaK	3270	0.86	0.12	...	15.52	0.80	0.98	0.50	12.02	9	yes
194	03 44 27.25	32 10 37.3	M1/26v,>K5(IR),M4.75/100 \pm 10	5,2,7	M4.75	A _V ,e,NaK	3161	0.86	0.090	...	15.88	0.89	1.08	0.71	11.95	9	yes
198	03 44 34.45	32 06 25.0	M5.5/4 \pm 0.5	7	M5.5	A _V ,NaK	3058	0.72	0.12	...	16.07	0.97	0.84	0.45	12.09	9	yes
200	03 43 33.67	32 01 45.4	M5/5 \pm 1	7	M5	A _V ,NaK	3125	0.66	0.10	...	15.65	0.86	0.79	0.35	12.22	3	no
201	03 45 01.49	32 12 29.1	M4/5 \pm 1	8	M4	A _V ,NaK	3270	0.55	0.11	...	15.25	0.71	0.88	0.28	12.12	9	yes
203	03 44 18.10	32 10 53.5	M0-M1.5/30 \pm 10	7	M0.75	A _V ,e	3741	1.28	0.021	1.64	18.24	0.82	2.14	1.63	12.27	9	no
205	03 44 29.80	32 00 54.6	M6/140 \pm 15	8	M6	A _V ,e,NaK	2990	0.66	0.095	...	16.46	1.04	0.76	0.56	12.26	9	yes
207	03 44 30.30	32 07 42.6	K6-M1(IR),M3-M4	2,7	M3.5	A _V	3342	1.78	0.17	2.31	17.16	1.04	1.31	0.55	12.15	9	no
210	03 44 20.02	32 06 45.5	M3.5/9 \pm 0.5	6	M3.5	A _V ,NaK	3342	0.90	0.12	...	15.81	0.78	0.93	0.37	12.22	9	yes
213	03 44 21.27	32 12 37.3	M4.75/6 \pm 2	7	M4.75	NaK	3161	0.59	0.073	...	15.92	0.81	0.83	0.38	12.48	9	yes
214	03 44 07.51	32 04 08.9	M4.75/7 \pm 1.5	7	M4.75	NaK	3161	0.59	0.099	...	15.59	0.81	0.76	0.38	12.22	9	yes
216	03 44 40.80	32 13 06.9	M4/6 \pm 1.5	7	M4	A _V ,NaK	3270	0.97	0.11	...	15.94	0.83	0.99	0.35	12.35	9	yes
217	03 44 43.05	32 10 15.3	M3/4,M4-M6(IR),M5/10 \pm 3	5,2,7	M5	A _V ,NaK	3125	0.90	0.11	...	16.07	0.93	0.90	0.43	12.21	9	yes
218	03 44 44.66	32 07 30.3	M4/8,K6-M1?(IR),M5.25/11 \pm 3	5,2,7	M5.25	A _V ,NaK	3091	1.15	0.11	2.43	16.87	1.08	1.01	0.52	12.27	9	no
221 ^h	03 44 40.24	32 09 33.2	>K5(IR),M4.5/40 \pm 5	2,7	M4.5	A _V ,e,NaK	3198	0.91	0.068	2.08	16.57	0.85	1.08	0.57	12.46	9	yes
223	03 44 41.45	32 13 09.8	M5/5 \pm 1	8	M5	NaK	3125	0.48	0.074	...	15.68	0.81	0.79	0.33	12.44	9	yes
224	03 44 55.36	32 09 34.8	M4.75/7.5 \pm 1	8	M4.75	A _V ,NaK	3161	0.97	0.11	...	16.32	0.92	0.93	0.41	12.30	9	yes
226 ^h	03 44 31.42	32 11 29.4	M2-M4(IR),M5.25/3 \pm 1	2,7	M5.25	NaK	3091	0.47	0.078	...	15.74	0.85	0.76	0.39	12.36	9	yes

Table 2—Continued

ID	α (J2000) ^a h m s	δ (J2000) ^a ° ' "	Spectral Type/ W_λ (H α) ^b	Ref	Adopt	Member ^c -ship	T_{eff} ^d	A_J	L_{bol}	$R - I^c$	I^f	$I - Z^g$	$J - H$	$H - K_s$	K_s	Ref	IMF?
228	03 44 31.18	32 05 58.8	K7-M2/200 \pm 50	7	M0.5	A_V, e	3778	1.95	0.097	...	18.28	0.98	1.64	1.25	12.18	9	no
229	03 44 57.86	32 04 01.8	M5.25/4.5 \pm 0.5	8	M5.25	NaK	3091	0.33	0.071	...	15.69	0.81	0.76	0.35	12.37	9	yes
230	03 44 35.52	32 08 04.5	>K5(IR),M5.25	2,7	M5.25	A_V, NaK	3091	0.81	0.094	...	16.30	0.95	0.88	0.44	12.34	9	yes
237	03 44 23.57	32 09 34.0	M3/5,M5/7,M4-M6?(IR)	5,2,2	M5	A_V, NaK	3125	0.48	0.074	...	15.74	0.81	0.80	0.40	12.36	9	yes
240	03 44 52.10	32 04 46.9	M3.5-M4.5	8	M4	A_V, NaK	3270	0.86	0.094	...	16.05	0.80	0.90	0.35	12.50	9	yes
241	03 44 59.84	32 13 32.2	M4.5/80 \pm 8	7	M4.5	A_V, e, NaK	3198	0.90	0.086	...	16.21	0.87	1.01	0.44	12.39	9	yes
242	03 44 32.80	32 04 13.3	M5/30 \pm 15	8	M5	A_V, NaK	3125	0.45	0.065	0.76	0.41	12.50	9	yes
243	03 44 07.71	32 05 05.1	M4.5/3 \pm 0.5	7	M4.5	A_V, NaK	3198	1.10	0.089	2.15	16.71	0.93	1.03	0.50	12.48	9	yes
247	03 44 37.33	32 07 11.1	M4.75	7	M4.75	A_V, NaK	3161	1.39	0.12	2.42	17.04	1.05	1.06	0.52	12.42	9	no
248	03 44 35.95	32 09 24.3	>K5(IR),M5.25/30 \pm 5	2,7	M5.25	A_V, NaK, e	3091	0.78	0.070	...	16.56	0.94	0.90	0.52	12.53	9	yes
252	03 44 29.12	32 07 57.4	M4/4,M0-M3(IR),M4.5	5,2,7	M4.5	NaK	3198	0.55	0.072	...	15.79	0.77	0.82	0.33	12.55	9	yes
253	03 44 31.65	32 06 53.4	M5.5/11 \pm 1	7	M5.5	A_V, NaK	3058	0.62	0.086	...	16.10	0.94	0.76	0.40	12.42	9	yes
254	03 43 53.80	32 07 30.3	M4.25/4 \pm 1	7	M4.25	A_V, NaK	3234	0.79	0.090	...	16.07	0.81	0.84	0.34	12.53	9	yes
255	03 44 35.70	32 04 52.7	M5.75/6.5 \pm 1	7	M5.75	NaK	3024	0.22	0.056	...	16.10	0.87	0.69	0.39	12.62	9	yes
256	03 43 55.27	32 07 53.4	M5.75/34 \pm 2	8	M5.75	e, NaK	3024	0.36	0.068	...	16.08	0.91	0.62	0.43	12.56	9	yes
259A ¹	03 44 03.64	32 02 35.1	M4.5-M6,M5/11 \pm 2	8,7	M5	A_V, NaK	3125	0.45	0.040	...	16.44	0.80	0.66	0.37	12.51	9	yes
259B	03 44 03.61	32 02 33.1	0.52	0.040	...	16.57	0.82	yes
261	03 43 48.62	32 13 50.9	M5/6 \pm 0.5	7	M5	A_V, NaK	3125	0.28	0.060	...	15.86	0.75	0.61	0.34	12.64	9	no
262	03 44 55.93	32 07 26.9	M4.75/5 \pm 1	7	M4.75	A_V, NaK	3161	0.69	0.075	...	16.15	0.84	0.85	0.36	12.56	9	yes
266	03 44 18.26	32 07 32.5	M4.75/4.5 \pm 0.5	8	M4.75	A_V, NaK	3161	0.69	0.078	...	16.04	0.84	0.80	0.36	12.57	9	yes
276	03 44 09.20	32 02 37.9	K7-M1/35 \pm 15	7	M0	A_V, e	3850	1.76	0.092	1.77	19.06	0.96	1.42	1.06	12.49	9	no
277	03 44 39.44	32 10 08.2	M5/5 \pm 1	8	M5	A_V, NaK	3125	0.55	0.057	...	16.06	0.83	0.81	0.35	12.75	9	yes
278	03 44 31.03	32 05 45.9	M5.5/6.5 \pm 1	7	M5.5	A_V, NaK	3058	0.69	0.061	...	16.75	0.96	0.85	0.42	12.76	9	yes
285	03 44 31.84	32 12 44.2	M4-M5	8	M4.5	A_V	3198	1.90	0.093	2.58	18.08	1.20	1.35	0.65	12.76	9	no
286	03 45 06.71	32 09 30.7	M5.75/6 \pm 1	8	M5.75	A_V, NaK	3024	0.48	0.061	0.75	0.37	12.74	9	yes
287	03 44 41.12	32 08 07.5	M5-M5.5	2	M5.25	A_V, NaK	3091	1.44	0.071	2.60	17.97	1.17	1.14	0.59	12.86	9	no
291	03 44 34.05	32 06 56.9	M7.25/45 \pm 5	7	M7.25	A_V, e, NaK	2838	0.30	0.032	...	17.09	1.10	0.79	0.55	12.73	9	yes
292	03 43 59.88	32 04 41.5	M4.5-M6.5,M5.75/13 \pm 1	8,7	M5.75	A_V, NaK	3024	0.49	0.048	2.30	16.78	0.95	0.78	0.46	12.89	9	yes
294	03 44 24.58	32 10 02.9	M4.5	2	M4.5	NaK	3198	0.45	0.040	...	16.32	0.74	0.85	0.35	13.04	9	yes
295	03 44 29.52	32 04 04.5	M5-M5.5/10?,M5	8,7	M5	A_V, NaK	3125	1.17	0.071	2.38	17.16	1.02	0.92	0.47	12.89	9	no
298	03 44 38.88	32 06 36.4	M6/10 \pm 1	7	M6	NaK	2990	0.31	0.047	2.27	16.60	0.95	0.72	0.44	12.82	9	yes
300	03 44 38.98	32 03 19.8	M5/110 \pm 10	7	M5	A_V, e, NaK	3125	0.52	0.046	...	16.40	0.82	0.76	0.46	12.89	9	yes
301	03 44 22.70	32 01 42.4	M4.5-M5.5/30?,M4.75/40 \pm 5	8,7	M4.75	A_V, e, NaK	3161	1.74	0.055	2.65	18.70	1.15	1.35	0.84	12.96	9	no
302	03 44 20.28	32 05 43.7	M4.75/4 \pm 0.5	7	M4.75	A_V, NaK	3161	1.17	0.075	2.27	17.04	0.99	0.92	0.47	12.85	9	no
303	03 44 04.43	32 04 54.0	M5.75/9 \pm 4	7	M5.75	A_V, NaK	3024	0.47	0.050	...	16.60	0.94	0.68	0.44	12.94	9	yes
308	03 44 21.23	32 01 14.6	M3-M5	7	M4	A_V	3270	3.00	0.072	...	21.03	1.42	1.94	1.16	13.08	9	no
309	03 44 31.34	32 09 29.2	M3/10	5	M3	A_V	3415	1.80	0.14	2.46	16.75	0.92	0.78	0.41	13.09	9	no
312	03 43 55.09	32 07 14.6	M6	8	M6	A_V, NaK	2990	0.41	0.046	2.32	16.80	0.99	0.68	0.43	13.01	9	yes
314	03 44 22.56	32 01 27.8	M4.5-M5.5	8	M5	A_V	3125	1.60	0.049	2.62	18.80	1.16	1.33	0.72	13.08	9	no
316	03 44 57.73	32 07 41.9	M6.5/4 \pm 1	7	M6.5	NaK	2935	0.35	0.033	2.48	17.18	1.05	0.74	0.48	13.05	9	yes
319	03 45 01.00	32 12 22.5	M5.5/16 \pm 1	8	M5.5	e, NaK	3058	0.31	0.038	...	16.51	0.85	0.77	0.38	13.03	9	yes
322	03 44 19.59	32 02 24.9	M4/9 \pm 2,M4.25	8,7	M4.25	A_V, NaK	3234	1.25	0.053	2.25	17.53	0.90	1.04	0.52	13.18	9	no
324	03 44 45.23	32 10 55.9	M5.5-M6/25 \pm 12	2	M5.75	A_V, NaK	3024	0.53	0.034	2.33	17.14	0.96	0.91	0.45	13.20	9	yes
325	03 44 30.06	32 08 49.0	M6	2	M6	A_V, NaK	2990	0.86	0.044	2.72	17.55	1.07	0.88	0.56	13.19	9	yes

Table 2—Continued

ID	α (J2000) ^a h m s	δ (J2000) ^a ° ' "	Spectral Type/ W_λ (H α) ^b	Ref	Adopt	Member ^c -ship	T_{eff}^d	A_J	L_{bol}	$R - I^e$	I^f	$I - Z^g$	$J - H$	$H - K_s$	K_s	Ref	IMF?
329	03 44 15.58	32 09 21.9	M7.5/15±2	7	M7.5	A _V ,e,NaK	2795	0.16	0.018	2.53	17.64	1.12	0.72	0.52	13.33	9	yes
334	03 44 26.66	32 02 36.4	M5.75/27±1	8	M5.75	e,NaK	3024	0.36	0.033	2.28	16.88	0.88	0.73	0.44	13.25	9	yes
335	03 44 44.24	32 08 47.5	M5.75/6	2	M5.75	NaK	3024	0.73	0.040	2.42	17.34	1.03	0.80	0.48	13.28	9	yes
336	03 44 32.36	32 03 27.4	M5-M6/200±50	8	M5.5	e	3058	0.68	0.028	2.28	17.63	0.97	0.84	0.52	13.50	9	yes
341	03 44 12.98	32 13 15.7	M5.25	7	M5.25	NaK	3091	0.62	0.039	2.19	16.77	0.88	0.80	0.42	13.19	9	yes
342	03 44 41.32	32 04 53.5	M5/7±1	7	M5	A _V ,NaK	3125	0.90	0.046	2.27	17.02	0.91	0.83	0.40	13.26	9	yes
344	03 45 00.64	32 08 19.3	M4.5-M5.5/6±2,M4.5/5.5±1	8,7	M4.5	NaK	3198	0.45	0.037	...	16.36	0.74	0.74	0.30	13.27	9	yes
347	03 44 27.28	32 07 17.6	M4.75/4.5±0.5	7	M4.75	A _V ,NaK	3161	0.65	0.038	2.01	16.72	0.81	0.81	0.36	13.29	9	yes
350	03 44 19.18	32 05 59.9	M5.75/10±1	7	M5.75	NaK	3024	0.44	0.038	2.25	16.91	0.94	0.72	0.38	13.22	9	yes
351	03 44 25.76	32 09 06.0	M5.5	2	M5.5	A _V ,NaK	3058	0.88	0.040	2.43	17.62	1.02	0.93	0.49	13.27	9	yes
353	03 44 38.16	32 10 21.6	M6/12	2	M6	NaK	2990	0.44	0.035	2.46	16.87	0.94	0.76	0.45	13.25	9	yes
355	03 44 39.21	32 08 13.8	M8	2	M8	NaK	2710	0.38	0.016	2.76	18.17	1.25	0.85	0.57	13.46	9	yes
358	03 44 12.76	32 10 55.3	M5.5/6±0.5	7	M5.5	NaK	3058	0.26	0.024	2.07	16.79	0.82	0.69	0.36	13.56	9	yes
360	03 44 43.72	32 10 48.1	M4/8,M4.75/9	5,2	M4.75	NaK	3161	0.24	0.024	...	16.40	0.71	0.70	0.30	13.54	9	yes
363	03 44 17.27	32 00 15.4	M8/12±4	8	M8	NaK	2710	0.19	0.013	2.62	17.97	1.11	0.76	0.56	13.60	9	yes
365	03 44 10.23	32 07 34.5	M5.75/4±1	7	M5.75	A _V ,NaK	3024	0.40	0.028	2.22	17.26	0.93	0.72	0.47	13.45	9	yes
366	03 44 35.01	32 08 57.4	M4.75/5	2	M4.75	NaK	3161	0.83	0.032	...	17.33	0.88	0.79	0.45	13.60	9	yes
367	03 43 59.16	32 05 56.7	M6-M7,M5.75/8±1	8,7	M5.75	NaK	3024	0.52	0.029	2.32	17.36	...	0.73	0.46	13.49	9	yes
373	03 44 27.97	32 05 19.6	M5.5/13.5±1	7	M5.5	NaK	3058	0.35	0.021	2.10	17.18	0.86	0.70	0.40	13.74	9	yes
382	03 44 30.95	32 02 44.2	M6-M7/60±20,M5-M6/60±30	8,7	M5.5	A _V ,e,NaK	3058	1.44	0.032	2.63	18.95	1.25	1.01	0.70	13.77	9	no
385	03 44 28.87	32 04 22.9	M5.75/10±1	7	M5.75	A _V ,NaK	3024	0.78	0.027	2.45	17.94	1.05	0.77	0.49	13.79	9	yes
391	03 44 46.59	32 09 01.9	M5.75/11±1.5	7	M5.75	A _V ,NaK	3024	1.08	0.026	2.63	18.63	1.14	0.97	0.56	13.85	9	yes
396	03 44 02.33	32 10 15.6	M5.25/7±1.5	7	M5.25	A _V ,NaK	3091	0.87	0.029	2.45	17.57	0.91	0.80	0.44	13.74	9	yes
405	03 44 21.15	32 06 16.6	M8/8±2	8	M8	NaK	2710	0.20	0.010	2.62	18.34	1.20	0.72	0.57	13.91	9	yes
407	03 45 04.13	32 05 04.7	M6.5-M7.5/100±20	8	M7	A _V ,e,NaK	2880	0.76	0.0062	2.77	19.50	1.10	0.96	0.67	14.69	9	yes
413	03 44 45.66	32 11 10.9	M4/3,M4.75	5,2	M4.75	A _V ,NaK	3161	0.97	0.028	2.39	17.29	0.82	0.79	0.36	13.97	9	yes
414	03 44 44.29	32 10 37.0	M5.25/7	2	M5.25	NaK	3091	0.68	0.017	2.33	17.68	0.85	0.73	0.37	14.31	9	yes
415	03 44 29.97	32 09 39.5	M6-M7/250±30,M6.5/160±20	2,7	M6.5	A _V ,e,NaK	2935	0.82	0.022	2.72	18.43	1.23	0.84	0.66	13.70	9	yes
432	03 44 45.94	32 03 57.0	M5-M6.5	8	M5.75	A _V	3024	0.81	0.025	2.48	18.18	1.05	0.87	0.56	13.71	9	yes
435	03 44 30.29	32 11 35.2	M1.5-M3/155±15	7	M2.25	A _V ,e	3524	0.75	0.0050	1.45	19.19	0.71	1.21	0.84	14.90	9	no
437	03 43 56.38	32 09 59.1	M7.25	7	M7.25	NaK	2838	0.36	0.0099	2.67	18.61	1.08	0.79	0.52	14.10	9	yes
454	03 44 41.58	32 10 39.5	M5.75/140±20	2	M5.75	e,NaK	3024	0.37	0.014	2.14	17.81	0.95	0.77	0.41	14.20	9	yes
456	03 45 05.32	32 12 16.4	M5-M6/38±5	8	M5.5	A _V ,e,NaK	3058	0.81	0.022	2.47	17.95	0.96	0.84	0.47	13.96	9	yes
462	03 44 24.46	32 01 43.8	M2-M4/∼200	6	M3	A _V ,e	3415	2.32	0.062	2.50	19.18	1.20	1.09	0.77	13.81	9	no
468	03 44 11.07	32 01 43.7	M8.25/400±50	7	M8.25	A _V ,e,NaK	2632	0.61	0.0045	...	20.55	1.38	1.11	0.82	14.60	9	yes
478	03 44 35.94	32 11 17.5	M6-M7/100±20	2	M6.25	A _V ,e,NaK	2962	0.56	0.0097	2.52	18.50	1.04	0.85	0.49	14.54	9	yes
486	03 44 59.10	32 10 11.2	M5.75	7	M5.75	A _V ,NaK	3024	0.61	0.0063	2.31	19.27	1.01	0.89	0.43	15.13	9	yes
555	03 44 41.23	32 06 27.2	M5.75/28±3	7	M5.75	A _V ,e,NaK	3024	0.43	0.039	2.31	16.86	0.91	0.74	0.44	13.10	9	yes
598	03 44 25.80	32 10 58.8	M6-M9?	7	M6	A _V	2990	1.38	0.0056	...	21.65	1.25	1.69	0.92	14.77	9	no
603	03 44 33.42	32 10 31.4	M8.5/35±5	7	M8.5	e,NaK	2555	0.11	0.0035	...	19.95	1.18	0.72	0.59	15.02	9	yes
611	03 44 30.36	32 09 44.7	M8	8	M8	NaK	2710	0.33	0.0040	...	19.61	1.17	0.86	0.50	14.99	9	yes
613	03 44 26.88	32 09 26.2	M8.25	8	M8.25	NaK	2632	0.28	0.0024	...	19.80	1.12	0.85	0.61	15.40	9	yes
621	03 44 37.64	32 08 32.9	M5-M6/300±100	7	M5.5	A _V ,e	3058	0.93	0.00095	...	21.73	1.03	1.59	0.68	16.54	9	no
622	03 44 31.34	32 08 11.5	M6/95±10	7	M6	A _V ,e,NaK	2990	0.59	0.0023	...	20.13	1.02	0.63	0.52	16.39	9	no

Table 2—Continued

ID	α (J2000) ^a h m s	δ (J2000) ^a ° ' "	Spectral Type/ W_λ (H α) ^b	Ref	Adopt	Member ^c -ship	T_{eff} ^d	A_J	L_{bol}	$R - I$ ^e	I^f	$I - Z$ ^g	$J - H$	$H - K_s$	K_s	Ref	IMF?
624	03 44 26.36	32 08 09.9	M8.5-M9.25	7	M9	NaK	2400	0.45	0.0015	...	21.55	1.31	0.84	0.61	16.25	9	yes
690	03 44 36.39	32 03 05.5	M8.75/40 \pm 20	7	M8.75	e,NaK	2478	0.14	0.0028	...	20.02	1.22	0.84	0.49	15.29	9	yes
694	03 45 00.46	32 03 20.4	M5.5	7	M5.5	A_V ,NaK	3058	1.69	0.043	2.76	19.58	1.34	1.43	0.88	13.12	9	no
703	03 44 36.62	32 03 44.3	M8/140 \pm 30	7	M8	A_V ,e,NaK	2710	0.49	0.0035	...	20.10	1.22	0.95	0.56	15.14	9	yes
705	03 44 27.18	32 03 46.6	M8.5-M9.25	7	M9	NaK	2400	0.66	0.0030	...	20.93	1.43	0.84	0.48	15.79	9	yes
725	03 44 33.69	32 05 20.5	M5.5-M6.5/90 \pm 20	7	M6	A_V ,e	2990	0.14	0.00087	...	20.91	0.89	0.79	0.38	16.99	9	no
738	03 44 33.69	32 05 46.7	M8.75/70 \pm 40	7	M8.75	e,NaK	2478	0.07	0.0012	...	20.92	1.16	0.57	0.71	16.19	9	yes
761	03 44 19.66	32 06 45.9	M6.5-M7.5/28 \pm 7	7	M7	e,NaK	2880	0.49	0.0089	...	20.03	1.14	0.33	0.79	14.54	9	yes
906	03 45 03.61	32 12 14.0	M8.25	7	M8.25	...	2632	0.00	0.0016	...	20.08	1.08	0.78	0.50	15.78	9	yes
935	03 44 26.91	32 12 50.6	M8.25	7	M8.25	NaK	2632	0.00	0.0028	2.17	19.32	1.09	0.73	0.61	15.09	9	yes
1434	03 44 22.97	32 07 18.9	M5.5-M6.5/40 \pm 15	7	M6	A_V ,e,NaK	2990	1.14	0.0018	...	21.11	1.18	0.95	0.18	17.26	9	no
1676	03 45 01.09	32 02 26.3	M5.75/9.5 \pm 1.5	7	M5.75	NaK	3024	0.35	0.034	2.22	16.74	0.90	0.72	0.38	13.24	9	yes
1684	03 44 23.30	32 01 54.5	M5.75/13.5 \pm 1.5	7	M5.75	NaK	3024	0.46	0.026	2.32	17.29	0.92	0.73	0.48	13.57	9	yes
1719	03 44 59.20	32 17 32.1	M2.25/5 \pm 2	7	M2.25	A_V	3524	1.85	0.31	2.22	16.66	1.00	1.38	0.51	11.69	9	no
1868	03 45 01.59	32 13 17.0	M4	7	M4	A_V ,NaK	3270	1.00	0.059	...	16.89	0.84	1.01	0.40	12.99	9	yes
1928	03 45 05.43	32 03 08.1	M5.5/25 \pm 10	7	M5.5	A_V ,e,NaK	3058	0.79	0.12	...	16.96	0.99	0.74	0.48	12.20	9	yes
1936	03 45 04.26	32 03 05.8	M4.25/3.5 \pm 0.5	7	M4.25	A_V ,NaK	3234	0.62	0.056	...	16.18	0.76	0.81	0.35	12.89	9	yes
1937	03 45 05.77	32 03 08.2	M0/3 \pm 0.5	7	M0	A_V	3850	0.48	0.54	...	13.51	0.54	0.82	0.24	10.71	3	yes
1939	03 44 52.75	32 00 56.8	M4.75/3 \pm 0.5	7	M4.75	NaK	3161	0.38	0.16	...	14.74	0.75	0.86	0.35	11.43	9	yes
1940	03 45 01.09	32 03 20.2	M4.25/5 \pm 1	7	M4.25	A_V ,NaK	3234	0.38	0.047	...	15.87	0.69	0.75	0.29	12.96	9	yes
4044	03 44 16.19	32 05 41.0	M8.5-M9.25/>100	7	M9	e,NaK	2400	0.45	0.0017	...	21.47	1.39	0.93	0.62	15.97	9	yes
10289	03 45 32.30	32 03 14.9	M3/7 \pm 1	7	M3	NaK	3415	0.34	0.13	...	14.55	0.59	0.75	0.25	11.89	3	no
10343	03 45 25.15	32 09 30.2	M3.75/45 \pm 5	7	M3.75	A_V ,e	3306	0.74	0.40	...	14.23	0.75	0.94	0.52	10.59	3	no
10352	03 45 20.46	32 06 34.4	M1/11.5 \pm 1	7	M1	A_V ,e	3705	0.90	1.4	...	13.31	0.69	1.13	0.64	9.35	3	no
10363	03 45 30.61	32 01 55.6	K6/0.6 \pm 0.3	7	K6	A_V	4205	0.66	0.71	...	13.29	0.54	0.79	0.30	10.57	3	no

^aFrom the 2MASS Point Source Catalog for 1, 2, 3, 4, 6, 7, 8, 10, 16, 19, 63, 88, 90, 122, 242, 286, and 367. The coordinates for 91 are derived in the manner described in § 4.1. All other coordinates are from the I -band images in this work.

^bMeasurement uncertainties for the optical spectral types from Luhman (1999) and this work are ± 0.5 and 0.25 subclass for K and M types, respectively, unless noted otherwise. For W_λ (H α) from Luhman et al. (1998b), Luhman (1999), and this work, uncertainties are 0.5-1 Å unless noted otherwise.

^cMembership in IC 348 is indicated by $A_V \gtrsim 1$ and a position above the main sequence for the distance of IC 348 (“ A_V ”), emission lines (“e”), spectral features such as Na I and K I (“NaK”), K_s excess emission (“ex”), or proper motion measurements (“pm”; Fredrick (1956)).

^dTemperature scale from Schmidt-Kaler (1982) ($\leq M0$) and Table 8 ($> M0$).

^eFrom Luhman (1999) for stars with $R - I \geq 1.5$ and for 435 and from Herbig (1998) for the remaining objects.

^fFrom Herbig (1998) for 16, 33, 63, 71, 88, 90, and 91, from Luhman (1999) for 367, and from this work for the remaining objects.

^gFrom this work.

^hSources 1, 6, 9, 52, 86, 92, 221, and 226 are resolved as binaries with separations of 0''.61, 0''.559, 0''.409, 1''.028, 0''.249, 0''.26, 0''.13, and 0''.70 and magnitude differences of $\Delta H = 0.14, 1.49, 1.84, 1.48, 0.67, 0.67, 1.35,$ and 0.75, respectively (Duchêne et al. 1999).

ⁱ $R - I$ and JHK_s are for A+B.

^j JHK_s are for A+B.

^kSpectral type and JHK_s are for A+B. L_{bol} is for A.

^lSpectral type and JHK_s are for A+B.

References. — (1) Harris et al. (1954); (2) Luhman et al. (1998b); (3) 2MASS Point Source Catalog; (4) Strom et al. (1974); (5) Herbig (1998); (6) Measurements described by Luhman (1999) and presented here for the first time; (7) this work; (8) Luhman (1999); (9) Muench et al. (2003).

Table 3. Foreground Stars

ID	$\alpha(\text{J2000})^{\text{a}}$ h m s	$\delta(\text{J2000})^{\text{a}}$ ° ' "	Spectral Type	Ref	Foreground ^b Evidence	$R - I^{\text{c}}$	I^{d}	$I - Z^{\text{d}}$	$J - H^{\text{e}}$	$H - K_s^{\text{e}}$	K_s^{e}
18	03 43 58.04	32 09 47.1	F8	1	pm	0.28	0.13	9.36
28	03 44 21.06	32 07 38.7	F8	1	pm	0.30	0.11	9.62
54	03 44 49.59	32 16 45.7	K1-K2	2	Li, A_V	...	12.04	0.32	0.50	0.16	10.50
57	03 44 48.51	32 15 28.1	K3-K4	2	pm	...	12.45	0.36	0.68	0.15	10.56
77	03 44 43.44	32 08 17.4	M1,K5-M0(IR)	3,2	pm	0.96	12.90	0.37	0.62	0.23	10.85
107	03 43 55.81	32 19 44.3	M1,K6-M1(IR)	2,2	pm	...	13.33	0.45	0.68	0.26	11.21
121	03 44 25.95	32 16 30.7	K4-K7(IR)	2	pm	...	13.39	0.37	0.80	0.12	11.36
134	03 43 59.88	32 11 16.2	M3.5,M2-M4(IR)	2,2	pm	...	13.56	0.49	0.64	0.20	11.34
189	03 43 41.52	32 15 00.2	M0	2	Li, A_V	...	14.33	0.41	0.62	0.27	12.06
281	03 44 06.82	32 04 40.9	M2.5	4	pm	...	15.09	0.51	0.61	0.26	12.79
320	03 43 34.44	32 18 44.2	pm	...	16.48	0.59	1.00	0.31	13.31
326	03 43 53.26	32 13 00.2	pm	...	15.76	0.55	0.56	0.25	13.35
354	03 44 59.56	32 14 24.9	pm	...	15.90	0.57	0.63	0.22	13.50
400	03 43 43.93	31 59 43.2	pm	1.60	17.05	0.62	0.68	0.27	14.54
404	03 44 44.47	32 10 05.8	M3,M3,M3	3,2,5	A_V	1.52	16.65	0.57	0.68	0.23	14.16
958	03 44 55.49	32 13 07.9	M5.5	5	A_V ,NaK	2.32	19.36	0.80	0.76	0.32	16.07
1674	03 45 13.57	32 00 20.5	pm	1.42	16.64	0.50	0.60	0.01	14.34
1696	03 45 05.92	32 08 26.5	pm	0.98	17.54	0.40	0.68	0.07	15.38
1701	03 45 03.04	32 11 25.7	pm	1.04	17.42	...	0.69	0.12	15.07
1788	03 44 02.08	32 20 24.7	pm	0.86	17.40	0.34	0.56	0.45	15.30

^aFrom the 2MASS Point Source Catalog for 18 and 28. All other coordinates are from the I -band images in this work.

^bForeground nature is indicated by proper motion measurements (“pm”; Blaauw (1952); Scholz et al. (1999)) or a combination of no Li absorption (“Li”), $A_V \sim 0$ (“ A_V ”), and spectral features such as strong Na I and K I (“NaK”; Luhman et al. (1998b); this work).

^cFrom Herbig (1998) for 77 and from Luhman (1999) for the remaining objects.

^dFrom this work.

^eFrom 2MASS for 18, 28, 54, 57, 77, 189, 320, 400, and 1788 and from Muench et al. (2003) for the remaining objects.

References. — (1) Fredrick (1956); (2) Luhman et al. (1998b); (3) Herbig (1998); (4) Measurements described by Luhman (1999) and presented here for the first time; (5) this work.

Table 4. Background Stars

ID	α (J2000) ^a h m s	δ (J2000) ^a ° ' "	Spectral Type	Ref	$R - I^b$	I^c	$I - Z^d$	$J - H^e$	$H - K_s^e$	K_s^e
14	03 44 54.95	32 12 11.3	K0-III,K1-2III(IR)	1,1	...	12.77	0.77	1.04	0.43	8.93
27	03 43 36.16	32 13 32.9	F7-G6,giant(IR)	1,2	...	12.57	0.54	0.83	0.29	9.68
34	03 44 15.48	32 02 35.1	G8III(IR)	1	2.28	16.91	1.18	1.98	0.98	9.89
43	03 45 03.19	32 04 05.7	giant(op,IR)	3,2	...	14.64	0.83	1.21	0.45	10.29
73	03 45 09.64	32 16 03.6	giant	2	...	13.73	0.55	0.83	0.28	10.81
80	03 44 27.88	32 10 52.2	K1III(IR)	1	2.60	18.52	1.35	2.19	1.03	10.87
84	03 44 42.14	32 02 57.8	giant(op,IR)	3,2	...	15.04	0.74	1.19	0.39	11.01
89	03 44 57.58	32 12 24.4	giant(op,IR)	3,2	...	14.40	0.71	0.99	0.28	11.04
106	03 44 14.13	32 10 28.3	giant	2	1.49	14.65	0.72	0.91	0.37	11.26
114	03 44 05.77	32 12 29.0	giant	2	...	13.85	0.53	0.77	0.17	11.35
127	03 44 59.79	32 06 47.9	F2-F5,<F8(IR)	1,1	...	13.53	0.44	0.59	0.14	11.36
131	03 43 46.81	32 15 08.9	F0-F4,<F8(IR)	1,1	...	13.45	0.41	0.54	0.20	11.41
143	03 44 16.51	32 05 32.7	F(op,IR)	2	1.85	16.50	0.97	1.26	0.58	11.50
152	03 43 47.54	32 19 43.8	F0-F6	1	...	13.56	0.38	0.52	0.20	11.71
164	03 43 57.27	32 12 57.8	giant	2	...	14.56	0.53	0.79	0.19	11.85
195	03 44 08.06	32 06 56.4	early or giant	2	...	16.28	0.83	1.01	0.46	12.10
206	03 43 54.53	32 10 14.0	giant	2	1.26	15.11	...	0.85	0.24	12.22
212	03 44 30.13	32 01 18.3	early or giant	3	2.61	18.73	1.15	1.68	0.85	12.34
219	03 44 29.70	32 05 52.1	late F/early G(op,IR)	2	...	16.09	0.78	0.96	0.40	12.29
232	03 44 36.41	32 09 19.7	F7-G7(IR)	1	...	17.71	1.02	1.26	0.61	12.46
235	03 44 20.92	32 12 37.5	giant	2	...	15.65	0.59	0.81	0.26	12.79
236	03 44 59.54	32 10 39.6	giant	3	...	14.68	0.49	0.68	0.17	12.36
246	03 44 46.24	32 03 12.9	early or giant	3	...	15.69	0.63	0.84	0.30	12.57
269	03 44 34.36	32 04 21.8	early or giant	2	...	16.65	0.79	1.00	0.38	12.72
282	03 44 57.63	32 07 01.8	early or giant	3	...	15.30	0.52	0.70	0.21	12.79
284	03 44 56.83	32 05 45.3	early	2	...	15.15	0.48	0.62	0.20	12.85
311	03 44 41.06	32 02 17.0	early or giant	3	1.91	17.88	0.87	1.36	0.52	13.08
317	03 44 46.01	32 12 05.5	early or giant	3	2.09	18.46	1.07	1.38	0.62	13.16
339	03 45 00.40	32 12 48.4	early or giant	3	...	15.95	0.54	0.73	0.21	13.42
352	03 44 23.76	32 11 56.0	early or giant	1	1.69	17.45	0.77	1.22	0.43	13.36
369	03 45 07.49	32 09 09.5	early or giant	3	...	16.53	0.54	0.99	0.20	13.56
370	03 45 06.87	32 12 42.6	giant	2	1.34	16.98	...	1.00	0.24	13.81
384	03 44 24.34	32 07 58.6	early or giant	3	...	18.72	0.95	1.38	0.51	13.82
434	03 44 20.58	32 03 12.2	early or giant	2	...	20.46	1.21	1.70	0.65	14.35
442	03 44 40.67	32 09 41.3	early or giant	1	1.33	17.40	0.69	0.87	0.34	14.09
450	03 44 01.93	32 11 21.9	early or giant	2	1.06	16.76	0.48	0.77	0.17	14.25
479	03 44 51.54	32 04 29.3	M2.5-M3.5	2	2.67	19.92	1.00	1.31	0.64	14.77
547	03 44 31.32	32 07 29.7	giant	3	...	18.86	0.15	0.93	0.40	15.71
548	03 44 33.32	32 07 52.3	early or giant	3	1.75	19.91	...	1.33	0.32	15.79
550	03 44 36.42	32 10 29.2	early or giant	3	2.52	19.22	0.90	1.53	0.51	14.40
609	03 44 44.91	32 09 37.5	early or giant	2	...	21.15	0.77	1.14	0.82	16.43
618	03 44 43.94	32 08 37.0	M2.5-M3.5	2	...	20.87	0.98	1.23	0.48	16.58
630	03 44 25.51	32 07 46.0	early or giant	2	...	22.78	1.31	1.21	0.12	17.81
631	03 44 33.88	32 07 29.9	M1	3	1.89	19.97	0.87	1.14	0.50	15.49
681	03 44 46.30	32 02 15.0	early or giant	2	...	20.79	0.98	1.34	0.65	15.59
689	03 44 40.54	32 03 03.9	M2-M4	2	...	20.85	1.01	1.06	0.57	15.93
702	03 44 53.56	32 03 43.4	M3-M4.5	2	...	21.04	1.00	1.31	0.63	15.65
709	03 44 56.08	32 03 55.8	M3.5-M4.5	2	2.22	20.37	1.01	1.14	0.52	15.70
713	03 44 54.19	32 04 26.9	M0-M2	2	2.51	20.68	0.90	1.15	0.64	16.27
719	03 44 42.02	32 04 46.6	M1.5-M3.5	2	...	20.72	0.74	0.96	0.51	16.52
741	03 44 01.37	32 05 50.0	early or giant	2	2.25	19.83	1.03	1.42	0.62	14.40
746	03 44 49.96	32 06 14.6	M4-M6	2	...	20.91	0.96	0.88	0.87	16.26
774	03 44 31.52	32 07 06.5	early or giant	2	2.39	20.29	0.77	1.38	0.55	15.83
813	03 44 49.96	32 08 41.3	M2.25	2	2.61	19.79	0.83	1.05	0.41	15.59
817	03 44 50.16	32 08 43.9	M3-M4	2	2.22	20.43	0.89	1.21	-0.03	15.96
829	03 44 56.88	32 09 14.3	M0-M2	3	1.97	18.85	0.66	1.10	0.44	14.82
842	03 44 51.42	32 09 45.9	M3.25	2	2.26	20.01	...	1.05	0.44	15.90
850	03 44 16.98	32 10 13.4	M1-M3	2	...	20.33	0.87	1.17	0.59	15.64

Table 4—Continued

ID	$\alpha(\text{J2000})^{\text{a}}$ h m s	$\delta(\text{J2000})^{\text{a}}$ ° ' "	Spectral Type	Ref	$R - I^{\text{b}}$	I^{c}	$I - Z^{\text{d}}$	$J - H^{\text{e}}$	$H - K_s^{\text{e}}$	K_s^{e}
863	03 44 10.61	32 10 55.1	M0-M1.5	2	3.31	20.13	0.80	1.13	0.51	16.05
934	03 45 03.12	32 12 52.1	M4.5	2	2.50	20.30	0.84	1.15	0.50	16.24
944	03 44 01.91	32 12 53.1	M3.5-M4.5	2	2.27	20.16	0.80	1.04	0.38	16.43
963	03 44 24.14	32 13 14.7	<M1 or giant	2	...	20.22	0.77	1.13	0.45	16.20
983	03 44 28.74	32 13 43.8	M3.5-M4.5	2	...	20.13	1.05	1.24	0.60	15.36
991	03 44 55.37	32 13 51.5	M2-M3.5	2	2.26	19.94	0.99	1.24	0.53	15.25
1010	03 44 04.20	32 14 06.5	M2-M4	2	...	20.22	1.00	1.02	0.53	16.09
1383	03 44 29.59	32 01 37.8	early or giant	2	...	21.50	0.93	1.05	0.66	16.69
1387	03 44 28.68	32 01 50.3	early or giant	2	...	21.35	1.09	1.45	0.48	16.02
1389	03 44 23.41	32 02 28.8	early or giant	2	...	21.15	1.12	1.18	0.52	15.98
1400	03 44 57.39	32 02 58.9	early or giant	2	...	21.06	1.04	1.49	0.74	15.39
1416	03 44 39.03	32 05 14.6	early or giant	2	...	21.77	0.99	0.90	0.09	17.87
1418	03 44 35.57	32 05 18.2	early or giant	2	...	21.50	0.46	1.22	-0.07	17.83
1424	03 44 50.45	32 07 53.9	mid-M	2	...	21.72	0.56	0.61	0.36	18.03
1426	03 44 38.50	32 06 52.4	early or giant	2	...	21.18	0.77	-0.24	0.71	17.29
1432	03 44 03.83	32 06 49.0	early or giant	2	...	21.72	0.96	1.30	0.45	16.93
1461	03 44 57.73	32 08 38.1	M3-M5	2	...	21.02	0.73	0.96	0.60	16.93
1463	03 44 57.50	32 09 43.1	M5-M6	2	...	21.29	1.12	0.88	0.76	16.73
1464	03 45 02.44	32 10 16.8	M4.5-M5.5	2	...	21.24	0.88	0.97	0.34	17.37
1476	03 44 30.41	32 13 10.5	M6-M7/20±10	2	...	21.07	0.82	0.33	0.60	18.00
1481	03 44 16.51	32 10 29.9	early or giant	2	...	20.70	0.76	1.11	0.56	16.29
1483	03 44 03.74	32 08 19.9	M4-M5	2	...	21.46	1.05	0.94	0.69	16.56
1511	03 43 58.72	32 08 30.8	early or giant	2	...	21.32	0.67	1.01	0.43	17.40
1689	03 44 55.42	32 05 16.2	early or giant	2	1.00	17.11	0.48	0.67	0.18	14.69
1863	03 45 12.13	32 10 29.4	giant	2	...	14.01	0.44	0.70	0.14	11.82
1903	03 44 09.90	32 03 03.1	early or giant	2	...	21.86	1.29	1.79	0.83	15.36
1932	03 45 13.56	32 01 20.4	giant	2	...	12.76	0.34	0.65	0.15	10.81
1941	03 45 15.69	32 08 12.7	giant	2	...	13.02	0.52	0.61	0.28	10.47
2096	03 44 12.94	32 13 24.1	M5-M7	2	...	20.97	0.87	0.78	1.31	15.95
2110	03 44 26.50	32 13 52.5	early or giant	2	...	21.28	0.84	1.26	0.74	16.83
3006	03 44 52.58	32 10 06.4	M1-M3	2	...	21.68	0.93
3039	03 45 05.60	32 11 30.6	M2-M4	2	...	21.48	0.79
3042	03 44 46.79	32 11 53.6	early or giant	2	...	21.85	0.73	1.73	0.41	17.06
3051	03 45 04.84	32 12 19.4	early or giant	2	...	21.82	0.85
3086	03 45 02.13	32 13 56.2	M2-M4	2	...	20.97	0.80	0.90	0.46	17.00
4037	03 44 16.56	32 05 25.9	early or giant	2	...	21.84	0.93	1.20	0.30	16.28
4048	03 44 19.61	32 05 57.9	early or giant	2	...	21.30	0.82	0.93	0.59	16.94
4053	03 44 14.89	32 06 12.2	early or giant	2	...	21.58	1.07	1.36	0.77	15.70
4098	03 43 59.83	32 09 22.3	M2-M4	2	...	22.01	0.80	0.89	0.32	17.65
5012	03 44 57.23	32 02 34.2	early or giant	2	...	21.69	0.86	1.31	0.66	16.34
5194	03 44 41.29	32 09 37.0	early or giant	2	...	22.33	0.94	16.87
5200	03 44 49.76	32 09 41.6	early or giant	2	...	21.69	0.97	1.20	0.09	17.77
10226	03 45 26.95	31 56 57.4	giant	2	...	14.11	0.47	0.56	0.22	11.94
10252	03 45 23.49	31 58 57.4	giant	2	...	11.39	0.73	1.01	0.39	7.65
10338	03 45 23.31	32 00 15.9	early	2	...	12.00	0.68	0.66	0.39	9.00

^aFrom the 2MASS Point Source Catalog for 206 and 370 and from Luhman (1999) for 842. All other coordinates are from the I -band images in this work.

^bFrom Herbig (1998) for 106 and 206 and from Luhman (1999) for the remaining objects.

^cFrom Herbig (1998) for 206, from Luhman (1999) for 370 and 842, and from this work for the remaining objects.

^dFrom this work.

^eFrom 2MASS for 14, 27, 34, 43, 73, 80, 131, 1932, 1941, 10226, 10252, and 10338 and from Muench et al. (2003) for the remaining objects.

References. — (1) Luhman et al. (1998b); (2) this work; (3) Measurements described by Luhman (1999) and presented here for the first time.

Table 5. Sources with Uncertain Membership Status

ID	$\alpha(\text{J2000})^{\text{a}}$ h m s	$\delta(\text{J2000})^{\text{a}}$ ° ' "	Spectral Type	Ref	Status ^b	$R - I^{\text{c}}$	I^{d}	$I - Z^{\text{d}}$	$J - H^{\text{e}}$	$H - K_s^{\text{e}}$	K_s^{e}
81	03 44 50.00	32 03 45.7	F2-G2 or giant	1	m or b	...	15.08	0.81	1.04	0.46	10.97
197	03 44 29.11	32 07 51.0	G6-K1(IR)	2	m or b	2.02	17.36	1.00	1.37	0.61	12.15
1927	03 45 07.74	32 00 27.6	K3-K4	3	m or f	...	11.71	0.36	0.63	0.17	9.67

^aFrom the I -band images in this work.

^bm=member, b=background, f=foreground.

^cFrom Luhman (1999).

^dFrom this work.

^eFrom 2MASS for 81 and 1927 and from Muench et al. (2003) for 197.

References. — (1) Measurements described by Luhman (1999) and presented here for the first time; (2) Luhman et al. (1998b); (3) this work.

Table 6. Recent Identifications for Sources in IC 348

ID ^a	Herbig (1998)	Najita et al. (2000)	Preibisch & Zinnecker (2002)	2MASS
1	J03443419+3209462
2	124	J03443536+3210045
3	187	J03445064+3219067
4	254	...	98	J03443118+3206220
5	114	...	73	J03442602+3204304
6	166	...	133	J03443694+3206453
7	J03440847+3207165
8	J03440915+3207093
9	184	063-08	151	J03443916+3209182
10	261	...	66	J03442466+3210150
11	209	J03450796+3204018
12A	139	084-02	...	J03443200+3211439
12B	140	084-01	...	J03443200+3211439
13	J03435964+3201539
14	J03445493+3212110
15	176	J03444472+3204024
16	144	024-06	108	J03443274+3208374
17	J03444770+3219117
18	20	J03435803+3209470
19	252	013-01	94	J03443081+3209558
20	208	J03450762+3210279
21	194	J03445614+3209152
22	3	J03435123+3213091
23	182	015-03	149	J03443871+3208420
24A	157	043-03	122	J03443503+3207370
24B	158	043-02	123	J03443537+3207362
25	J03450142+3205017
26	J03435602+3202132
27	J03433616+3213327
28	89	J03442106+3207386
29	137	023-03	103	J03443153+3208449
30	83	104-04	40	J03441912+3209313
31	79	...	38	J03441816+3204570
32	173	025-03	142	J03443788+3208041
33	143	024-05	106	J03443259+3208424
34	J03441548+3202350
35	187	054-01	153	J03443924+3207355
36	178	054-02	145	J03443845+3207356
37	143	J03443798+3203296
38	103	092-02	62	J03442398+3211000
39	203	J03450174+3214276
40	124	083-03	88	J03442972+3210398
41	94	091-01	51	J03442161+3210376
42A	202	062-05	165	J03444207+3209009
42B	203	062-04	165	J03444207+3209009
43	J03450319+3204055
44	J03440885+3216105
45	104	...	63	J03442428+3210194
46	J03441162+3203131
47	14	...	8	J03435550+3209321
48	155	041-01	119	J03443487+3206337
49	J03435759+3201373
50	192	J03445561+3209198
51	29	J03441297+3201354
52	211	052-06	170	J03444351+3207427
53	70	...	32	J03441642+3209552
54	J03444957+3216454
55	99	J03443137+3200140
56	43	...	20	J03440499+3209537

Table 6—Continued

ID ^a	Herbig (1998)	Najita et al. (2000)	Preibisch & Zinnecker (2002)	2MASS
57	J03444848+3215279
58	179	025-02	146	J03443854+3208006
59	190	073-02	159	J03444011+3211341
60A	110	093-05	71	J03442555+3211307
60B	109	093-04	71	J03442555+3211307
61	97	...	55	J03442228+3205427
62	75	J03442663+3203583
63	22	...	11	J03435890+3211270
64	70	J03442557+3212299
65	148	024-01	114	J03443398+3208541
66	121	033-02	83	J03442847+3207224
67	J03434461+3208177
68	84	J03442851+3159539
69	116	...	77	J03442702+3204436
71	142	024-04	107	J03443257+3208558
72	57	J03442257+3201536
73	J03450964+3216033
74	150	012-01	115	J03443426+3210497
75	214	064-01	173	J03444376+3210304
76	155	J03443979+3218041
77	210	053-02	169	J03444342+3208172
78A	115	022-04	76	J03442668+3208203
78B	115	022-05	76	J03442668+3208203
79	202	J03450151+3210512
80	...	082-03	...	J03442787+3210522
81	J03444998+3203455
82	171	041-02	137	J03443740+3206118
83	170	015-02	138	J03443741+3209009
84	J03444212+3202576
85	81	J03442812+3216002
86	119	033-01	80	J03442787+3207316
87	12	J03435970+3214028
88	145	...	109	J03443276+3209157
89	J03445757+3212240
90	146	...	113	J03443330+3209396
91	185	011-04	152	J03443919+3209448
92	102	032-01	61	J03442366+3206465
93	36	J03441791+3212203
94	J03433205+3206172
95	54	J03442191+3212115
96	154	...	120	J03443486+3209535
97	111	032-03	69	J03442554+3206171
98	180	...	147	J03443860+3205064
99A	85	...	41	...
99B	82
100	56	J03442232+3212007
101	188	J03445096+3216093
103	219	052-04	174	J03444458+3208125
105	63	...	26	J03441125+3206121
106	65	J03441412+3210283
107	J03435580+3219441
108	181	015-01	148	J03443869+3208567
110	...	085-01	139	J03443739+3212241
111	J03434875+3207332
112	178	J03444495+3213364
113	168	014-01	135	J03443719+3209161
114	J03440576+3212287
115	127	023-01	89	J03442999+3209210
116	93	091-02	49	J03442155+3210174

Table 6—Continued

ID ^a	Herbig (1998)	Najita et al. (2000)	Preibisch & Zinnecker (2002)	2MASS
119	92	...	47	J03442125+3205024
120	98	093-02	59	J03442297+3211572
121	J03442595+3216306
122	112	J03443321+3215290
123	64	J03442457+3203571
124	J03435463+3200298
125	95	...	52	J03442166+3206248
127	J03445980+3206476
128	87	104-02	...	J03442017+3208565
129	91	...	48	J03442129+3211563
130	18	J03440424+3213497
131	J03434680+3215087
133	164	J03444173+3212022
134	26	J03435988+3211160
135	J03443918+3220089
136	30	J03441361+3215542
137	J03441143+3219401
138	179	J03444508+3214130
139	107	...	68	J03442530+3210128
140	J03443568+3203035
141	131	...	93	J03443054+3206297
142	16	...	9	J03435619+3208362
143	71	J03441651+3205327
144	144	J03443838+3212597
145	198	071-03	163	J03444129+3210252
146	205	055-01	166	J03444261+3206194
147	2	J03434939+3210398
149	167	015-05	...	J03443698+3208342
150	204	J03450285+3207006
151	153	084-03	118	J03443482+3211180
152	J03434753+3219437
153	206	053-01	...	J03444276+3208337
154	...	085-02	140	J03443777+3212181
156	50	...	22	J03440678+3207540
157	J03441857+3212530
158	191	063-07	158	J03444016+3209129
159	231	075-02	184	J03444760+3210555
160	14	J03440257+3201348
163	62	...	25	J03441122+3208161
164	J03435728+3212576
165	159	014-04	...	J03443545+3208563
166	204	064-05	...	J03444256+3210025
167	195	064-06	...	J03444116+3210100
168	133	083-01	...	J03443134+3210469
169	74	...	35	J03441776+3204476
170	...	082-01	82	J03442842+3211225
171	221	075-05	177	J03444484+3211055
173	J03441012+3204045
174	39	...	17	J03440410+3207170
175	186	J03444978+3203340
176	J03450464+3215010
177	J03450521+3209544
178	185	J03444881+3213218
180	53	J03442176+3212312
182	78	J03441820+3209593
184	250	...	190	J03445374+3206519
186	228	...	181	J03444631+3211165
187A	48	...	21	J03440613+3207070
187B	49	...	21	J03440613+3207070

Table 6—Continued

ID ^a	Herbig (1998)	Najita et al. (2000)	Preibisch & Zinnecker (2002)	2MASS
188	193	J03445611+3205564
189	J03434150+3215000
190	87	J03442922+3201157
191	172	011-03	141	J03443783+3210074
192	J03442364+3201526
193	174	073-03	...	J03443800+3211370
194	117	094-05	...	J03442724+3210373
195	57	J03440806+3206564
197	122	021-07	...	J03442911+3207510
198	152	041-03	116	J03443444+3206250
200	J03433365+3201451
201	J03450148+3212288
203	75	...	37	J03441810+3210534
205	J03442980+3200545
206	10	J03435452+3210139
207	130	021-06	90	J03443030+3207426
210	86	...	44	J03442001+3206455
212	J03443013+3201182
213	J03442127+3212372
214	J03440750+3204088
216	161	J03444078+3213067
217	207	064-04	167	J03444303+3210151
218	220	051-01	175	J03444464+3207301
219	125	045-03	...	J03442970+3205522
221	192	063-03	...	J03444024+3209331
223	J03444144+3213096
224	J03445535+3209344
226	136	084-05	101	J03443141+3211293
228	253	045-01
229	197	J03445785+3204016
230	160	025-04	126	J03443551+3208046
232	165	014-03	...	J03443641+3209196
235	J03442091+3212373
236	J03445952+3210393
237	99	101-01	...	J03442356+3209338
240	242	...	189	J03445209+3204467
241	J03445983+3213319
242	J03443280+3204133
243	56	...	23	J03440770+3205050
246	J03444623+3203127
247	169	042-01	136	J03443732+3207111
248	163	014-02	130	J03443595+3209243
252	123	022-06	86	J03442912+3207573
253	138	044-04	104	J03443165+3206534
254	6	J03435379+3207303
255	161	...	127	J03443569+3204527
256	13	J03435526+3207533
259A	J03440362+3202341
259B	J03440362+3202341
261	J03434862+3213507
262	J03445591+3207266
266	80
269	151	J03443435+3204218
276	24	J03440920+3202376
277	189	011-02	154	J03443943+3210081
278	132	045-02	95	J03443103+3205460
281	51	J03440680+3204407
282	J03445762+3207015
284	J03445682+3205450

Table 6—Continued

ID ^a	Herbig (1998)	Najita et al. (2000)	Preibisch & Zinnecker (2002)	2MASS
285	J03443184+3212441
286	J03450671+3209307
287	196	053-03	...	J03444111+3208073
291	149	043-06
292	29	J03435987+3204414
294	106	101-02	...	J03442457+3210030
295	J03442952+3204045
298	183	042-03	150	J03443886+3206364
300	J03443896+3203196
301	J03442270+3201423
302	88	J03442027+3205437
303	42	...	19	J03440442+3204539
308	J03442122+3201144
309	134	013-05	100	J03443134+3209291
311	J03444104+3202168
312	11	J03435508+3207145
314	J03442256+3201277
316	J03445771+3207416
317	J03444599+3212052
319	J03450100+3212222
320	J03433441+3218442
322	J03441959+3202247
324	223	075-06	180	J03444522+3210557
325	128	023-04	...	J03443005+3208489
326	J03435326+3212599
329	68	105-01	...	J03441558+3209218
334	J03442666+3202363
335	216	062-03	...	J03444423+3208473
336	J03443237+3203274
339	J03450040+3212480
341	J03441297+3213156
342	200	J03444130+3204534
344	201	J03450063+3208190
347	118	033-03	78	J03442728+3207177
350	84	J03441918+3205599
351	113	J03442575+3209059
352	101	093-01	...	J03442375+3211560
353	176	011-01	...	J03443814+3210215
354	J03445954+3214246
355	186	015-06	...	J03443920+3208136
358	64	...	28	J03441276+3210552
360	212	075-07	172	J03444371+3210479
363	J03441726+3200152
365	60	J03441022+3207344
366	156	014-05	...	J03443501+3208573
367	25	J03435915+3205567
369	J03450748+3209091
370	J03450686+3212426
373	120	J03442798+3205196
382	J03443095+3202441
384	105	034-01	...	J03442434+3207586
385	J03442887+3204229
391	259	062-01	...	J03444658+3209017
396	34	J03440233+3210154
400	J03434392+3159429
404	218	064-03	...	J03444445+3210056
405	90
407	J03450414+3205043
413	227	075-03	...	J03444564+3211106

Table 6—Continued

ID ^a	Herbig (1998)	Najita et al. (2000)	Preibisch & Zinnecker (2002)	2MASS
414	217	075-08	...	J03444428+3210368
415	126	013-06	...	J03442997+3209394
432	J03444593+3203567
434	J03442057+3203121
435	129	081-02	91	J03443030+3211353
437	J03435638+3209591
442	193	063-02	...	J03444066+3209411
450	32	J03440192+3211217
454	201	071-01	...	J03444157+3210394
456	J03450531+3212161
462	J03442445+3201437
468	J03441106+3201436
478	162	072-03	...	J03443593+3211175
479	J03445153+3204292
486	J03445909+3210111
547	135	021-08
548	147	021-03
550	164	J03443640+3210292
555	197	055-02	...	J03444121+3206271
598	...	094-04	...	J03442581+3210588
603	...	012-02	...	J03443341+3210314
609	...	061-02
611	...	013-04	...	J03443035+3209446
613	...	102-01	...	J03442685+3209257
618	...	062-06
621	...	015-04
622	...	021-02
624	...	022-09
631	...	043-04
690	J03443638+3203054
694	J03450045+3203201
703	J03443661+3203442
741	J03440136+3205499
774	J03443151+3207066
829	J03445686+3209140
935	J03442691+3212506
983	J03442874+3213437
1426	...	042-02
1434	...	031-01
1674	J03451356+3200203
1676	J03450109+3202260
1684	J03442330+3201544
1689	J03445541+3205159
1696	J03450591+3208261
1701	J03450304+3211254
1719	200	J03445919+3217319
1788	J03440208+3220244
1863	J03451212+3210293
1868	J03450158+3213167
1903	J03440989+3203030
1927	J03450773+3200272
1928	J03450543+3203079
1932	J03451356+3201202
1936	J03450427+3203056
1937	207	J03450577+3203080
1939	J03445274+3200565
1940	J03450108+3203200
1941	J03451569+3208125
10226	J03452694+3156574

Table 6—Continued

ID ^a	Herbig (1998)	Najita et al. (2000)	Preibisch & Zinnecker (2002)	2MASS
10252	J03452349+3158573
10289	J03453230+3203150
10338	J03452331+3200157
10343	J03452514+3209301
10352	J03452046+3206344
10363	J03453061+3201557

^aIdentifications from Luhman et al. (1998b), Luhman (1999), and this work.

Table 7. Adopted Intrinsic Colors

Spectral Type	$R - I$	$I - Z$
K0	0.39	0.23
K1	0.43	0.25
K2	0.47	0.27
K3	0.50	0.29
K4	0.50	0.31
K5	0.63	0.33
K6	0.70	0.35
K7	0.76	0.37
M0	0.75	0.40
M1	0.92	0.43
M2	1.00	0.46
M3	1.10	0.49
M4	1.25	0.55
M5	1.65	0.67
M6	2.10	0.85
M7	2.30	0.98
M8	2.50	1.10
M9	2.50	1.21

Table 8. Adopted Temperature Scale

Spectral Type	$T_{\text{eff}}(\text{K})$
M1	3705
M2	3560
M3	3415
M4	3270
M5	3125
M6	2990
M7	2880
M8	2710
M9	2400

Table 9. Frequencies of Brown Dwarfs and High-Mass Stars

Population	$\mathcal{R}_1 = \frac{N(0.02-0.08)}{N(0.08-10)}$	$\mathcal{R}_2 = \frac{N(1-10)}{N(0.15-1)}$	Reference
Taurus	0.14 ± 0.04	0.08 ± 0.04	1,2
IC 348	0.12 ± 0.03	0.18 ± 0.04	3
Trapezium	0.26 ± 0.04	0.21 ± 0.04	4
Pleiades	...	0.27 ± 0.02	5
M35	...	0.22 ± 0.01	6

References. — (1) Briceño et al. (2002); (2) Luhman et al. (2003a); (3) this work; (4) Luhman et al. (2000); (5) Bouvier et al. (1998); (6) Barrado y Navascués et al. (2001).

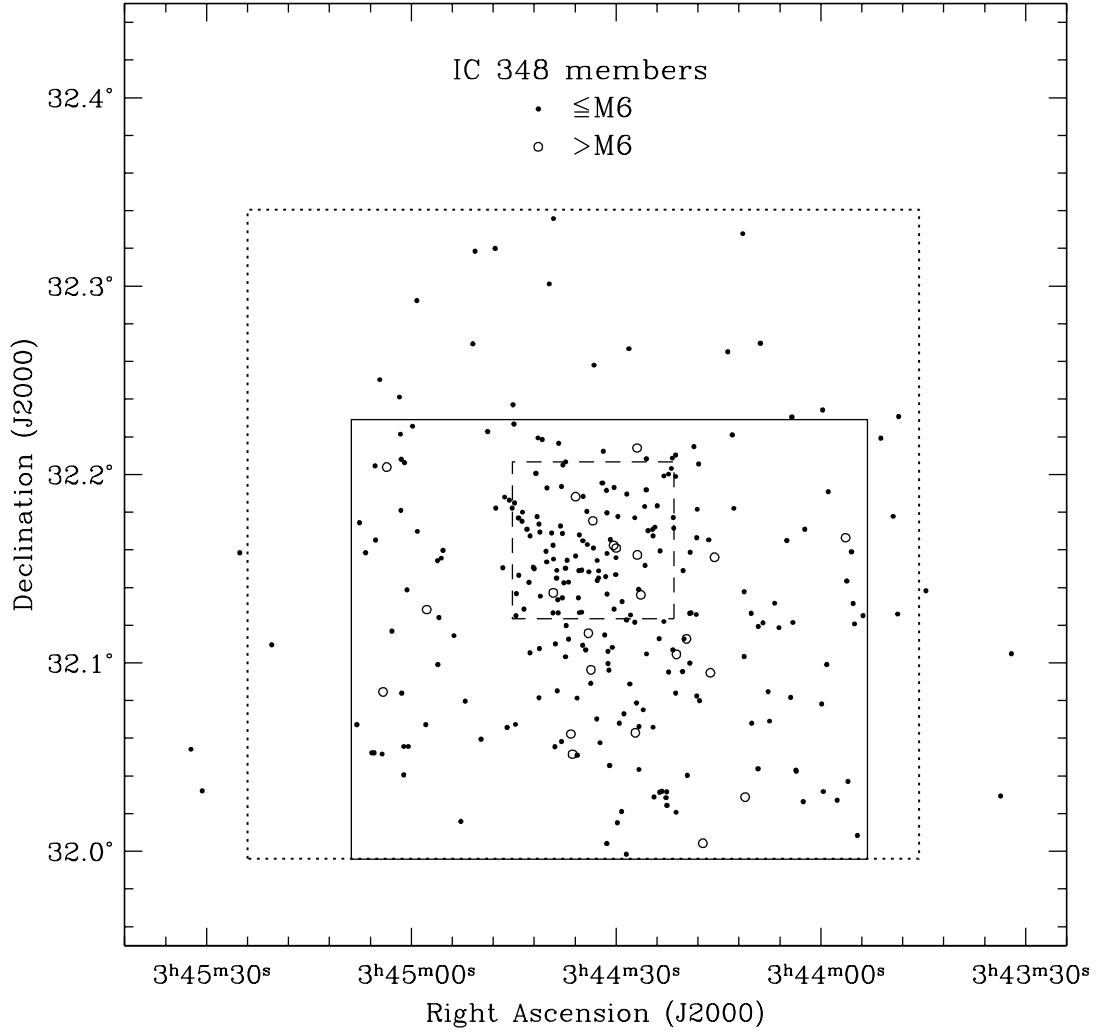


Fig. 1.— Spatial distribution of the 283 members of the IC 348 cluster that have measured spectral types from this work and from previous studies. The 23 members with spectral types later than M6 are likely to be brown dwarfs. Most of the analysis in this work applies to the $16' \times 14'$ field indicated here (*solid line*). For reference, the IMF of Luhman et al. (1998b) was measured for the $5' \times 5'$ center of the cluster (*dashed line*), which was closely matched by the region observed by NTC00. The near-IR imaging and luminosity function modeling of Muench et al. (2003) was performed for the $20.5' \times 20.5'$ field (*dotted line*).

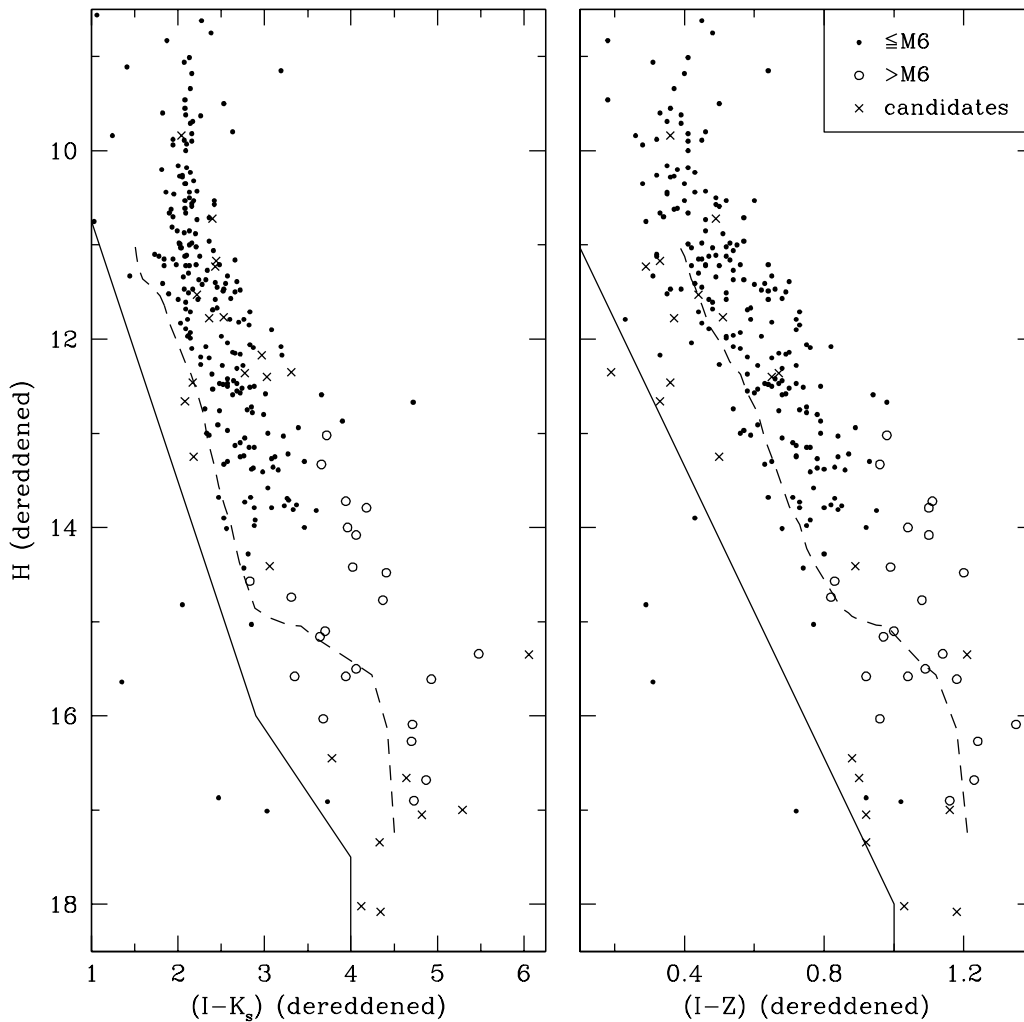


Fig. 2.— Extinction-corrected color-magnitude diagrams for the $16' \times 14'$ field in the IC 348 cluster in Figure 1. We show the cluster members at $\leq M6$ and $> M6$ (*points and circles*) that have been identified through spectroscopy in this work and in previous studies. We have omitted the foreground and background stars that appear in spectroscopic and proper motion measurements (Tables 3 and 4) as well as objects that are likely to be field stars by their location below either of the solid boundaries in this diagram. Sources that lack spectroscopic measurements and that are above both of the boundaries are candidate members of IC 348 (*crosses*). One star that is below the boundary in the right diagram shows other evidence of youth and thus is marked as a candidate (§ 3.1). We omit stars that are too faint to be reliably identified as either field stars or candidate members ($I > 22$). The dashed line is the 10 Myr isochrone ($1-0.015 M_{\odot}$) from the evolutionary models of Baraffe et al. (1998).

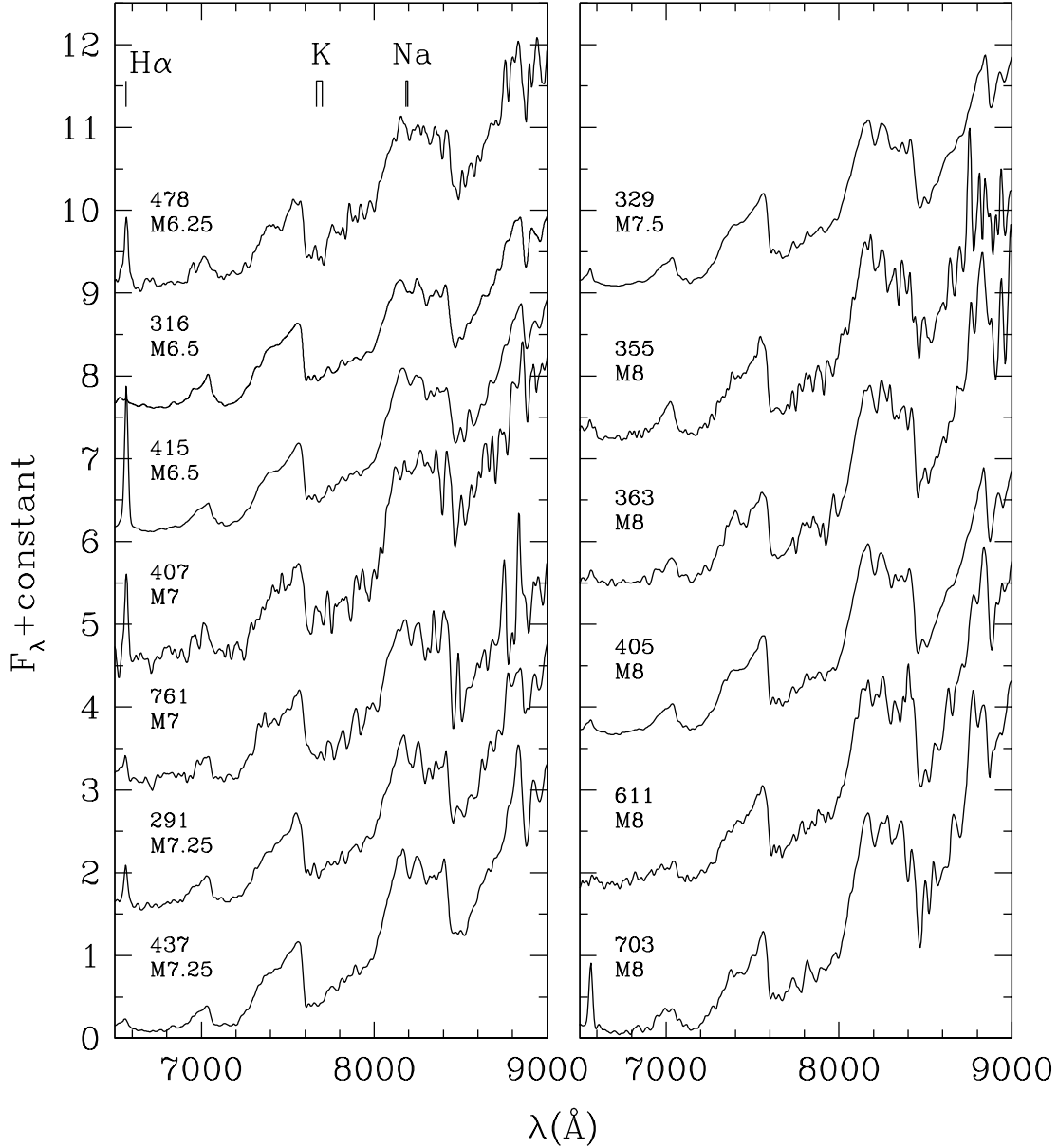


Fig. 3.— Low-resolution spectra of the 13 known members of the IC 348 cluster with spectral types of M6.5 to M8 (Luhman et al. (1998b); Luhman (1999); this work), which are below the hydrogen burning mass limit by the H-R diagram and evolutionary models in Figure 9. These spectra exhibit reddenings of $A_V = 0.4$. All data are smoothed to a resolution of 25 \AA and normalized at 7500 \AA .

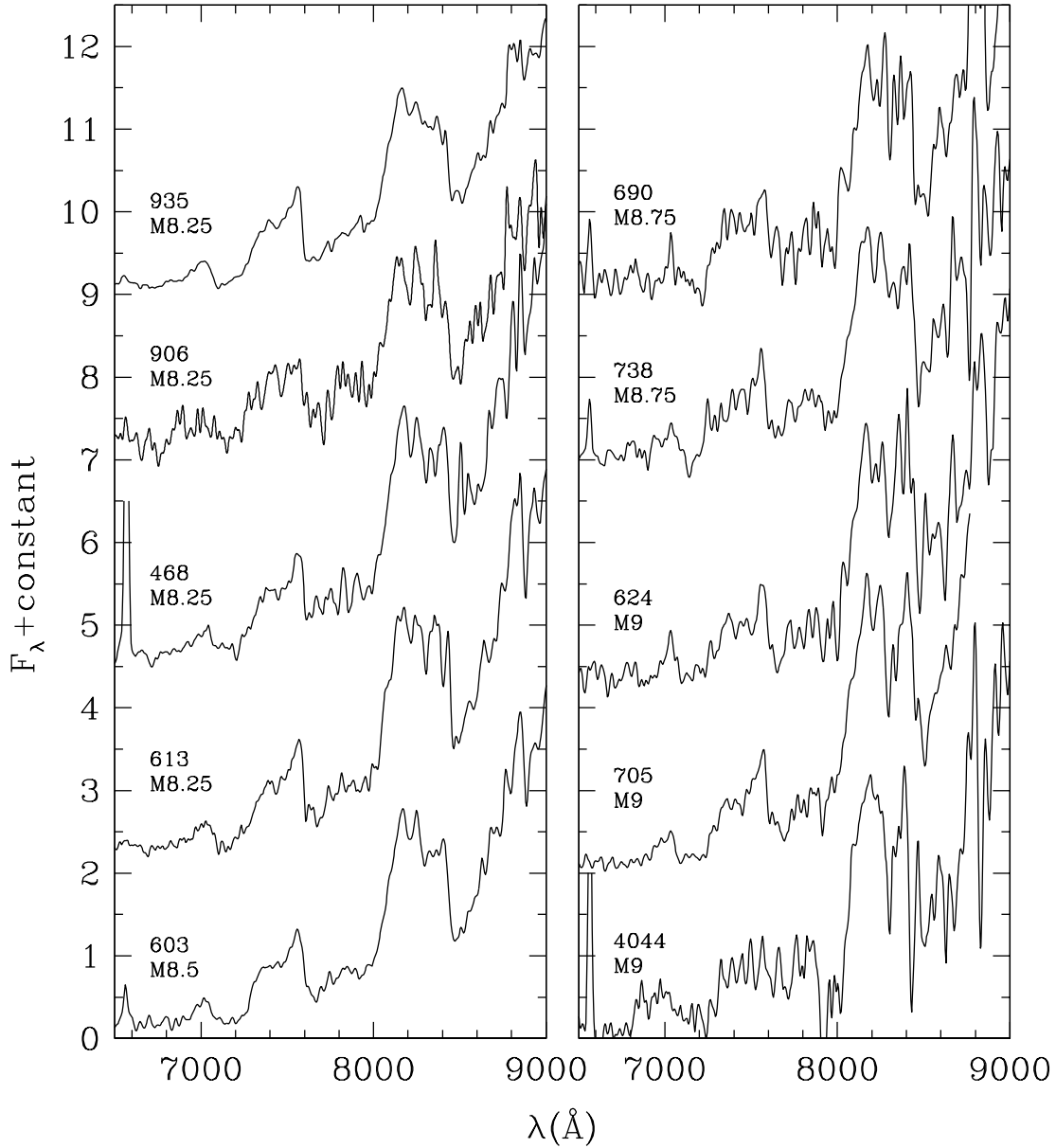


Fig. 4.— Low-resolution spectra of the 10 known members of the IC 348 cluster with spectral types of M8.25 to M9 (Luhman et al. (1998b); Luhman (1999); this work), which are below the hydrogen burning mass limit by the H-R diagram and evolutionary models in Figure 9. These spectra exhibit reddenings of $A_V = 0-2$. All data are smoothed to a resolution of 25 \AA and normalized at 7500 \AA .

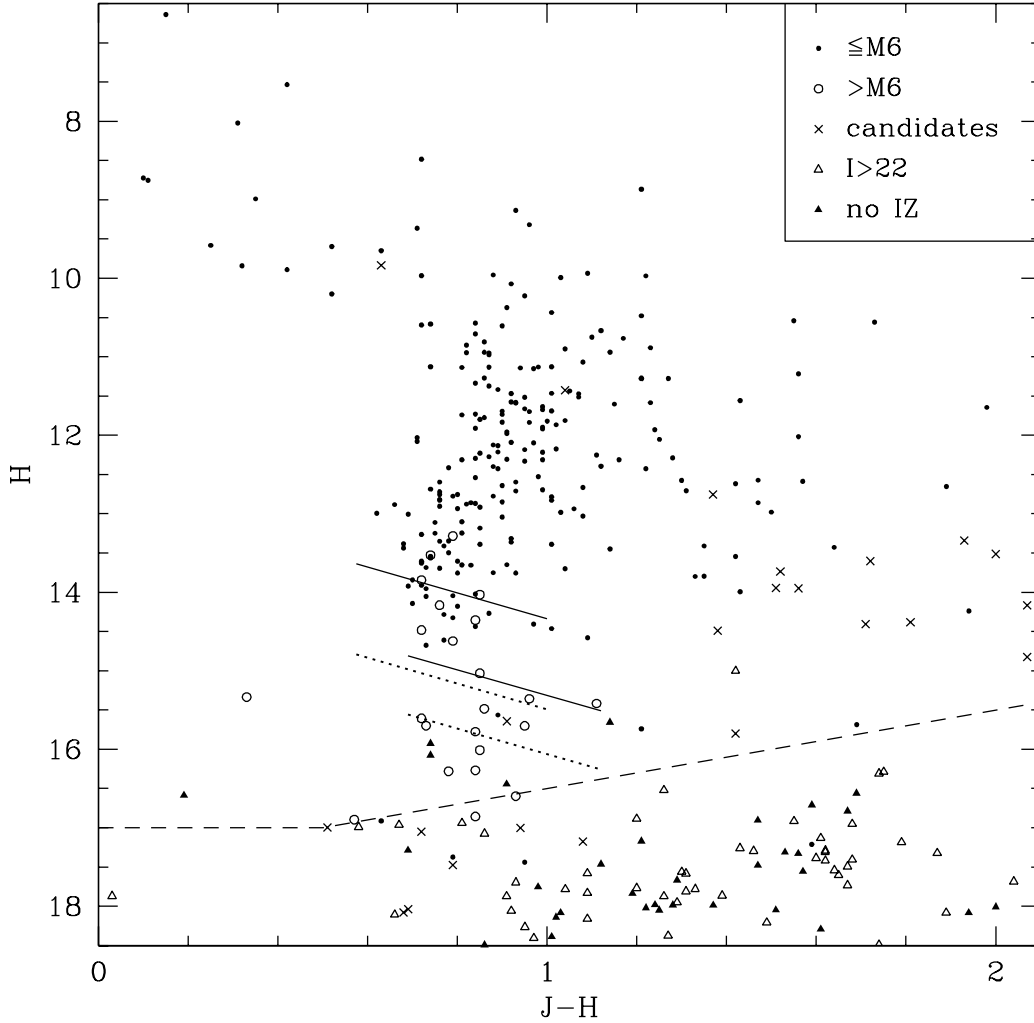


Fig. 5.— $J - H$ versus H for the $16' \times 14'$ field in the IC 348 cluster in Figure 1. The symbols are the same as in Figure 2, with the addition of stars with uncertain optical photometry ($I > 22$, *open triangles*) and sources detected only in these IR data (*solid triangles*). The reddening vectors from $A_V = 0-4$ are plotted for 0.08 ($\sim M6.5$) and $0.03 M_\odot$ ($\sim M8$) for ages of 3 Myr (*upper and lower solid lines*) and 10 Myr (*upper and lower dotted lines*) (CBAH00). Most of these J and H measurements are from 2MASS and Muench et al. (2003). The dashed line represents the completeness limits for the data from Muench et al. (2003).

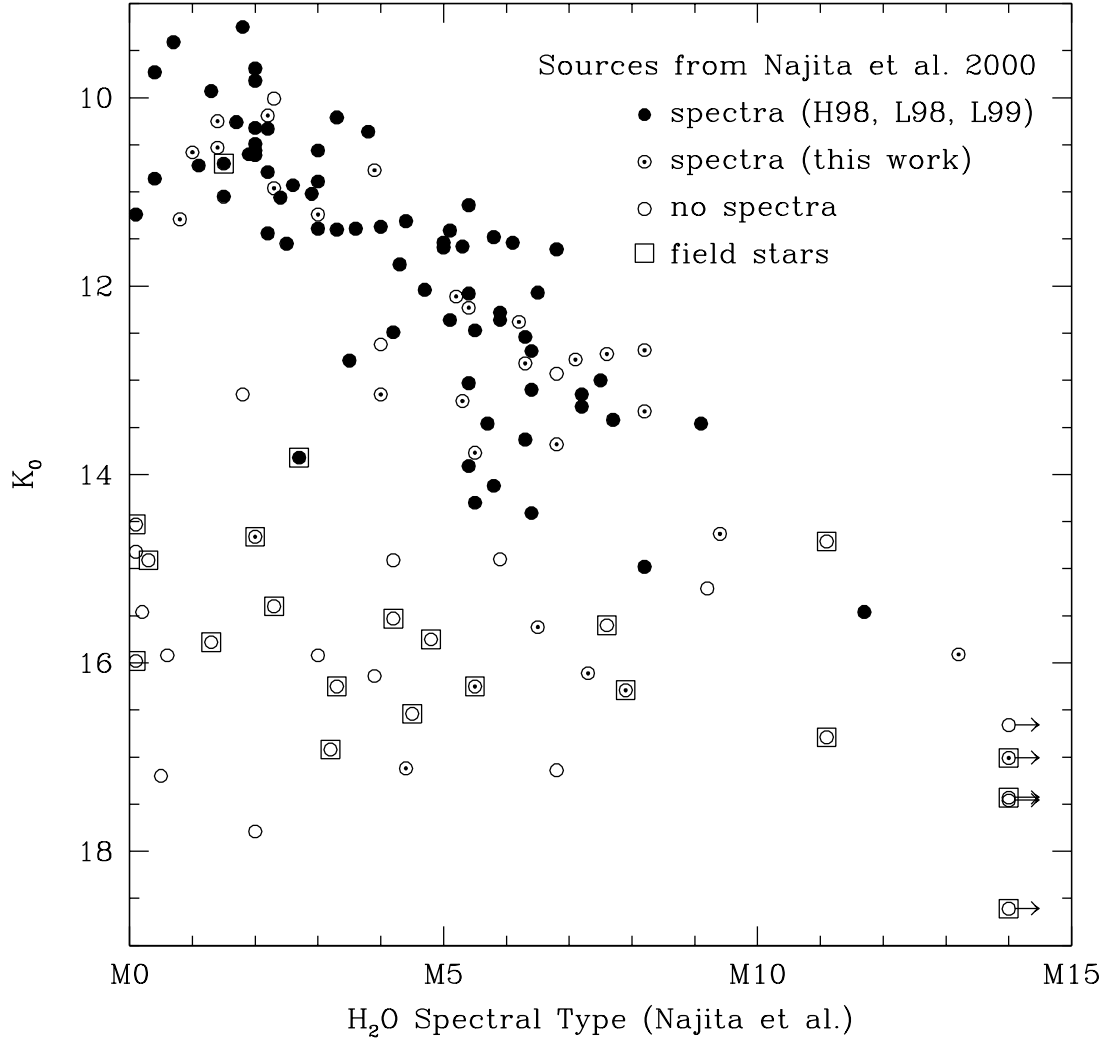


Fig. 6.— Spectral types estimated from *HST* NICMOS narrow-band photometry of H_2O absorption versus dereddened K -band data for the $5' \times 5'$ center of IC 348, as reported by NTC00. We indicate sources that have been observed spectroscopically by Herbig (1998), Luhman et al. (1998b), and Luhman (1999) (*large points*) and in this work (*circled points*), sources that lack spectra (*circles*), and objects that are identified as foreground or background field stars by spectroscopy or the color-magnitude diagrams in Figure 2 and in Luhman et al. (2003b) (*squares*).

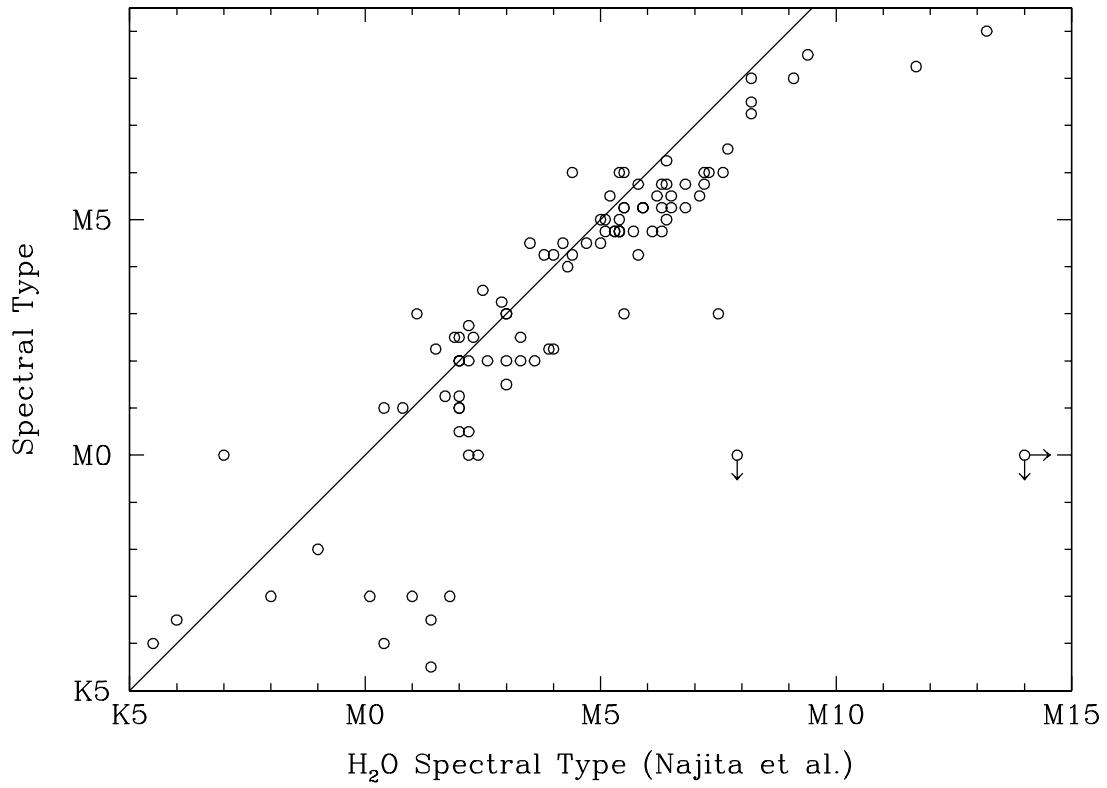


Fig. 7.— Spectral types estimated from *HST* NICMOS narrow-band photometry of H₂O absorption by NTC00 versus spectral types measured from optical spectra by Herbig (1998), Luhman et al. (1998b), and Luhman (1999) and in this work. The typical uncertainties in the spectral types on the vertical axis are ± 0.25 -0.5 subclass.

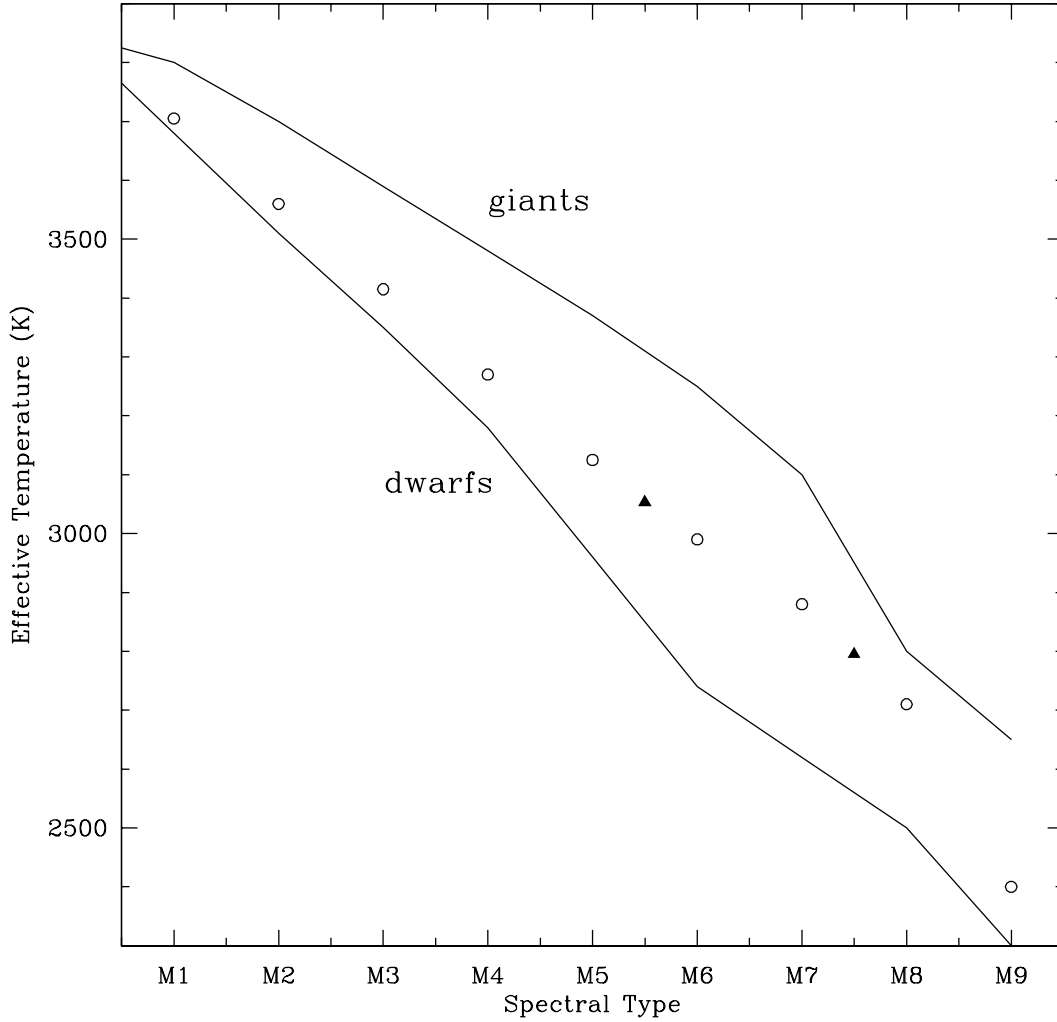


Fig. 8.— For GG Tau Ba and Bb (M5.5, M7.5) to have the same age as GG Tau Aa and Ab (K7, M0.5) on the model isochrones of BCAA98 and CBAH00, the first two objects must have the temperatures indicated by the solid triangles. We have constructed a temperature scale (*circles*; Table 8) that coincides with these two points and thus produces coevality for GG Tau. At $>M7.5$, the scale has been designed so that the M8-M9 members of Taurus and IC 348 have model ages that are similar to those of the earlier members. Temperature scales for dwarfs and giants are shown for comparison (*solid lines*). The dwarf scale compiled by Luhman (1999) has been adjusted by -50 K at M5 and -100 K at M6-M9 to be consistent with the latest temperature estimates for young disk dwarfs (Leggett et al. 2000, 2001; Burgasser et al. 2002). The references for the giant scale are provided in Luhman (1999).

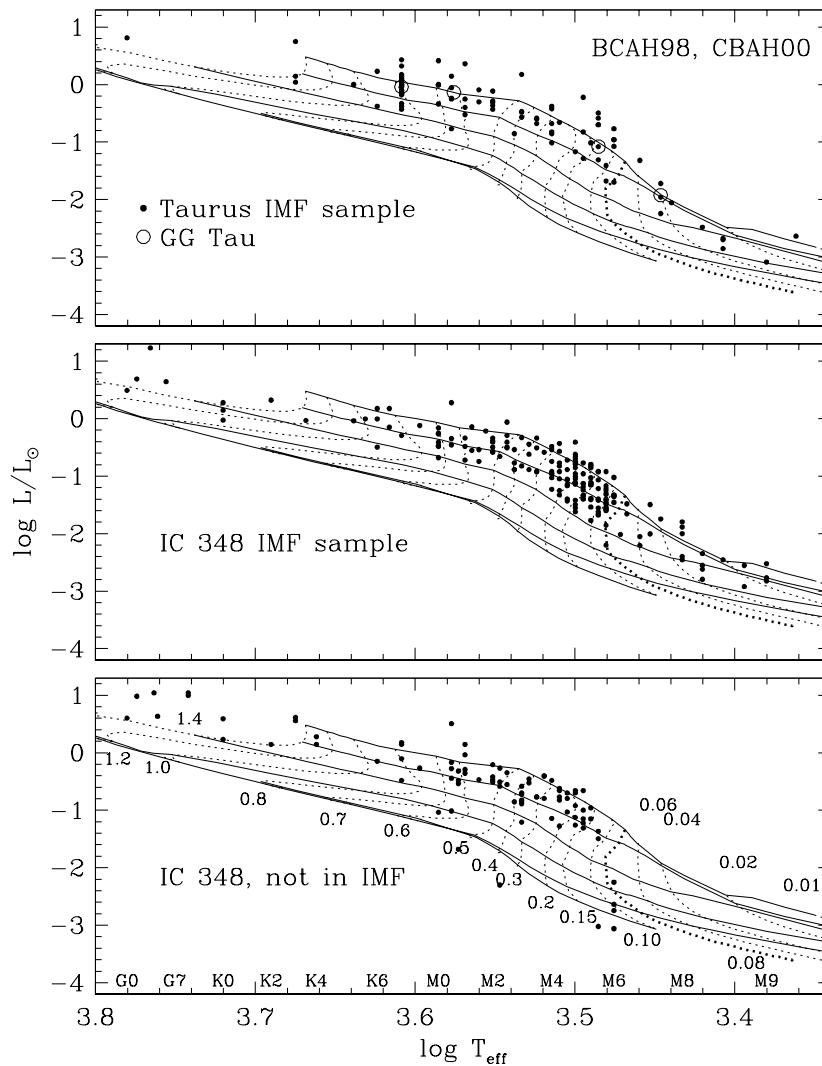


Fig. 9.— H-R diagrams at low masses for objects in the IMFs for Taurus (Briceño et al. 2002; Luhman et al. 2003a) and for IC 348 (this work) (*top and middle*) that are shown in Figure 12. These IMF samples are extinction-limited ($A_V \leq 4$) and apply to 8.4 deg^2 in Taurus and to the $16' \times 14'$ field in IC 348 in Figure 1. Members of IC 348 that are beyond the extinction threshold of $A_V = 4$ or that have anomalously low luminosities for their spectral types are not included in the IMF (*bottom*). The latter sources are probably detected primarily in scattered light. The theoretical evolutionary models of BCAH98 and CBAH00 are shown, where the horizontal solid lines are isochrones representing ages of 1, 3, 10, 30, and 100 Myr and the main sequence, from top to bottom. The M spectral types have been converted to effective temperatures with a scale such that GG Tau Ba and Bb fall on the same model isochrone as Aa and Ab and that the M8-M9 members of Taurus and IC 348 have model ages that are similar to those of the earlier members (Table 8, Figure 8).

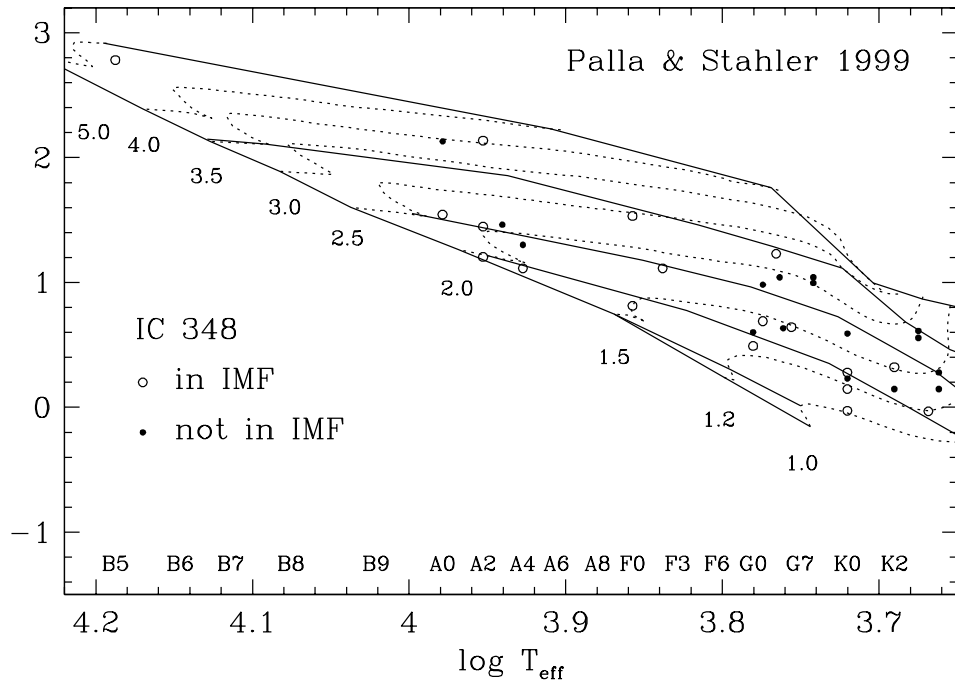


Fig. 10.— H-R diagram at high masses for members of IC 348. The theoretical evolutionary models of Palla & Stahler (1999) are shown, where the horizontal solid lines are isochrones representing ages of 0.1, 1, 3, 10, and 30 Myr and the zero-age main sequence, from top to bottom.

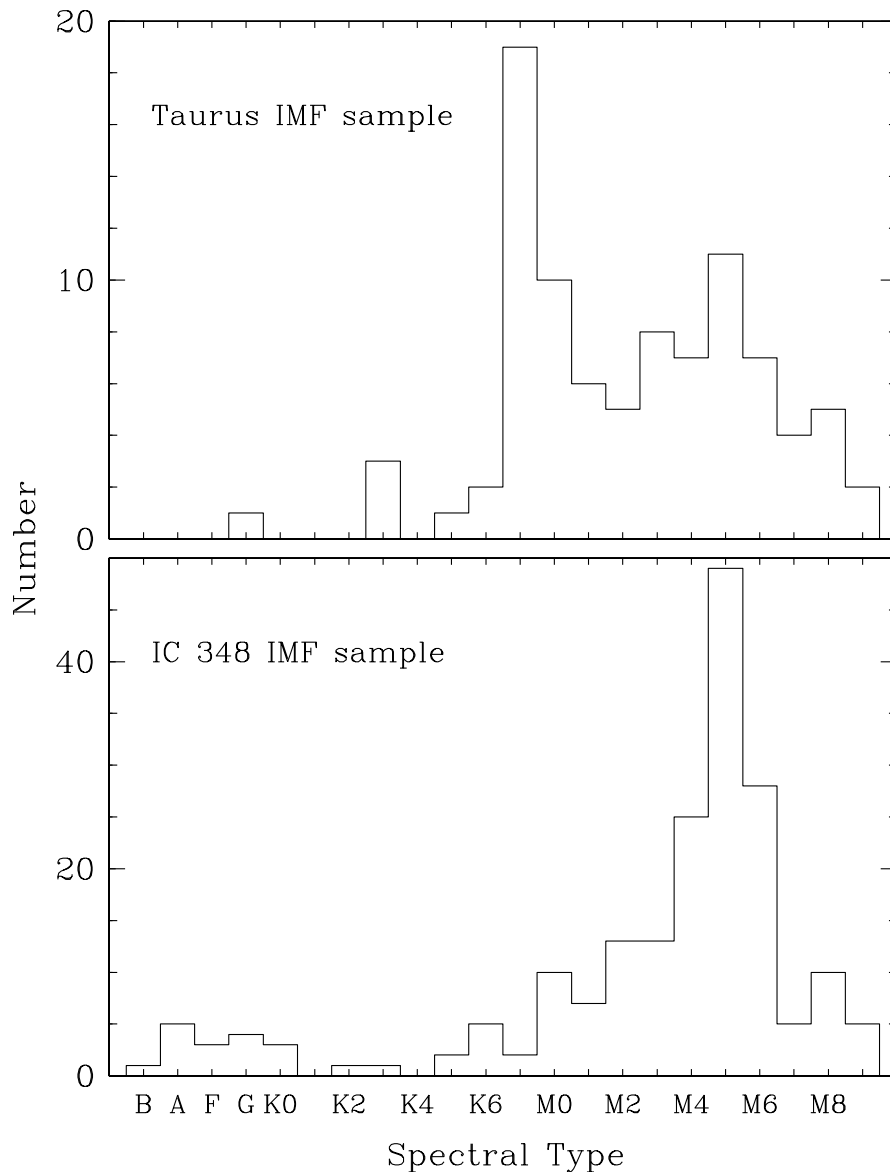


Fig. 11.— Distributions of spectral types for objects in the IMFs for Taurus (Briceño et al. 2002; Luhman et al. 2003a) and for IC 348 (this work) that are shown in Figure 12. These samples are extinction-limited ($A_V \leq 4$) and apply to 8.4 deg^2 in Taurus and to the $16' \times 14'$ field in IC 348 in Figure 1 and are nearly 100% complete for spectral types of $\leq M9$ and $\leq M8$, respectively. Because the evolutionary tracks for young low-mass stars are mostly vertical, spectral types should be closely correlated with stellar masses. As a result, these distributions of spectral types should directly reflect the IMFs in IC 348 and Taurus. This comparison provides clear, model-independent evidence for significant differences in the IMFs of these two regions.

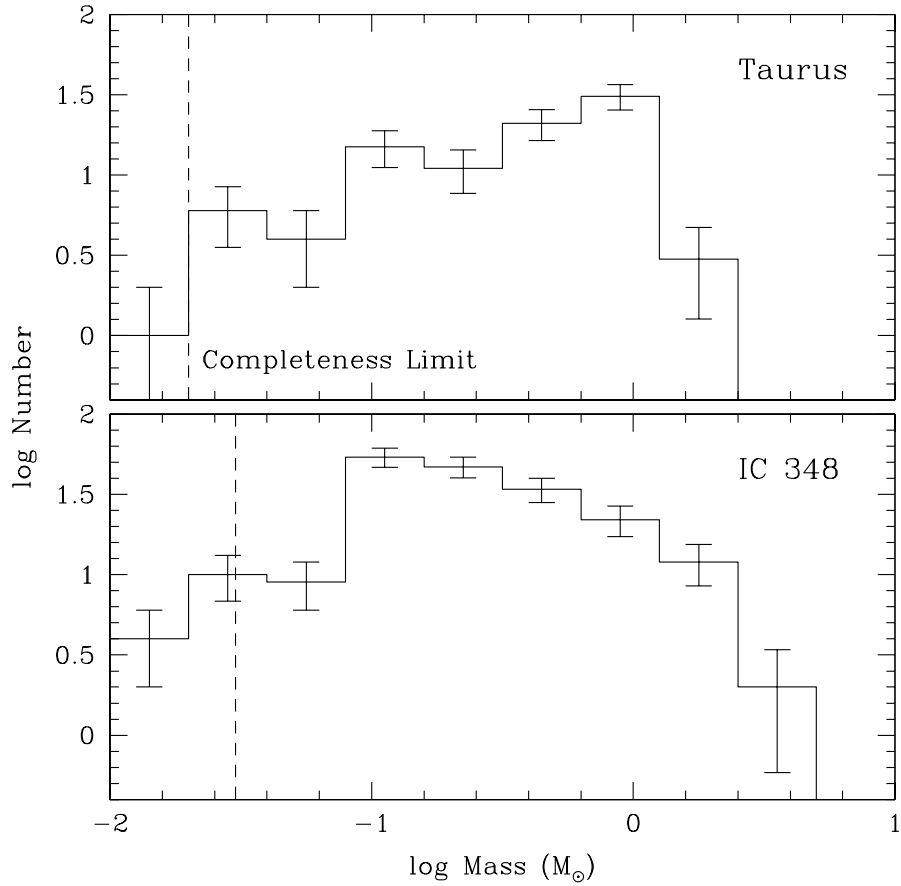


Fig. 12.— IMFs for extinction-limited samples ($A_V \leq 4$) in 8.4 deg^2 in Taurus (Briceño et al. 2002; Luhman et al. 2003a) and in the $16' \times 14'$ field in IC 348 in Figure 1 (this work). These samples are unbiased in mass for $M/M_{\odot} \geq 0.02$ and 0.03 , respectively. In the units of this diagram, the Salpeter slope is 1.35.

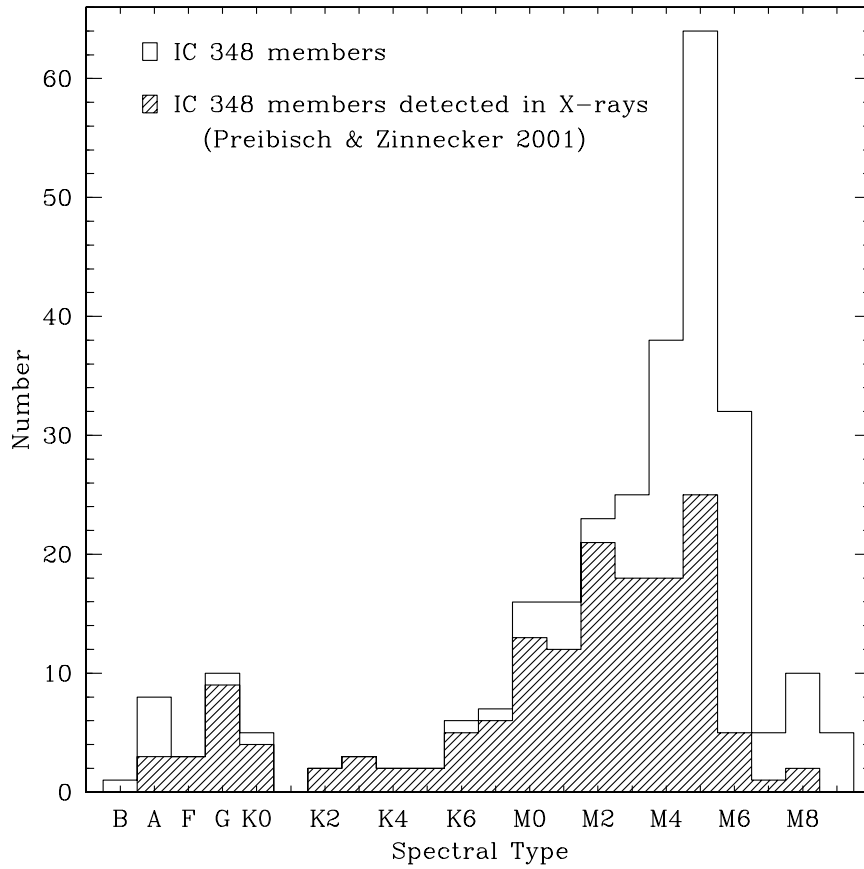


Fig. 13.— Distribution of spectral types for the 283 members of IC 348 that have accurate classifications. Preibisch & Zinnecker (2001) have detected X-rays from 154 of these sources, as indicated by the shaded histogram.

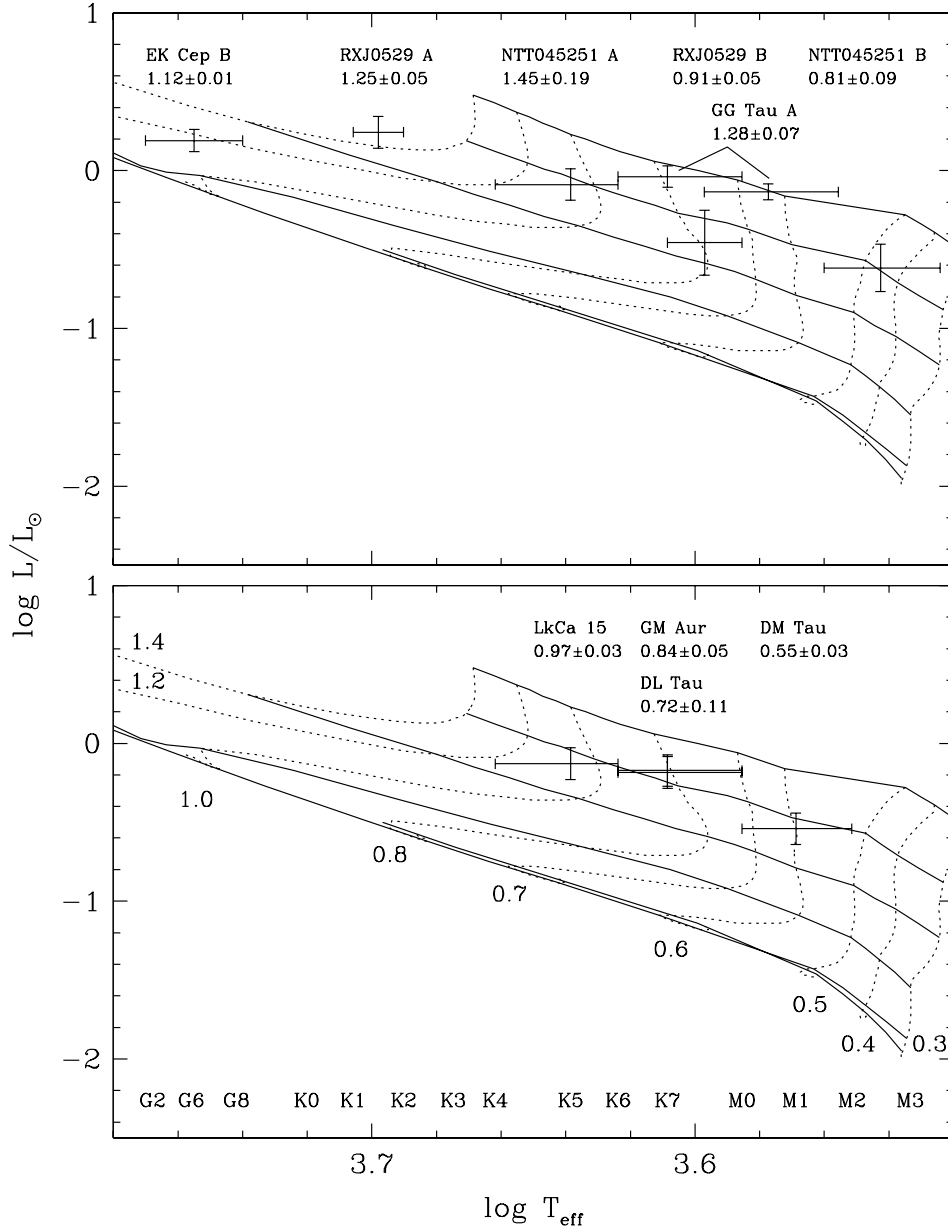


Fig. 14.— Young stars that have dynamical mass estimates are shown with the evolutionary models of BCAH98 ($M/M_{\odot} > 0.1$) and CBAH00 ($M/M_{\odot} \leq 0.1$) with $l_{mix}/H_p = 1.0$ ($M/M_{\odot} \leq 0.6$) and 1.9 ($M/M_{\odot} > 0.6$). The horizontal solid lines are isochrones representing ages of 1, 3, 10, 30, and 100 Myr and the main sequence, from top to bottom. For clarity, these sources are divided into single and binary stars (*lower and upper*). Mass estimates in solar masses are indicated, which are from Simon et al. (2000) (LkCa 15, GM Aur, DL Tau, DM Tau, GG Tau A), Steffen et al. (2001) (NTT045251+3016), Covino et al. (2000) (RXJ0529.4+0041), and Popper (1987) (EK Cep). The mass listed for GG Tau A is the combined mass of Aa and Ab, which are plotted individually.